

**PERFORMANCE ANALYSIS OF A POWER LINE
COMMUNICATION (PLC) SYSTEM WITH MULTICARRIER
DS-CDMA UNDER THE INFLUENCE OF CHANNEL
EFFECTS**

**By
S M Lutfor Rahman
Roll No- 0411062247F**

Under Supervision of :

**Dr. Satya Prasad Majumder
Professor, EEE Dept
BUET, Dhaka**

A Thesis Submitted in Partial Fulfillment of the Requirements for the

Degree of

Master of Science in Electrical and Electronic Engineering



**Department of Electrical and Electronic Engineering
Bangladesh University of Engineering and Technology**

December 2013

APPROVAL CERTIFICATE

This thesis titled **“PERFORMANCE ANALYSIS OF A POWER LINE COMMUNICATION (PLC) SYSTEM WITH MULTICARRIER DS-CDMA UNDER THE INFLUENCE OF CHANNEL EFFECTS”** submitted by S M Lutfor Rahman, Roll No- 0411062247F Session : April 2011 has been accepted as satisfactory in partial fulfillment of the requirements for the degree of **Master of Science in Electrical and Electronic Engineering on 07 December 2013.**

BOARD OF EXAMINERS

1. _____

Dr. Satya Prasad Majumder
Professor

Department of Electrical and Electronic Engineering (EEE)
Bangladesh University of Engineering & Technology (BUET)
Dhaka-1000, Bangladesh

Chairman

2. _____

Dr. Pran Kanai Saha
Professor and Head

Department of Electrical and Electronic Engineering (EEE)
Bangladesh University of Engineering & Technology (BUET)
Dhaka-1000, Bangladesh

Member
(Ex-Officio)

3. _____

Dr. Md. Forkan Uddin
Assistant Professor

Department of Electrical and Electronic Engineering (EEE)
Bangladesh University of Engineering & Technology (BUET)
Dhaka-1000, Bangladesh

Member

4. _____

Dr. Hossam-e-Haider
Senior Instructor

Department of Electrical, Electronic and Communication Engineering (EECE)
Military Institute of Science & Technology (MIST)
Dhaka-1216, Bangladesh

Member
(External)

DECLARATION

I, hereby declare that this thesis is based on the results found by myself. Materials of work found by other researchers are mentioned by reference. This thesis, neither in whole nor in part, has been previously submitted for any degree.

Signature of the Candidate

S M Lutfor Rahman

ACKNOWLEDGEMENT

First and Foremost praise is to ALLAH, the Almighty, the greatest of all, on whom eventually we depend for sustenance and guidance. I would like to thank Almighty Allah for giving me opportunity, determination and strength to do my research. His continuous grace and mercy was with me throughout my life and ever more during the tenure of my research.

I would like to thank my supervisor, Dr. Satya Prasad Majumder, Professor, Department of EEE, BUET, for the patient guidance, encouragement and advice he has provided throughout my time as his student. I have been extremely lucky to have a supervisor who cared so much about my work, and who responded to my questions and queries so promptly. In addition to being an admirable supervisor, he is a man of principles and has immense knowledge of research in general and his subject in particular. I appreciate all his contributions of time, support and ideas.

I would also like to thank the members of my thesis examination board, Dr. Pran Kanai Saha, Dr. Hossam-e-Haider and Dr.Md.Forkan Uddin for their encouragement and insightful comments.

I am grateful to my colleagues who have helped and provided me adequate support for successful completion of my research works.

Most importantly, none of this would have been possible without the love and patience of my family. I would like to express my heart-felt gratitude to my family.

ABSTRACT

Power line communication (PLC) system is evolving as a ubiquitous communication system for high speed broadband data communication. Multicarrier DS-CDMA (MC-DS-CDMA) technique is an attractive technique in achieving high data-rate transmission in wireless communication. In this thesis investigations are carried out to combine the MC-DS-CDMA technology with the features and characteristics of a PLC system. To find the effectiveness of MC-DS-CDMA system in a power line channel, a system model is proposed for high speed data communication through a power line channel using the DS-CDMA with multicarrier orthogonal FDM (OFDM) technique. Analysis is carried out by considering the combined effect of power line impulsive noise, channel transfer function, effect of load impedances and the number of branches in a PLC network without and with path diversity using rake receiver. Expressions of signal to interference and noise ratio and bit error rate (BER) at output of CDMA receiver are developed considering the above limitations. BER performance results are evaluated for different system parameters, channel parameters, processing gain, number of OFDM carriers and number of rake fingers. For a given performance level, the optimum values of system parameters like number of OFDM subcarriers, code length, number of rake fingers for a given system length, number of branches and load impedances are determined.

TABLE OF CONTENTS

APPROVAL	i
DECLARATION	ii
ACKNOWLEDGEMENT	iii
ABSTRACT	iv
TABLE OF CONTENTS	v
LIST OF TABLES	ix
LIST OF FIGURES	x
LIST OF ABBREVIATIONS	xii

Chapter -1 INTRODUCTION

1.1	Power Line Communication	1
1.2	Limiting Factors of a Wireless Communication System	1
1.3	Limiting Factors of Power Line Communication	2
1.4	Multiple Access Schemes for Power Line Communication	2
1.5	Single Carrier Vs Multicarrier CDMA System	4
1.6	OFDM Systems for Power Line Communications	5
1.7	Merits of Multicarrier DS CDMA Technique	5
1.8	Motivation of this Thesis	6
1.9	Review of Previous Works	6
1.10	Objectives of this Thesis Work	6
1.11	Organization of this Thesis Paper	7

Chapter-2 BACKGROUND AND RELATED WORKS

2.1	Introduction	8
2.2	Power Line Networks with One Interconnection	8
2.2.1	Signal Propagation	8
2.2.2	Power Line Transfer Function	10
2.3	Power Line Networks with One Interconnection and One Branch	10
2.3.1	Signal Propagation	10
2.3.2	Power Line Transfer Function	11
2.4	Power Line with Interconnection and a Number of Branches	12
2.5	Power Line Network with Distributed Branches	14

2.6	Noise in a Power Line Channel	15
2.7	Related Works	17
Chapter-3	ANALYTICAL MODEL OF POWER LINE COMMUNICATION (PLC) SYSTEM WITH MULTICARRIER DS-CDMA	
3.1	Introduction	19
3.2	Power Line Channel Model	19
3.3	Power Line Noise Model	19
3.4	Functional Block Diagram of PLC System with MC DS-CDMA	19
3.4.1	Transmitter Model	20
3.4.2	OFDM Modulator Model	20
3.4.3	Receiver Model	21
3.4.4	OFDM Demodulator Model	21
3.5	System Analysis without Diversity	22
3.5.1	Transmitted Signal	22
3.5.2	Receiver Output	23
3.5.3	Desired Signal of Receiver	25
3.5.4	Multiple Access Interference (MAI)	25
3.5.5	Noise	26
3.5.6	Signal to Interference and Noise Ratio (SINR)	26
3.5.7	Bit Error Rate (BER) of the Receiver	27
3.6	System Analysis with Diversity	27
3.6.1	Receiver Model with Diversity (Rake)	27
Chapter-4	RESULTS AND DISCUSSIONS	
4.1	Introduction	29
4.2	Performance of Power Line Communication System with Varying Channel Parameters	29
4.2.1	BER Vs SNR for Different Line Impedances (Value of R, L, and C varying)	30
4.2.2	BER Vs SNR for Different Branch Lengths	32
4.2.3	BER Vs SNR for Different Source Impedances	34
4.3	Performance of Power Line Communication System with Varying System Parameters (Without Diversity).	36
4.3.1	BER Vs SNR for Different Number of Subcarriers at Fixed Processing	36

Gain ($G_p=128$)	
4.3.2	BER Vs SNR for Different Number of Subcarriers at Fixed Processing Gain ($G_p=256$) 38
4.3.3	BER Vs SNR for Different Processing gains at Fixed Number of Subcarriers ($N_c=8$) 41
4.4	Performance of Power Line Communication System with Varying System Parameters (With Diversity using a Rake Receiver) 44
4.4.1	BER Vs SNR for Different Number of Subcarriers at Fixed Processing Gain ($G_p=128$) with a Rake Receiver having Number of Rake Fingers, $N_r=3$ 44
4.4.2	BER Vs SNR for Different Number of Subcarriers at Fixed Processing Gain ($G_p=128$) with a Rake Receiver having Number of Rake Fingers, $N_r=4$ 47
4.4.3	BER Vs SNR for Different Number of Subcarriers at Fixed Processing gain ($G_p=256$) with a Rake Receiver having Number of Rake Fingers, $N_r=3$ 49
4.4.4	BER Vs SNR for Different Number of Subcarriers at Fixed Processing Gain ($G_p=256$) with a Rake Receiver having Number of Rake Fingers, $N_r=4$ 52
4.4.5	BER Vs SNR for Different Processing Gains at Fixed number of subcarriers ($N_c=8$) with a Rake Receiver having Number of Rake Fingers, $N_r=3$ 54
4.4.6	BER Vs SNR for Different Processing Gains at fixed number of subcarriers ($N_c=8$) with a Rake Receiver having Number of Rake Fingers, $N_r=4$ 57
4.5	Optimum System Parameters 60
4.5.1	N_c (Subcarrier) Vs SNR for Different Users at G_p (Processing gain)=128 60
4.5.2	User Vs SNR for Different Number of Subcarriers (N_c) at $G_p=128$ 63
4.5.3	Subcarrier (N_c) Vs User for a Certain SNR (15dB) at $G_p=128$ 64
4.5.4	Subcarrier (N_c) Vs SNR for Different Users at G_p (Processing gain)=256 66
4.5.5	User Vs SNR for Different Number of Subcarriers (N_c) at $G_p=256$ 68
4.5.6	Subcarrier (N_c) Vs User for a Certain SNR (15dB) at $G_p=256$ 70
4.5.7	Processing Gain (G_p) Vs User for a Fixed Number of Subcarriers ($N_c=8$) 72
4.6	Performance Comparison of PLC with Wireless Communication 74
4.6.1	BER Vs SNR for Different Number of Subcarriers at Fixed Processing Gain ($G_p=256$) for Wireless Communication 74
4.6.2	User Vs SNR for Different Number of Subcarriers (N_c) at $G_p=256$ for Wireless Communication 76

Chapter-5	CONCLUSIONS AND FUTURE WORKS	
5.1	Conclusions	77
5.2	Scope for Future Works	78
	REFERENCES	79

LIST OF TABLES

<u>Table</u>	<u>Title of the Table</u>	<u>Page</u>
4-1	List of channel and system parameters	29
4-2	Values of SNR(dB) corresponding to $BER=10^{-3}$, $G_p=128$	61
4-3	Number of users at different number of subcarriers (at SNR=15dB), $G_p=128$	64
4-4	Values of SNR(dB) corresponding to $BER=10^{-3}$, $G_p=256$	66
4-5	Number of users at different number of subcarriers (at SNR=15dB), $G_p=256$	70
4-6	Values of SNR(dB) for different processing gains for different users at a fixed number of subcarriers ($N_c=8$)	72
4-7	Comparison of capacity between PLC and wireless communication at particular SNR =15 dB, $G_p=256$	76

LIST OF FIGURES

<u>Figure</u>	<u>Title of the Figure</u>	<u>Page</u>
Fig. 1-1	Various CDMA Schemes	4
Fig. 2-1	Transmission Line with One Interconnection	8
Fig. 2-2	Transmission Line with One Interconnection and One Branch	11
Fig. 2-3	Power Line with Two Branches at the Same Node	12
Fig. 2-4	Transmission Line with One Interconnection and Branch	13
Fig. 2-5	Power Line Network with Distributed Branches	14
Fig. 2-6	Bad and Good Background Noise PSD	16
Fig. 3-1	Functional Block Diagram of PLC System with MC-DS CDMA	19
Fig. 3-2(a)	Block Diagram of MC DS-CDMA Transmitter	20
Fig. 3-2(b)	Block Diagram of OFDM Modulator Model	20
Fig. 3-3(a)	Block Diagram of MC DS-CDMA Receiver	21
Fig. 3-3(b)	Block Diagram of OFDM Demodulator Model	21
Fig. 3-4	Block Diagram of MC DS-CDMA Receiver with Diversity	27
Fig. 4-1	Plots of BER Vs SNR for Different Line Impedances (Value of R, L, and C varying)	31
Fig. 4-2	Plots of BER Vs SNR for Different Branch Lengths	33
Fig. 4-3	Plots of BER Vs SNR for Different Source Impedances	35
Fig. 4-4	Plots of BER Vs SNR for Different Number of Subcarriers at Fixed Processing Gain ($G_p=128$)	38
Fig. 4-5	Plots of BER Vs SNR for Different Number of Subcarriers at Fixed Processing Gain ($G_p=256$)	40
Fig. 4-6	Plots of BER Vs SNR for Different Processing Gains at Fixed Number of Subcarriers ($N_c=8$)	43
Fig. 4-7	Plots of BER Vs SNR for Different Number of Subcarriers at Fixed Processing Gain ($G_p=128$) with a Rake Receiver having Number of Rake Fingers, $N_r=3$	46
Fig. 4-8	Plots of BER Vs SNR for Different Number of Subcarriers at Fixed Processing Gain ($G_p=128$) with a Rake Receiver having Number of Rake Fingers, $N_r=4$	49
Fig. 4-9	Plots of BER Vs SNR for Different Number of Subcarriers at Fixed Processing Gain ($G_p=256$) with a Rake Receiver having Number of Rake Fingers, $N_r=3$	51
Fig. 4-10	Plots of BER Vs SNR for Different Number of Subcarriers at Fixed Processing Gain ($G_p=256$) with a Rake Receiver having Number of Rake Fingers, $N_r=4$	54

Fig. 4-11	Plots of BER Vs SNR for Different Processing Gains at Fixed Number of Subcarriers ($N_c=8$) with a Rake Receiver having Number of Rake Fingers, $N_r=3$	57
Fig. 4-12	Plots of BER Vs SNR for Different Processing Gains at Fixed Number of Subcarriers ($N_c=8$) with a Rake Receiver with Number of Rake Fingers, $N_r=4$	60
Fig. 4-13	N_c (Subcarrier) Vs SNR for Different Users at G_p (Processing Gain)=128	62
Fig. 4-14	User Vs SNR for Different Number of Subcarriers (N_c) at $G_p=128$	64
Fig. 4-15	Subcarrier (N_c) Vs User for a Certain SNR (15dB) at $G_p=128$	66
Fig. 4-16	N_c (Subcarrier) Vs SNR for Different Users at G_p (Processing Gain)=256	68
Fig. 4-17	User Vs SNR for Different Number of Subcarriers (N_c) at $G_p=256$	69
Fig. 4-18	Subcarrier (N_c) Vs User for a Certain SNR (15dB) at $G_p=256$	71
Fig. 4-19	Processing Gain (G_p) Vs User for Fixed Number of Subcarriers ($N_c=8$)	73
Fig. 4-20	Plots of BER Vs SNR for Different Number of Subcarriers at Fixed Processing Gain ($G_p=256$) for Wireless Communication	75
Fig. 4-21	User Vs SNR for Different Number of Subcarriers (N_c) at $G_p=256$ for Wireless Communication	76

LIST OF ABBREVIATIONS

AWGN	Additive White Gaussian Noise
BER	Bit Error Rate
BPSK	Binary Phase Shift Keying
CDMA	Code Division Multiple Access
CFO	Carrier Frequency Offset
CP	Cyclic Prefix
DS/FH	Direct Sequence Frequency Hopping
DS/TH	Direct Sequence Time Hopping
DS-CDMA	Direct Sequence Code Division Multiple Access
EGC	Equal Gain Combining
FDMA	Frequency Division Multiple Access
FFT	First Fourier Transform
GIR	Gauss Impulsive power Ratio
ICI	Inter Carrier Interference
IFFT	Inverse First Fourier Transform
ISI	Inter Symbol Interference
ITU	International Telecommunication Union
LOS	Line of Sight
LPF	Low Pass Filter
MAI	Multiple Access Interference
MC- DS-CDMA	Multi Carrier Direct Sequence CDMA
MC-CDMA	Multi Carrier Code Division Multiple Access
MIMO	Maximum Input Maximum Output
MT-CDMA	Multi Tone Code Division Multiple Access
OFDM	Orthogonal Frequency Division Multiplexing
OFDMA	Orthogonal Frequency Division Multiple Access
PN	Pseudo-random Noise
PL	Power Line
PLN	Power Line Noise
PLC	Power Line Communication

PDF	Probability Density Function
PSD	Power Spectral Density
PSK	Phase Shift Keying
SINR	Signal to Interference and Noise ratio
SNR	Signal to Noise Ratio
SS	Spread-Spectrum
SSDR	Spread-Spectrum Diversity Receiver
SSMA	Spread-Spectrum Multiple Access
STBC	Space Time Block Code
TDMA	Time Division Multiple Access

CHAPTER-1

INTRODUCTION

1.1 Power Line Communication

The basic concept of power line communication (PLC) is to transmit information and electricity simultaneously along power lines as an alternative to constructing dedicated communications infrastructure. PLC technology integrates the activities of outside the building with those inside the building at a much higher bandwidth. This means voice and data transmission via the mains supply voltage network to every power socket in the building, as well as in the reverse direction at high speed. In recent days, major advances in the fields of modulation, coding and detection enabled the design of efficient broadband communication systems over power lines. Generally power line communication systems have been assumed as the systems of low speed and low reliability. The low qualities of the systems, however, are not inherent of PLC but the result of inadequate design strategy of the systems. The systems with proper considerations of the characteristics of power line as a communication medium achieve reliable high speed data transmission in power lines. PLC make it possible to use ubiquitous electricity power lines for the medium of communications [1]. With the increasing demand for broadband communications, the use of broadband PLC has become more attractive mainly due to advantages such as the availability of power lines worldwide and the low cost of installation.

1.2 Limiting Factors of a Wireless Communication System

A signal transmitted through a mobile radio channel undergoes all the mechanisms that govern the propagation of electromagnetic waves. There are four basic mechanisms influence the propagation of electromagnetic waves which are described below :

- a. **Path Loss :** The path loss describes a deterministic average attenuation of the signal strength depending only on the distance between the transmitter and receiver.
- b. **Shadowing :** Shadowing is caused by landscape details obstructing line of sight, such as hills, forests, bushes, buildings and so forth. It also reflects the changes in the propagation paths due to movements of the mobile.
- c. **Multipath Fading :** It is a result of the multiple propagation paths created by reflection, diffraction, and scattering mechanisms which leads to inter symbol interference (ISI). Multipath fading characteristics depend on whether the transmitter and receiver are in the line of sight (LOS) or not. The latter is modeled as a rayleigh distribution, while the former case is modeled as a rician distribution.
- d. **Carrier Frequency Offset :** It indicates the shift in frequency of the signal spectrum caused by the motion of the objects within the propagation environment.

1.3 Limiting Factors of Power Line Communication

Power lines provide a harsh environment for higher frequency communications signal. As power lines are not specifically designed for communication, a number of challenges exist as far as data transfer through this type of network [1]. The most crucial channel properties degrading the performance of high-speed communication over power lines are given below :

- a. **Power Line Noise :** Noise in a power line is not an additive white Gaussian noise. The noise is categorized into four different types of noise and extended into five types. The five types of noise are colored background noise, narrowband noise, periodic impulsive noise asynchronous to the mains frequency, periodic impulsive noise synchronous to the mains frequency and asynchronous impulsive noise. The first three types of noise usually remain stationary and are summarized as background noise. The last two noise types are time-variant and are classified as impulsive noise. The impulsive noise has a short duration with random occurrence and a high power spectral density (PSD). It may cause bit or burst errors in data transmission [1].
- b. **Multipath Effect :** Multipath effect is another serious problem for PLC because the distribution of power lines is complicated. Signal propagation usually travels along a shortest path between transmitter and receiver, but additional paths (echoes) should also be considered. This will result in a multipath scenario with frequency selective effect. In any given power line channel, the number of interconnected branches in the link between sending and receiving end, different terminal loads, and branch lengths cause multipath (due to transmission and reflection of signals between the transmission line segments) that are similar to wireless channels. This multipath causes degradation of the signals propagating in the link between the sending and receiving ends [2].
- c. **Attenuation :** There are two major causes of high frequency attenuation in a power line communication channel [3]. The first is attenuation due to ohmic absorption in the materials that make up the physical channel. This absorption varies with frequency. The second is attenuation due to reflections from abrupt discontinuities and mismatched impedances that occur along the power line. These reflections cause part of the signal to be diverted away from the receiver and absorbed in other parts of the system.
- d. **Effect of Channel Parameters :** Channel parameters like load impedances, line length, branches etc. affect the performance of power line communication.

1.4 Multiple Access Schemes for Power Line Communication

The capacity of a communication system is measured in bit/s Hz and it shows the maximum amount of information per spectrum unit that can be sent by all active users. In cellular network design, capacity refers to the maximum number of users simultaneously served by the system located on the unit area, or alternatively the maximum value of traffic served by the system per unit area. Multiple – access capacity has also been defined as the number of users who can be supported at a given error performance level. Multiple access schemes enable the radio system elements to be used in the most appropriate combination to efficiently meet the demand of the users at any given situation. The choice of a multiple-access scheme is one of the crucial decisions made in the design of a radio communication system since it is closely related with the system capacity. Frequency division

multiple access (FDMA), time division multiple access (TDMA) and code division multiple access (CDMA) are the major access techniques used in conventional mobile radio communication systems.

- a. **FDMA** : It assigns individual channels (frequency bands) to individual users. During the period of the call, no other user can share that frequency band. If an FDMA channel is not in use, it remains idle.
- b. **TDMA** : It divides the transmission time into time slots and in each slot, only one user is allowed to either transmit or receive. TDMA shares a single carrier frequency with several users, where each user makes use of non overlapping time slots. Analogous to FDMA, if a channel is not in use, the corresponding time slots sit idle and cannot be used by other users.

In both the cases, they assume that all users transmit continuously. But actually, the percentage of speaker remains active, ranges from 35% to 50%. Low frequency reuse factor reduces the number of channels per cell. Susceptible to fading, which is caused by interference between two or more versions of the transmitted signal that arrive at the receiver at slightly different time.

- c. **CDMA** : A completely different approach is realized in CDMA systems in which all resources are being allocated to all the active users [4]. Here, each user is assigned with a unique code sequence to encode its information-bearing signal. The receiver, knowing the code sequences of the user, decodes a received signal after reception and recovers the original data. This is possible since the cross-correlations between the code of the desired user and the codes of the other users are small. Since, the bandwidth of the code signal is chosen to be much larger than the bandwidth of the information-bearing signal, the encoding process spreads the spectrum of the signal and is therefore also known as spread-spectrum modulation. That's why, CDMA is often denoted as spread-spectrum multiple access (SSMA). However, if the number of simultaneously transmitting users rises above a certain limit, the multiple access interference (MAI) becomes too large for the desired signal to be extracted correctly and contention occurs. Therefore, CDMA system is essentially interference limited. The ratio of code signal bandwidth to information signal bandwidth is called the processing gain of the spread spectrum system. High data rate in multiuser wireless access is demanded by multimedia applications, which require very high bandwidth with mobility. CDMA is considered to be a strong candidate for next generation mobile systems to support multimedia services because it has the ability to cope with the asynchronous nature of multimedia traffic. There are number of properties that are behind the development of CDMA. Some of those are [5] :

- (1) Multiple access capability
- (2) Inherent frequency diversity
- (3) Interference rejection and anti-jamming capability
- (4) Low probability of interception
- (5) Universal frequency reuse
- (6) Soft handoff
- (7) Soft capacity

There are various schemes of CDMA system which are given below [6]:

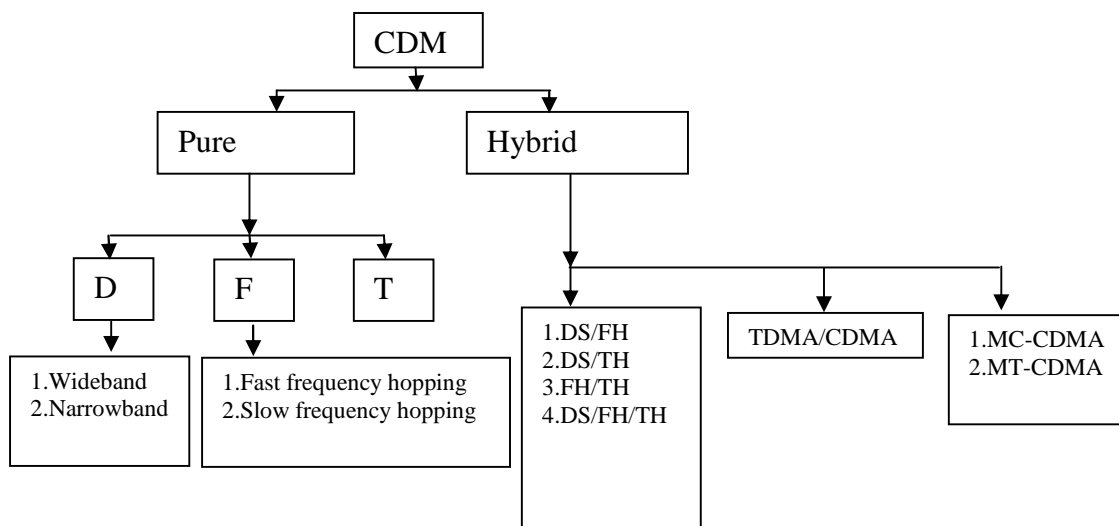


Fig. 1-1 Various CDMA Schemes

There are number of coding and modulation techniques that generate spread spectrum signals. Some important schemes are [6] :

- (1) **Direct Sequence CDMA (DS CDMA)** : The information bearing signal is multiplied directly by a high chip rate code signal.
- (2) **Frequency Hopping CDMA (FH CDMA)** : The carrier frequency at which the information-bearing signal is transmitted, is rapidly changed according to the code signal.
- (3) **Time Hopping CDMA (TH CDMA)** : The information-bearing signal is not transmitted continuously. Instead the signal is transmitted in short burst where the times of the bursts are decided by the code signal.
- (4) **Multi Carrier CDMA (MC CDMA)** : Two or more of the previously-mentioned modulation techniques can be used together to combine the advantages and to combat their disadvantages. In MC-CDMA, transmitter spreads the original data stream over different sub-carriers using a given spreading code in the frequency domain whereas, in MT-CDMA, spreading is done along the time domain. However, in MC-DS-CDMA, spreading of signal is done in time domain which is then modulated in diversified frequencies.

1.5 Single Carrier Vs Multicarrier CDMA System

The choice of a single carrier or multi carrier CDMA scheme is an important design consideration. Future mobile radio systems have to support a variety of services such as voice, video and high-rate data communications. Towards this goal, the system must be able to support variable and high bit-

rate transmission, and with high bandwidth efficiency, bearing in mind the limited radio frequency spectrum [7]. In mobile environments, high data-rate transmission will result in the channel delay exceeding the symbol duration. In this case, the single carrier DS-CDMA system is subject to a severe ISI. MC modulation, a technique to reduce the symbol rate, is then essential, where the carrier frequencies are chosen to be orthogonal to one another [8]. Combination of MC modulation techniques with DS-CDMA forms the MC-CDMA system. In multi-carrier CDMA systems, frequency diversity may be achieved by repeating the transmitted signal in the frequency domain with the aid of several sub-carriers to increase the capacity of the multicarrier CDMA systems. Additionally, it is also possible to use the spreading operation for multiple code transmissions to increase the data rate. As a result, a system operating with MC-CDMA technology can be flexibly changed from single-device transmission with high-data-rate transmission to multiple device transmission with a low data rate for each device. But all these achievements are obtained with the expense of increased system complexity.

1.6 OFDM Systems for Power Line Communications

Orthogonal frequency division multiplexing (OFDM) systems has been a major candidate for PLC systems [9]. OFDM performs better than single carrier in the presence of impulsive noise. OFDM spreads the effect of impulsive noise over multiple symbols due to discrete fourier transform operation in the receiver. The addition of cyclic prefix(CP) in OFDM symbols can mitigate the effect of multipath.

OFDM is based on parallel broadband data transmission which reduces the effects of multipath and leads to unnecessary equalization techniques. In the transmitter, the high speed data being transmitted are first coded, interleaved, and then mapped. The data are then converted into parallel data and transmitted in several channels. The transmitted data of each parallel sub channel are modulated by either phase shift keying (PSK) or quadrature amplitude modulation (QAM). The data are fed into an inverse first fourier transform (IFFT) circuit which generates OFDM signals. The signals are fed into a guard time insertion circuit to reduce ISI, which is connected to the power line channel. In the receiver, the guard time is removed, and the orthogonality of channels is maintained by using the FFT circuit. Since the data in the FFT circuit are parallel, parallel to serial conversion is performed by using coherent detection for which channel estimation is necessary. The estimates are necessary so that data can be demodulated correctly. Channel coding is also necessary to improve channel performance.

1.7 Merits of Multicarrier DS CDMA Technique

In comparison to the pure DS-CDMA using only time domain spreading and pure MC-CDMA using only frequency domain spreading, it has been demonstrated that the multi-carrier DS-CDMA has the highest flexibility and the highest number of degrees of freedom for reconfigurations [10]. With a multi-carrier modulation technique, the entire bandwidth of a multi-carrier direct sequence code-division multiple-access system (MC-DS-CDMA) system is subdivided into several narrow-band sub-channels operating at lower data rates. So, there is only flat fading, which has no inter-chip interference (ICI), in each subchannel if the number of sub-carriers is chosen properly. These properties render the MC DS-CDMA a versatile multiple access scheme that is suitable for cognitive and software-defined radios [10].

1.8 Motivation of this Thesis

Power line communication technology has emerged as a very attractive alternative for the provision of broadband communications services over medium and low-voltage power lines. The economic and operational viability of using this technology leans on the current availability of low cost PLC equipment, besides the utilization of the power network infrastructure already in place. For a PLC network, the available infrastructures are indoor and outdoor and the usable frequency band is narrowband and broadband. However, it is observed that a number of challenges exist as far as data transfer through this type of network [1]. Multicarrier DS CDMA has been considered to be an attractive technique in achieving high data-rate transmission. Therefore, this scheme has been analyzed and incorporated in PLC technology to evaluate its capabilities for applicability in different aspects. As the system performance is greatly influenced by the limiting factors like power line channel parameters, system parameters, interference, noise, fading, attenuation, multipath propagation, the evaluation in terms of BER performance is to be done at different extent of these effects.

In order to evaluate the above mentioned performance of the system, in this thesis, an analytical approach has been chosen for said work.

1.9 Review of Previous Works

Significant amount of investigations are reported already by different scholars to analyze the performance of PLC system by using various communication techniques [1-2],[9],[12],[14],[15-16],[20],[24],[26-27]. But in all the cases, the concentration was mainly on the effects of communication parameters, both the influence of power line network parameters and communication parameters together was not focussed. Some of the studies are briefly described in Section 2.7, Chapter 2.

1.10 Objectives of this Thesis Work

The objectives of this research are :

- a. To propose an analytical model of a PLC system with MC-DS CDMA and to carry out the performance analysis considering the combined effect of power line impulsive noise, channel transfer function and the effect of load impedance and the number of branches in a PLC network without and with path diversity using a rake receiver.
- b. To evaluate the BER performance results for different system parameters, channel parameters like line length, load impedance, number of branches, throughput, number of OFDM carriers, number of rake fingers etc.
- c. To determine the optimum values of system parameters like number of OFDM subcarriers, code length, number of rake fingers for a given system length and number of branches and load impedances at a given BER.

1.11 Organization of this Thesis Paper

The outline of this thesis paper is organized as follows :

Chapter 2: This chapter reviews the fundamental concept of power line communication channel with power line noise. For better understanding, it starts with the power line networks with one interconnection and its transfer function. It then discusses power line networks with one interconnection and one branch, power line with interconnection and a number of branches, power line network with distributed branches. Noise in a power line channel is also discussed here. Review of previous works on PLC is discussed.

Chapter 3: An analytical model of a PLC system with MC-DS-CDMA is proposed and analysis is carried out for the PLC link without and with diversity using a rake receiver. Analytical expression of received signal, MAI, Noise, SINR and BER has been developed without and with diversity using a rake receiver.

Chapter 4: This chapter presents the BER performance results obtained analytically for various system parameters and optimum system parameters are determined.

Chapter 5: It includes the conclusions and the scopes of future works on this subject.

CHAPTER-2

BACKGROUND AND RELATED WORKS

2.1 Introduction

With the increasing demand for broadband communications, the use of broadband power line communication has become more attractive mainly due to advantages such as the availability of power lines worldwide and the low cost of installation. However, as power lines are not specially designed for communication, a number of challenges exist as far as data transfer through this type of network is considered [1].

Power lines provide a harsh environment for higher frequency communication signal. The most influencing properties of this hostile medium in the performance of high speed communications are signal distortion due to frequency dependent cable losses, multipath propagation and noise [1]. Several techniques were adopted to model transfer characteristics of power line network. Considering the all drawbacks and difficulties of all models, transfer function of power line channel was developed that can ensure uniformity in obtained result. The derived model based on reflection and transmission factors, while taking into consideration of loads, distances, and interconnection nodes. In any given power line channel, the number of interconnected branches in the link between sending and receiving end, different terminal loads, and branch lengths cause multipath (due to transmission and reflection of signals between the transmission line segments) that are similar to wireless channels. This multipath causes degradation of the signals propagating in the link between the sending and receiving ends.

The power line noise has been analyzed using different models. The model suitable to analyze impulsive noise is the Middleton Class –A model [11]. The impulsive noise has a short duration with random occurrence and a high power spectral density (PSD). It may cause bit or burst errors in data transmission.

2.2 Power Line Networks with One Interconnection

2.2.1 Signal Propagation

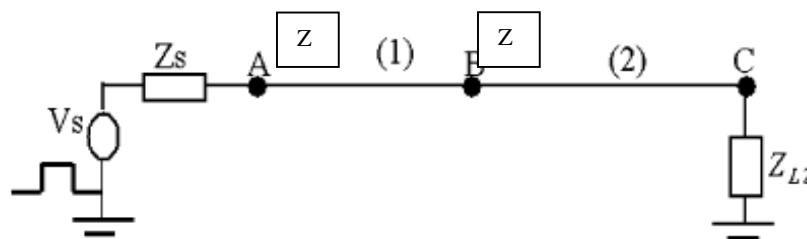


Fig. 2-1 Transmission line with one interconnection

Consider a transmission line shown in Fig. 2-1. V_s and Z_s are the source voltage and impedance, respectively[15], AB and BC are transmission lines with characteristics impedance Z_1 and Z_2 respectively while Z_{L2} is the load impedance. When the transmission line is excited with a pulse at point A, signal v^+ will propagate to B. The signal, which will propagate through the line, is given by $v^+ e^{-\gamma_1 l_1}$ where v^+ is a terminal voltage, γ_1 is the propagation constant, and l_1 is the arbitrary length that the signal travels toward B. The incident signal wave at point B is given by $v^+ e^{-\gamma_1 L_1}$, where L_1 is the length of transmission line 1. On reaching point B, two waves will be generated, the first being the reflected wave back to A and the second wave will travel toward C. The incidence wave at C will generate two waves, one will travel toward the load and another one is the reflected wave toward node B. Generally, in the first instant, there will be three waves traveling between nodes B and C. The first is the direct wave, the second is the wave reflected at node C, and the third is the wave reflected at B back to C. The reflections at all points will continue until all signals have been significantly attenuated. In addition, the wave reflected at node B from the initial pulse on reaching node A will be reflected back and initiate a similar trend. It is perceived that in transmission line 2, there will be three signals. The expression for the direct signal from transmission line 1 is given by Eq.(2.1), while the expression for the reflected signals at point B is given by Eq.(2.2). The reflected signal at point C is given by Eq.(2.3). Eq.(2.1) to Eq.(2.3) give the first signals transmitted from transmission line AB to BC and parameters $\beta_{21}, B_{21}, A_{21}$ and β_2 are given in Eq.(2.4) to Eq.(2.7), respectively. The parameters ρ_{21}, ρ_s and ρ_{12} are reflection factors from transmission line 2 to transmission line 1, that of the source and that of transmission line 1 to transmission line 2, respectively. T_{12} and T_{21} are transmission factors from transmission line 2 to transmission line 1 and vice-versa respectively. L_2 and l_2 are the length of transmission line 2 and arbitrary length that the signal has traveled respectively. The first transmitted signal (V_{21}) is given by Eq.(2.8). When the first signal is incident at point B, a reflected signal toward A will be generated with reflection coefficient ρ_{12} . On reaching point A, the signal will be reflected back with reflection coefficient ρ_s . The general trends are as expressed in Eq.(2.9). The parameter α_{21} and M are the reflection contribution in the source transmission line and reflection times respectively. The total incidence waves at point C are given by Eq.(2.10), where L is the total number of reflections at point C. The total received signal at load Z_{L2} is given by Eq.(2.11), where T_{L2} is the transmission factor to load Z_{L2}

$$V_{21ab} = (1 + \beta_{21})\beta_2 e^{-\gamma_2 l_2} \quad (2.1)$$

$$V_{21b} = \sum_{N=1}^L (1 + \beta_{21})\beta_2 \rho_{21}^N \rho_{L1}^N e^{-\gamma_2 (2NL_2 + l_2)} \quad (2.2)$$

$$V_{21c} = \sum_{N=1}^L (1 + \beta_{21})\beta_2 \rho_{21}^{N-1} \rho_{L1}^N e^{-\gamma_2 (2NL_2 - l_2)} \quad (2.3)$$

$$\beta_{21} = \frac{B_{21}}{1 - B_{21}} + \frac{B_{21}A_{21}}{1 - B_{21}A_{21}} + \frac{B_{21}A_{21}^2}{1 - B_{21}A_{21}^2} + \frac{B_{21}A_{21}^3}{1 - A_{21}B_{21}^3} + \dots \quad (2.4)$$

$$B_{21} = (e^{-\gamma_1 2L_1} T_{12} e^{-\gamma_2 2L_2}) \rho_{L2} T_{21} \rho_s \quad (2.5)$$

$$A_{21} = \rho_{L2} \rho_{21} e^{-\gamma_2 2L2} \quad (2.6)$$

$$\beta_2 = T_{12} e^{-\gamma_1 L_1} v^+ \quad (2.7)$$

$$V_{21} = V_{21ab} + V_{21b} + V_{21c} \quad (2.8)$$

$$\alpha_{21} = \rho_s^{M-1} \rho_{12}^{M-1} e^{-\gamma_1 (2(M-1)L_1)} \quad (2.9)$$

$$V_{Cincident} = \sum_{M=1}^L \alpha_{21} V_{21} \quad (2.10)$$

$$V_2 = \sum_{M=1}^L T_{L2} \alpha_{21} V_{21} \quad (2.11)$$

2.2.2 Power Line Transfer Function

The transfer function $H_2(f)$ is the ratio of the received signal at load Z_{L2} to the input signal at node A. The transfer function can be represented by Eq.(2.12) and Eq.(2.13). The parameter $H_{21}(f)$ is as given in Eq.(2.14), where H_{21a} , H_{21b} , H_{21c} and β_3 are given in Eq.(2.15)-Eq.(2.18) respectively. The parameters in Eq.(2.15)- Eq.(2.17) are in the frequency domain

$$H_2(f) = \frac{V_2}{v^+} \quad (2.12)$$

$$H_2(f) = \sum_{m=1}^L T_{L2} \alpha_{21} H_{21}(f) \quad (2.13)$$

$$H_{21}(f) = H_{21a} + H_{21b} + H_{21c} \quad (2.14)$$

$$H_{21a} = (1 + \beta_{21}) \beta_3 e^{-\gamma_2 l_2} \quad (2.15)$$

$$H_{21b} = \sum_{N=1}^L (1 + \beta_{21}) \beta_3 \rho_{21}^N \rho_{L1}^N e^{-\gamma_2 (2NL_2 + l_2)} \quad (2.16)$$

$$H_{21c} = \sum_{N=1}^L (1 + \beta_{21}) \beta_3 \rho_{21}^{N-1} \rho_{L1}^N e^{-\gamma_2 (2NL_2 - l_2)} \quad (2.17)$$

$$\beta_3 = T_{12} e^{-\gamma_1 L_1} \quad (2.18)$$

2.3 Power Line Networks with One Interconnection and One Branch

2.3.1 Signal Propagation

Fig. 2-2 shows a transmission line with one interconnections and a branch where,

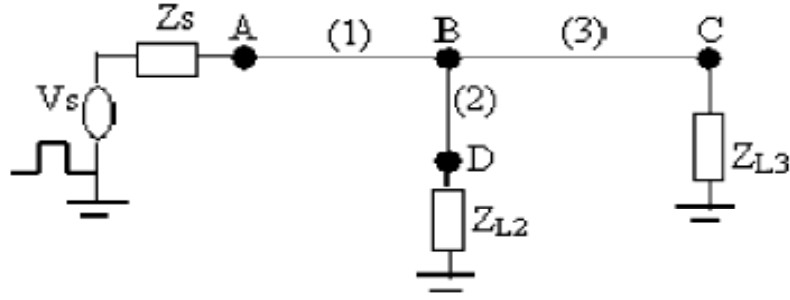


Fig. 2-2 Transmission line with one interconnection and one branch

L_1, L_2 and L_3 are the lengths of transmission lines and l_1, l_2 and l_3 are arbitrary distances the signal has travelled from node A to node B, node B to node D, and node B to node C respectively. Z_{L2} and Z_{L3} are the load impedances [15]. Assuming that the loads are not terminated in their characteristic impedances, the received signal at load 2 (Z_{L2}) is the contribution from transmission line 1 and transmission line 3. The signals at load 2 from transmission lines 1 (V_{21}) and 3 (V_{23}) can be represented by Eq.(2.19). The parameter α_{23} is shown in Eq.(2.20) where each parameter of transmission line 1 in Eq.(2.9) is replaced by that of transmission line 3. The other parameters are given in Eq.(2.21) – Eq.(2.28)

$$V_2 = \sum_{M=1}^L (\alpha_1 V_{21} + \alpha_{23} V_{23}) \quad (2.19)$$

$$\alpha_{23} = \rho_{L3}^{M-1} \rho_{32}^{M-1} e^{-\gamma_3(2(M-1)L_3)} \quad (2.20)$$

$$V_{23} = V_{23a} + V_{23b} + V_{23c} \quad (2.21)$$

$$V_{23a} = (1 + \beta_{23}) \beta_{132} e^{-\gamma_2 l_2} \quad (2.22)$$

$$V_{23b} = \sum_{N=1}^L (1 + \beta_{23}) \beta_{132} \rho_{23}^{N-1} \rho_{L1}^N e^{-\gamma_2(2NL_2 - l_2)} \quad (2.23)$$

$$V_{23c} = \sum_{N=1}^L (1 + \beta_{23}) \beta_{132} \rho_{23}^N \rho_{L1}^N e^{-\gamma_2(2NL_2 + l_2)} \quad (2.24)$$

$$\beta_{23} = \frac{B_{23}}{1 - B_{23}} + \frac{B_{23} A_{23}}{1 - B_{23} A_{23}} + \frac{B_{23} A_{23}^2}{1 - B_{23} A_{23}^2} + \frac{B_{23} A_{23}^3}{1 - A_{23} B_{23}^3} + \dots \quad (2.25)$$

$$\beta_{132} = T_{13} T_{23} \rho_{L3} e^{-\gamma_1 L_1} e^{-\gamma_3(2L_3) \nu_T} \quad (2.26)$$

$$B_{23} = \rho_{L3} \rho_{L2} T_{23} T_{32} e^{-\gamma_3(2L_3)} e^{-\gamma_1(2L_2)} \quad (2.27)$$

$$A_{23} = \rho_{L3} \rho_{23} e^{-\gamma_2(2L_2)} \quad (2.28)$$

2.3.2 Power Line Transfer Function

The transfer function at load 2 is given in Eq.(2.29). The parameter $H_{23}(f)$ is as shown in Eq.(2.30) where $H_{23a}, H_{23b}, H_{23c}$ and β_{133} are given in Eq.(2.31) – Eq.(2.34). The parameters in Eq.(2.31) – Eq.(2.33) are in frequency domains

$$H_2(f) = \sum_{M=1}^L (\alpha_{21} H_{21}(f) + \alpha_{23} H_{23}(f)) \quad (2.29)$$

$$H_{23}(f) = H_{23a} + H_{23b} + H_{23c} \quad (2.30)$$

$$H_{23a} = (1 + \beta_{23}) \beta_{133} e^{-\gamma_2 l_2} \quad (2.31)$$

$$H_{23b} = \sum_{N=1}^L (1 + \beta_{23}) \beta_{133} \rho_{21}^{N-1} \rho_{L1}^N e^{-\gamma_2 (2NL_2 - l_2)} \quad (2.32)$$

$$H_{23c} = \sum_{N=1}^L (1 + \beta_{23}) \beta_{133} \rho_{21}^N \rho_{L1}^N e^{-\gamma_2 (2NL_2 + l_2)} \quad (2.33)$$

$$\beta_{133} = T_{13} T_{23} \rho_{L3} e^{-\gamma_1 L_4} e^{-\gamma_3 (2L_3)} \quad (2.34)$$

$$\alpha_{23} = \rho_{L2}^{M-1} \rho_{23}^{M-1} e^{-\gamma_2 (2(M-1)L_2)} \quad (2.35)$$

2.4 Power Line with Interconnection and a Number of Branches

Consider a power line network with a number of branches connected at the same node as shown in Fig. 2-3 [15]. For an arbitrary number of branches, the signal along transmission line 1 to the receiver

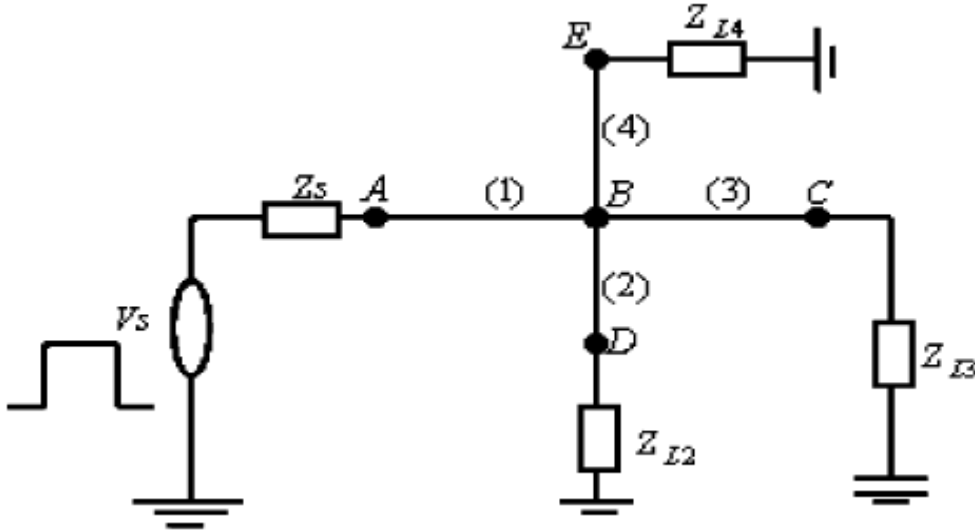


Fig.2-3 Power line with two branches at the same node

can be represented by Eq.(2.36) where N_T is the total number of transmission lines connected at node B and $n=1$ is the transmission line with the source signal. T_{Ln} is the load transmission factor, α_{mn} and $H_{mn}(f)$ are given in Eq.(2.37) and Eq.(2.38), respectively while H_{mna}, H_{mnb} and H_{mnc} are given in Eq.(2.39) – Eq.(2.41) respectively. In the general equations, m means the reference load where the transfer function is referred to. For example if the reference is load 3 then m will be to 3 and n is the transmission line which contributes signals to the referenced load. For example, in Fig. 2-4, if the reference is load 3,

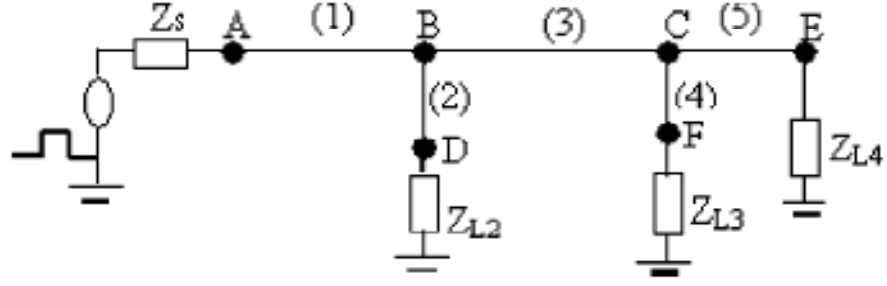


Fig. 2-4 Transmission line with one interconnections and branches

Then $n=1,2$ and 4 . β_{1nm} in Eq.(2.42) represents the contribution of the signal in either the source or loads while β_{mn} is as in Eq.(2.43). The parameters B_{mn}, A_{mn} and P_{Ln} are as in Eq.(2.44) – Eq.(2.46), respectively

$$H_m(f) = \sum_{M=1}^L \sum_{n=1}^{N_T} T_{Ln} \alpha_{mn} H_{mn}(f) \quad (2.36)$$

$$\alpha_{mn} = P_{Ln}^{M-1} \rho_{nm}^{M-1} e^{-\gamma_n(2(M-1)L_n)} \quad (2.37)$$

$$H_{mn}(f) = H_{mna} + H_{mnb} + H_{mnc} \quad (2.38)$$

$$H_{mna} = (1 + \beta_{mn}) \beta_{1nm} e^{-\gamma_n l_m} \quad (2.39)$$

$$H_{mnb} = \sum_{N=1}^L (1 + \beta_{mn}) \beta_{1nm} \rho_{mn}^{N-1} \rho_{Ln}^N \times e^{-\gamma_m(2NL_m - l_m)} \quad (2.40)$$

$$H_{mnc} = \sum_{N=1}^L (1 + \beta_{mn}) \beta_{1nm} \rho_{mn}^N \rho_{Ln}^N \times e^{-\gamma_m(2NL_m + l_m)} \quad (2.41)$$

$$\beta_{1nm} = \begin{cases} T_{nm} e^{-\gamma_n l_n} & n=1(\text{source}) \\ T_{1n} T_{nm} P_{Ln} \times e^{-\gamma_n l_n} e^{-\gamma_n(2L_n)} & \text{otherwise} \end{cases} \quad (2.42)$$

$$\beta_{mn} = \frac{B_{mn}}{1 - B_{mn}} + \frac{B_{mn} A_{mn}}{1 - B_{mn} A_{mn}} + \frac{B_{mn} A_{mn}^2}{1 - B_{mn} A_{mn}^2} \dots \quad (2.43)$$

$$B_{mn} = \rho_{Ln} P_{Ln} T_{nm} T_{nm} e^{-\gamma_n(2L_n)} e^{-\gamma_m(2L_m)} \quad (2.44)$$

$$A_{mn} = \rho_{Ln} \rho_{mn} e^{-\gamma_m(2L_m)} \quad (2.45)$$

$$P_{Ln} = \begin{cases} \rho_S & n=1(\text{source}) \\ \rho_{Ln} & \text{otherwise} \end{cases} \quad (2.46)$$

2.5 Power Line Network with Distributed Branches

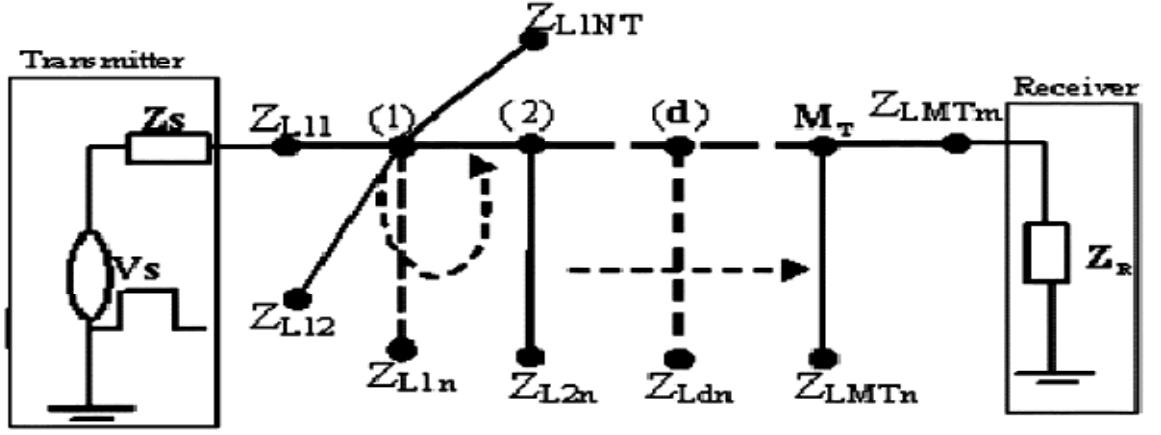


Fig. 2-5 Power Line network with distributed branches

In Fig. 2-5 the branches are either concentrated at a given node or distributed in the link between the transmitting on and receiving end [15]. The transfer function of this network is given by Eq.(2.47).

$$H_{mM_T}(f) = \prod_{d=1}^{M_T} \sum_{M=1}^L \sum_{n=1}^{N_T} T_{Lmd} \alpha_{mnd} H_{mnd}(f) \quad (2.47)$$

$$\alpha_{mnd} = P_{Lnd}^{M-1} \rho_{nmd}^{M-1} e^{-\gamma_{nd}(2(M-1)l_{nd})} \quad (2.48)$$

$$P_{Lnd} = \begin{cases} \rho_s & d=n=1(\text{source}) \\ \rho_{Lnd} & \text{otherwise} \end{cases} \quad (2.49)$$

In Eq.(2.47), N_T is the total number of branches connected, say at node “1” and terminated in any arbitrary load. $n, m, M, H_{mnd}(f)$ and T_{Lmd} represent any branch number, any referenced (terminated) load, number of reflections (with total L number of reflections), transfer function between line n to a referenced load m at the referred load d , and the transmission factor at the referenced load m at referred node d , respectively. With these, the signal contribution factor α_{mnd} is given by Eq.(2.48), where ρ_{nmd} is the reflection factor at node “d” between line n to the referenced load m , γ_{nd} is the propagation constant of line n that has line length l . All terminal reflection factors P_{Lnd} , in general, are given by Eq.(2.49), except at the source where $\rho_{L11} = \rho_s$ is the source reflection factor.

Considering,

$m =$ Reference load (3)
 $n =$ Number of branches (1,2,4)

$$\rho_s = \frac{Z_s - Z_1}{Z_s + Z_1} \quad (2.50)$$

$$\text{For, } \rho_{nm}, \quad \rho_{12} = \frac{Z_2 \parallel Z_3 - Z_1}{Z_2 \parallel Z_3 + Z_1} \quad \text{and} \quad \rho_{21} = \frac{Z_1 \parallel Z_3 - Z_2}{Z_1 \parallel Z_3 + Z_2} \quad (2.51)$$

$$\text{For, } \rho_{Ln}, \quad \rho_{L2} = \frac{Z_L - Z_2}{Z_L + Z_2} \quad (2.52)$$

$$\gamma = \alpha + j\beta = \sqrt{(R + j\omega L)(G + j\omega C)} \quad (2.53)$$

$$H_{mn}(f) = H_{mna} + H_{mnb} + H_{mnc} \quad (2.54)$$

$$H_{mna} = (1 + \beta_{mn})\beta_{1nm} e^{-\gamma_m l_m} \quad (2.55)$$

$$\beta_{mn} = \frac{B_{mn}}{1 - B_{mn}} + \frac{B_{mn} A_{mn}}{1 - B_{mn} A_{mn}} + \frac{B_{mn} A_{mn}^2}{1 - B_{mn} A_{mn}^2} \dots \quad (2.56)$$

$$B_{mn} = \rho_{Lm} \rho_{Ln} T_{mn} T_{nm} e^{-\gamma_n (2L_n)} e^{-\gamma_m (2L_m)} \quad (2.57)$$

$$A_{mn} = \rho_{Lm} \rho_{mn} e^{-\gamma_n (2L_m)} \quad (2.58)$$

$$\beta_{1nm} = \begin{cases} T_{nm} e^{-\gamma_n L_n} & n=1(\text{source}) \\ T_{1n} T_{mn} \rho_{Ln} * e^{-\gamma_1 L_1} e^{-\lambda_n (2L_n)} & \text{otherwise} \end{cases} \quad (2.59)$$

$$H_{mnb} = \sum_{N=1}^L (1 + \beta_{mn}) \beta_{1nm} \rho_{mn}^{N-1} \rho_{Lm}^N * e^{-\gamma_m (2NL_m - l_m)} \quad (2.60)$$

$$H_{mnc} = \sum_{N=1}^L (1 + \beta_{mn}) \beta_{1nm} \rho_{mn}^N \rho_{Lm}^N * e^{-\lambda_2 (2NL_m + l_m)} \quad (2.61)$$

$$T_{Lm} = 1 + \rho_{Lm} \quad (2.62)$$

$$\rho_{Lm} = \frac{Z_L - Z_m}{Z_L + Z_m} \quad (2.63)$$

2.6 Noise in a Power Line Channel

The power line channel suffers impulsive noise interference that is generated from connected electrical appliances. Middleton class A noise model is one of the appropriate models for impulsive noise environment [11]. Based on the model, the combination of impulsive plus background noise is a sequence of iid complex random variables with the probability density function of class A noise is given by,

$$P_z(z) = \sum_{m=0}^{\alpha} \frac{\alpha_m}{2\pi\sigma_m^2} \exp\left(-\frac{z^2}{2\sigma_m^2}\right) \quad (2.64)$$

where, m is the number of impulsive noise sources and is characterized by poisson distribution with mean parameter A called the impulsive index (which is the product of the average rate of impulsive noise and the mean duration of typical impulse)

$$\alpha_m = e^{-A} \frac{A^m}{m!} \quad (2.65)$$

$$\sigma_m^2 = (\sigma_g^2 + \sigma_i^2) \frac{\left(\frac{m}{A}\right) + \Gamma}{1 + \Gamma} \quad \text{and} \quad \Gamma = \frac{\sigma_g^2}{\sigma_i^2} \quad (2.66)$$

$$\sigma_m^2 = \left(1 + \frac{1}{\Gamma}\right) \left(\frac{(m/A) + \Gamma}{1 + \Gamma}\right) \sigma_g^2 \quad (2.67)$$

where, σ_g^2 and σ_i^2 are the power of background noise and impulsive noise respectively. For small A, we get highly structured impulsive noise where as for large values of A, the noise PDF becomes Gaussian. The parameter Γ (GIR- Gauss Impulsive power ratio) is called background – to – Impulsive noise ratio. Eq. (2.64) shows that the PDF of noise is a weighted sum of Gaussian PDF's with zero mean, therefore has a mean of $\mu_z=0$ and a variance of

$$\sigma_z^2 = E\{z^2\} = \sum_{m=0}^{\alpha} \alpha_m \cdot \frac{1}{2\pi\sigma_m^2} \int z^2 \cdot \exp\left(-\frac{z^2}{2\sigma_m^2}\right) \quad (2.68)$$

$$= \frac{e^{-A} \sigma_g^2}{\Gamma} \sum_{m=0}^1 \frac{A^m}{\Gamma m} \left(\frac{m}{A} + \Gamma\right) = (\sigma_g^2 + \sigma_i^2) \quad (2.69)$$

Colored background noise is caused by the superimposition of numerous noise sources, e.g, computers, dimmers or hair dryers, which can create disturbances in the frequency range 0-100 MHz. A commonly accepted model is the simple three-parameter model where the noise is considered non white Gaussian with the power spectral density (PSD).

$$R_{nb}(f) = a + b|f|^c \left[\frac{dBm}{Hz} \right] \quad (2.70)$$

where a, b and c are parameters derived from measurements and f is the frequency in MHz. By setting the parameters $[a,b,c] = [-145, 53.23, -0.337]$, a worst case is obtained while with the parameters $[a,b,c] = [-140, 38.75, -0.72]$, a best case is obtained. The resulting PSDs are depicted in Fig. 2-6, where the considered frequency band is between 1 MHz and 100 MHz [12]. σ_g^2 is the power of background noise which can be given as $\sigma_g^2 = \text{Trapz}(R_{nb-w}) \times \Delta f$.

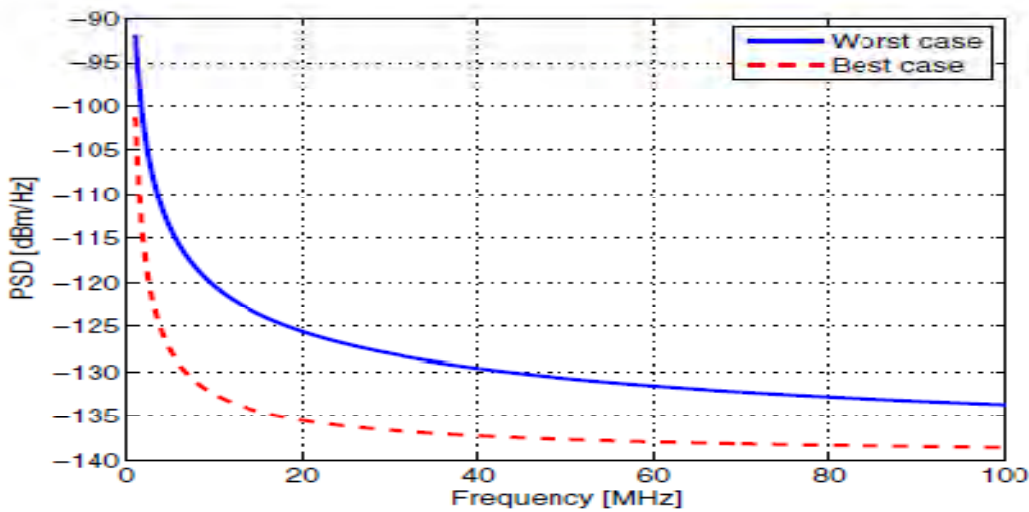


Fig. 2-6 Bad and good background noise PSD

2.7 Related Works

Significant amount of investigations are reported already by different scholars to analyze the performance of PLC system by using various communication techniques [1-2],[9],[12],[14],[15-16],[20],[24],[26-27]. But in all the cases, the concentration was mainly on the effects of communication parameters, both the influence of power line network parameters and communication parameters together was not focussed. Some of the studies are briefly described below :

- Ma. Y. H., P. L. So and Gunawan. E. [1] present a comparison between CDMA and OFDM systems for power line communications. The BER performance and the optimum overall data rate of the CDMA and OFDM systems are analyzed and compared, using the criteria of the same bandwidth occupation, the same transmission power for each user, the same total number of users in the system and the same power line channel. In both the cases, the effect of power line network parameters are not considered.
- Anatory J., Nelson T., Rajeev T. [2] investigate the performance of indoor channels of a PLC system that uses OFDM techniques. They also discuss various situations like addition of new branches, terminal impedances that degrade the overall performance of the system and sought possible solutions to overcome such degradations.
- Ma. Y. H., P. L. So and Gunawan. E. [9] theoretically analyze the BER performance of the OFDM system for PLC under the impulsive noise and multipath effects in terms of closed form formulas. They also determine optimum guard interval to achieve the best BER performance.
- Di Bert L., Caldera P., David S., and Tonello A. M [12] reviews existing noise models including both background and impulsive noise for the PLC scenario.
- Khalifa S. A. M., Fawaz S. A.Q and Zahir M. H. [14] shows the effect of impulsive noise in adaptive power loading in OFDM-based PLC systems. They also present a simple power loading algorithm with uniform bit allocation and non uniform BER distribution in a widely accepted power line channel impaired by impulsive noise.
- Anatory J., Kissaka M M., and Mvungi N H. [15] present a novel approach to model the transfer function of a power line network. The channel frequency response of a power line channel with interconnections are derived considering different loading at different branches. However the effect of transfer function on link performance is not reported.
- Anatory J., Nelson T., Rajeev T., Kissaka M M., and Mvungi N H. [16] present analytically the effects of load impedance, line length and branches on the performance of PLC network. The observations presented in the paper could be helpful in the suitable design of the PLC systems for a better data transfer and system performance.
- Saimoon Ara Amin, Mahbulul Alam Rafel and S.P Majumder [20] present performance analysis of multicarrier DS-CDMA wireless communication system.
- S.D. Paul, S. Asif and S. P. Majumder [24] present performance analysis of a MC-DS-CDMA wireless communication system with RAKE receiver over a rayleigh fading channel with receiver diversity.

- Kazi Abu Taher, Md Ruhul Minhaz and S. P. Majumder [26] present performance analysis of multicarrier direct sequence (MC DS) CDMA with fading.
- Yong-tao Ma, Kai-hua Liu, Zhi-jun Zhang, Jie-xiao Yu, Xiao-lin Gong [27] have derived the model for colored background noise of PLC channel based on artificial neural network and evaluate the performance of a PLC system with colored noise.

CHAPTER – 3

ANALYTICAL MODEL OF POWER LINE COMMUNICATION (PLC) SYSTEM WITH MULTICARRIER DS-CDMA

3.1 Introduction

In this chapter, a model of a power line communication system (PLC) with multicarrier DS-CDMA is presented which includes different number of branches, different types of devices and loads. Analysis is carried out for a power line communication link considering the transfer function of the power line with different number of branches, load impedances, line length and device characteristics. Analysis is done to find out the expression of the signal at the output of the power line at the receiving end along with the channel noise. The analytical approach has been carried out for determining the expression of MAI and power line noise. The expression for signal to interference and noise (SINR) ratio and the expression of BER is developed without diversity and with diversity using a rake receiver. The performance results are evaluated in terms of output signal spectrum and BER performance for several system parameters and power line parameters.

3.2 Power Line Channel Model

The generalized channel model described in section 2.5, chapter-2 is considered here for a power line network.

3.3 Power Line Noise Model

The generalized noise model described in section 2.6, chapter-2 is considered here for a power line noise model.

3.4 Functional Block Diagram of PLC system with MC DS-CDMA

The functional block diagram of a power line communication system with MC DS-CDMA is shown in Fig. 3-1. It includes S/P converter, transmitter, power line channel, receiver and P/S converter.

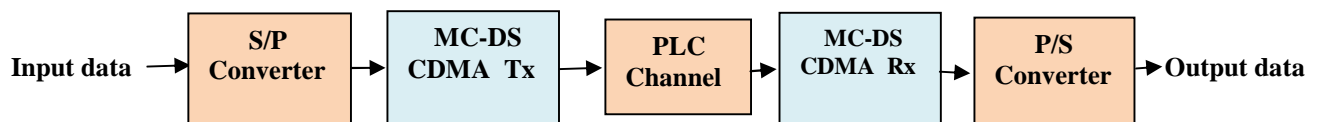


Fig. 3-1 Functional block diagram of PLC System with MC-DS CDMA

3.4.1 Transmitter Model

Block diagram of a DS-CDMA with multicarrier OFDM transmitter is shown in Fig. 3-2(a). In the transmitter, the high-speed data are converted into parallel data stream and are OFDM modulated. The output of OFDM modulator is fed to PLC channel after RF amplification.

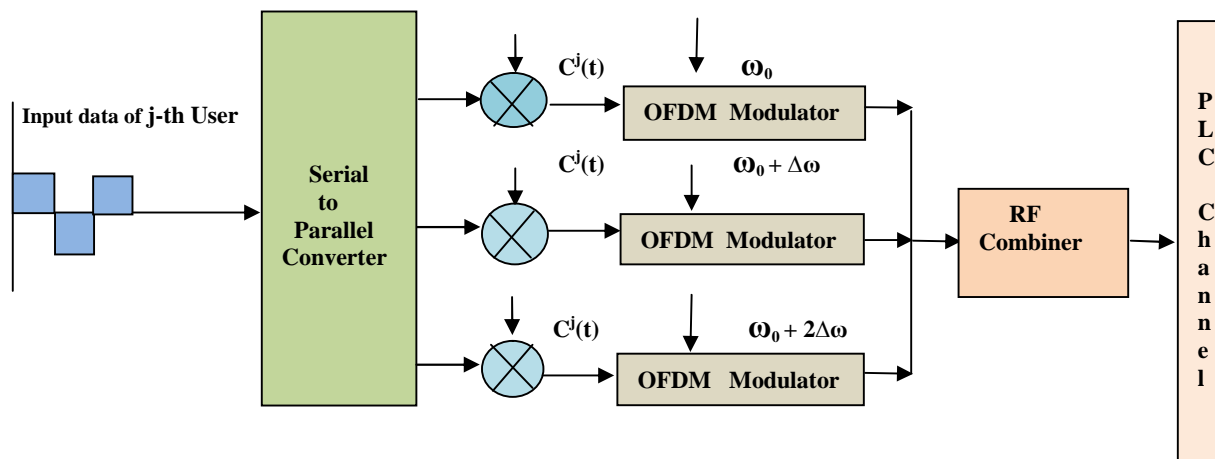


Fig. 3-2(a) Block diagram of MC DS-CDMA transmitter

3.4.2 OFDM Modulator Model

The OFDM modulator model is shown in Fig. 3-2(b). It includes modulator circuit, inverse first fourier transform (IFFT) circuit, combiner and arrangements for adding cyclic prefix. The transmitted data of each parallel subchannel are modulated and fed into an IFFT circuit which generates OFDM signals. All parallel data are then combined and fed into a cyclic prefix addition circuit which is connected to the PLC channel through RF amplification.

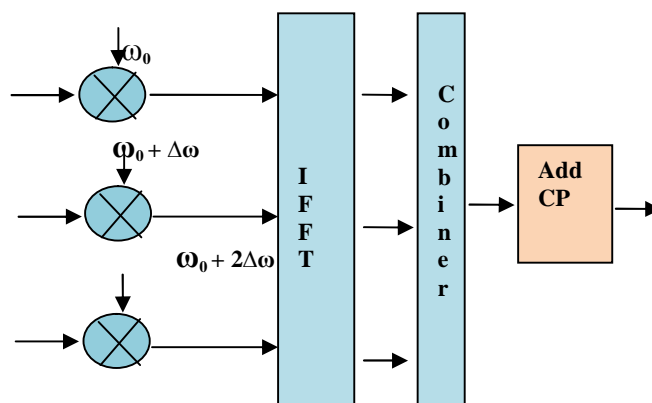


Fig. 3-2(b) Block diagram of OFDM Modulator Model

3.4.3 Receiver Model

Block diagram of MC DS-CDMA receiver is shown in Fig. 3-3(a). The received signal is first

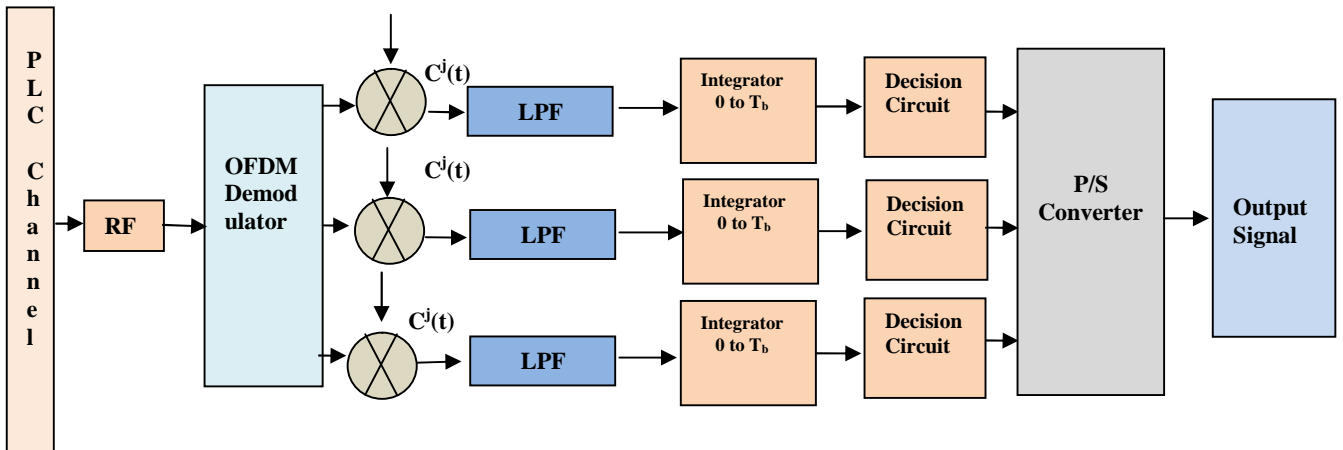


Fig. 3-3(a) Block diagram of MC DS-CDMA receiver

amplified by RF amplification and passed to a coherent OFDM demodulator. Output of OFDM demodulator is passed to the decoder blocks. Decoding is carried out using a locally generated code sequence. To be able to perform the despreading operation, the receiver must not only know the code sequence used to spread the signal, but the codes of the received signal and the locally generated code must also be synchronized. The decoded outputs are passed through integrator and passed to data decision circuit. The output of the decision circuit is then converted to serial data.

3.4.4 OFDM Demodulator Model

The block diagram of OFDM demodulator model is shown in Fig. 3-3(b). In the receiver, CP is removed and the orthogonality of channels is maintained by using the FFT circuit. Since the data in

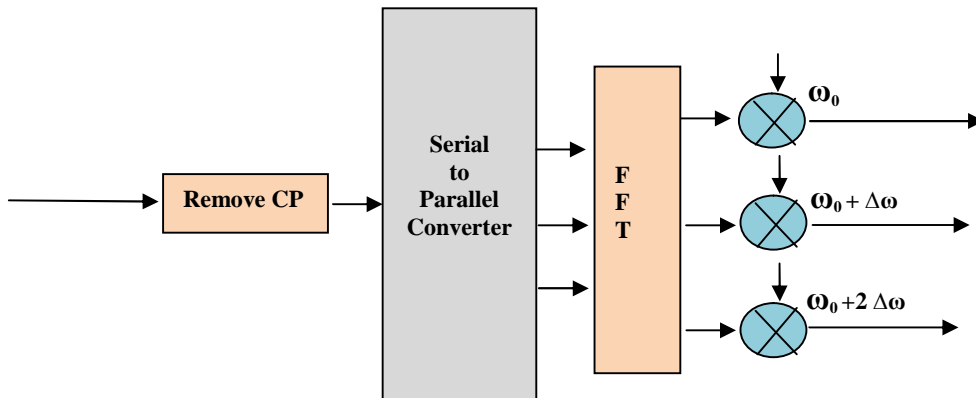


Fig. 3-3(b) Block diagram of OFDM Demodulator Model

the FFT circuit are parallel , parallel-to-serial conversion is performed by using coherent detection.

3.5 System Analysis Without Diversity

3.5.1 Transmitted Signal

Let us consider an MC DS-CDMA system, the block diagram of MC DS-CDMA is shown in the Fig. 3-1. Let for any period of time, there are J number of users and j is the reference user. Now to have a system model, let us make following assumptions :

- a. All the users are active at any time
- b. All the user's transmitter power levels are equal
- c. The bit rate is much larger than chip rate

Now, let us consider the following terms for this system :

- J = Total no of user
- P = Chip power of each user
- N_c = Number of sub-carriers
- N = Number of chip of the code for each sub-carrier channel
- L = Code length of each user
- C^j = Code of j-th user
- R_b = Bit-rate
- $m_j(t)$ = Input data stream of the j-th user
- b_n^j = n-th bit of $m_j(t)$

Thus,

$$m_j(t) = \sum_{n=-\infty}^{\infty} b_n^j \quad ; \text{ where } b = \pm 1$$

Now, the input data of the j-th user are converted into N_c parallel data streams and each of the parallel data is coded by the code of the j-th user. Thus each data bit is spreaded in time domain and then modulated by the respective subcarrier. To write the general expression of the subcarriers, let us consider the following :

ω_0 = Frequency of the reference channel

$\Delta\omega$ = Frequency spacing between two subcarrier channel

So, the general expression of a subcarrier is :

$$\sqrt{2P} \cos(\omega_0 t + k\Delta\omega)$$

(3.1)

Thus, the expression of the transmitted signal of the j-th user is as follows :

$$S_T(t) = \sum_{k=1}^{N_c} \left\{ \sqrt{2P} b_{n,k}^j \left(\sum_{i=1}^{G_p} C_i^j \times P(t - it_c) \right) \cos(\omega_0 t + k\Delta\omega) \right\} \quad (3.2)$$

Here,

$b_{n,k}^j = n$ -th bit of the j -th user, which is being modulated by the k -th subchannel.

$C_i^j = i$ -th chip of the j -th user's code.

3.5.2 Receiver Output

While reception, the receiver of the j -th user receives signals transmitted by all the J number of users [20],[24],[26]. Thus, the expression of the received signal is :

$$r(t) = \sum_{j=1}^J \left[\sqrt{2P} \sum_{k=1}^{N_c} \left\{ b_{n,k}^j \left(\sum_{i=1}^{G_p} C_i^j * P(t-it_c) \cos(\omega_0 t + k\Delta\omega t) \right) \right\} \otimes h_{ch}(t) \right] + \sum_{k=1}^{N_c} n(t) \quad (3.3)$$

where, $h_{ch}(t)$ is the impulse response of the PLC channel, \otimes denotes convolution and $n(t)$ is the channel noise.

The signal while propagating through power line channel, suffers frequency-selective multipath fading. To account the fading, consider that α be the instantaneous amplitude fading.

$$r(t) = \sum_{j=1}^J \left[\alpha \sqrt{2P} \sum_{k=1}^{N_c} \left\{ b_{n,k}^j \left(\sum_{i=1}^{G_p} C_i^j * g(t-it_c) \cos(\omega_0 t + k\Delta\omega t) \right) \right\} \right] + \sum_{k=1}^{N_c} n(t) \quad (3.4)$$

Where,

$$g(t) = P(t) \otimes h_{ch}(t)$$

$$G(f) = P(f) \cdot H_{ch}(f)$$

$$G(f_k) = P(f_k) \cdot H(f_k)$$

This signal is then coherently demodulated by the respective carriers and the output $y(t)$ can be represented as:

$$y(t) = \sum_{j=1}^J \alpha \sqrt{2P} \sum_{k=1}^{N_c} \left\{ b_{n,k}^j \sum_{i=1}^{G_p} C_i^j * g(t-it_c) \cos(\omega_0 t + k\Delta\omega t) * \cos(\omega_0 t + k\Delta\omega t) \right\} + \sum_{k=1}^{N_c} n(t) * \cos(\omega_0 t + k\Delta\omega t) \quad (3.5)$$

$$= \sum_{j=1}^J \alpha \sqrt{2P} \sum_{k=1}^{N_c} \left\{ b_{n,k}^j \sum_{i=1}^{G_p} C_i^j * g(t-it_c) \cos^2(\omega_0 t + k\Delta\omega t) \right\} + \sum_{k=1}^{N_c} n(t) * \cos(\omega_0 t + k\Delta\omega t) \quad (3.6)$$

$$= \sum_{j=1}^J \alpha \sqrt{2P} \sum_{k=1}^{N_c} \left\{ b_{n,k}^j \sum_{i=1}^{G_p} C_i^j * g(t-it_c) \cdot \frac{1}{2} (1 + \cos(2\omega_0 t + 2k\Delta\omega t)) \right\} + \sum_{k=1}^{N_c} n(t) * \cos(\omega_0 t + k\Delta\omega t) \quad (3.7)$$

$$= \sum_{j=1}^J \alpha \sqrt{2P} \sum_{k=1}^{N_c} \left\{ b_{n,k}^j \sum_{i=1}^{G_p} C_i^j * g(t-it_c) (1 + \cos(2\omega_0 t + 2k\Delta\omega t)) \right\} + \sum_{k=1}^{N_c} n(t) * \cos(\omega_0 t + k\Delta\omega t) \quad (3.8)$$

It is then decoded and the output of the correlator is given by :

$$y(t) = \sum_{j=1}^J \alpha \sqrt{2P} \sum_{k=1}^{N_c} \left\{ b_{n,k}^j \left[\sum_{i=1}^{G_p} C_i^j * g(t-it_c) * \sum_{i=1}^{G_p} C_i^1 P(t-it_c) \right] (1 + \cos(2\omega_0 t + 2k\Delta\omega t)) \right\} + \sum_{k=1}^{N_c} n(t) \sum_{i=1}^{G_p} C_i^j P(t-it_c) \cos(\omega_0 t + k\Delta\omega t) \quad (3.9)$$

$$y(t) = \sum_{j=1}^J \alpha \sqrt{2P} \sum_{k=1}^{N_c} b_{n,k}^j \left\{ \sum_{i=1}^{G_p} C_i^j g(t-it_c) * \sum_{i=1}^{G_p} C_i^1 P(t-it_c) \right\} + \sum_{j=1}^J \alpha \sqrt{2P} \sum_{k=1}^{N_c} b_{n,k}^j \left\{ \sum_{i=1}^{G_p} C_i^j g(t-it_c) * \sum_{i=1}^{G_p} C_i^1 P(t-it_c) * \cos(2\omega_0 t + 2k\Delta\omega t) \right\} + \sum_{k=1}^{N_c} n(t) \sum_{i=1}^{G_p} C_i^j P(t-it_c) \cos(\omega_0 t + k\Delta\omega t) \quad (3.10)$$

After passing through low pass filter (LPF), the output of the LPF is given by :

$$y_0(t) = \alpha \sqrt{2P} \sum_{k=1}^{N_c} \left[b_{n,k}^j \sum_{i=1}^{G_p} C_i^1 g(t-it_c) * \sum_{i=1}^{G_p} C_i^1 P(t-it_c) \right] + \sum_{j=2}^J \alpha \sqrt{2P} \sum_{k=1}^{N_c} \left[b_{n,k}^j \left\{ \sum_{i=1}^{G_p} C_i^1 g(t-it_c) * \sum_{i=1}^{G_p} C_i^j P(t-it_c) \right\} \right] + \sum_{k=1}^{N_c} n(t) \sum_{i=1}^{G_p} C_i^j P(t-it_c) \cos(\omega_0 t + k\Delta\omega t) \quad (3.11)$$

$$y_0(t) = \alpha \sqrt{2P} \sum_{k=1}^{N_c} \left[b_{n,k}^j \sum_{i=1}^{G_p} C_i^1 g(t-it_c) * \sum_{i=1}^{G_p} C_i^1 P(t-it_c) \right] + \sum_{j=2}^J \alpha \sqrt{2P} \sum_{k=1}^{N_c} \left[b_{n,k}^j \left\{ \sum_{i=1}^{G_p} C_i^1 g(t-it_c) * \sum_{i=1}^{G_p} C_i^j P(t-it_c) \right\} \right] \quad [i \neq j, j=2] + \sum_{k=1}^{N_c} n(t) \sum_{i=1}^{G_p} C_i^j P(t-it_c) \cos(\omega_0 t + k\Delta\omega t) \quad (3.12)$$

Now, after integrating over 0 to T_b , we get the following,

$$y_0(t) = \alpha \sqrt{2P} \sum_{k=1}^{N_c} \left[b_{n,k}^1 \frac{1}{T_b} \int_0^{T_b} \sum_{i=1}^{G_p} g(t-it_c) * \sum_{i=1}^{G_p} P(t-it_c) dt \right] \quad [C_i^1 \times C_i^1 = 1] + \sum_{j=2}^J \alpha \sqrt{2P} \sum_{k=1}^{N_c} \left[b_{n,k}^j \frac{1}{T_b} \int_0^{T_b} \left\{ \sum_{i=1}^{G_p} C_i^1 g(t-it_c) * \sum_{i=1}^{G_p} C_i^j P(t-it_c) dt \right\} \right] + \frac{1}{T_b} \int_0^{T_b} \sum_{k=1}^{N_c} n(t) \sum_{i=1}^{G_p} C_i^j P(t-it_c) \cos(\omega_0 t + k\Delta\omega t) dt \quad (3.13)$$

$$y_0(t) = y_j(t) + y_{MAI} + n(t) \quad (3.14)$$

Here, $y_j(t)$ = Desired signal of j-th user

y_{MAI} = Multiple access interference

$n(t)$ = Noise

3.5.3 Desired Signal of Receiver

$$\begin{aligned} y_j(t) &= \alpha \sqrt{2P} \sum_{k=1}^{N_c} \left[b_{n,k}^1 \frac{1}{T_b} \int_0^{T_b} \sum_{i=1}^{G_p} g(t - it_c) * \sum_{i=1}^{G_p} P(t - it_c) dt \right] \\ &= \alpha \sqrt{2P} N_c [\mu_{11}] \end{aligned} \quad (3.15)$$

where,

$$\mu_{11} = \frac{1}{T_b} \int_0^{T_b} \sum_{i=1}^{G_p} g(t - it_c) * P(t - it_c) dt \quad \text{and} \quad N_c = \sum_{k=1}^{N_c} b_n^j$$

Thus, for the j-th user, the desired signal power, P_s is given as :

$$P_s = \alpha^2 2P N_c^2 \times (\mu_{11})^2 \quad (3.16)$$

3.5.4 Multiple Access Interference (MAI)

The multiple access interference term of Eq (3.13) can be represented as :

$$\begin{aligned} y_{MAI}(t) &= \sum_{j=2}^J \alpha \sqrt{2P} \sum_{k=1}^{N_c} \left[b_{n,k}^j \frac{1}{T_b} \int_0^{T_b} \left\{ \sum_{i=1}^{G_p} C_i^1 g(t - it_c) * \sum_{i=1}^{G_p} C_i^j P(t - it_c) dt \right\} \right] \\ &= (J - 1) \alpha \sqrt{2P} N_c \times \frac{1}{G_p} \sum_{j=2}^J \mu_{ij} \end{aligned} \quad (3.17)$$

where,

$$\mu_{ij} = \frac{1}{T_b} \int_0^{T_b} \left\{ \sum_{i=1}^{G_p} C_i^1 g(t - it_c) * \sum_{i=1}^{G_p} C_i^j P(t - it_c) dt \right\} \quad \text{and} \quad N_c = \sum_{k=1}^{N_c} b_n^j$$

So the interference power is given as,

$$P_{MAI} = \frac{(J - 1) \alpha^2 2P N_c^2 \times |\mu_{ij}|^2}{G_p} \quad (3.18)$$

3.5.5 Noise

The noise at the output of integrator is given by :

$$n(t) = \frac{1}{T_b} \int_0^{T_b} \sum_{k=1}^{N_c} n(t) \sum_{i=1}^{G_p} C_i^j P(t - it_c) \cos(\omega_0 t + k\Delta\omega t) dt \quad (3.19)$$

Here the noise is power line noise and the variance of the noise is given (section 2.6, chapter-2) as,

$$\sigma_n^2 = \sigma_g^2 + \sigma_i^2 \quad (3.20)$$

$$\sigma_n^2 = (\sigma_g^2 + \sigma_i^2) \frac{\left(\frac{m}{A}\right) + \Gamma}{1 + \Gamma} \quad (3.21)$$

where,

$$\Gamma = \frac{\sigma_g^2}{\sigma_i^2} ; N_m = \frac{\sigma_n^2}{R_b}$$

σ_g^2 and σ_i^2 represents the Gaussian and Impulsive noise variance respectively. Γ represent Gauss Impulsive power ratio and R_b is bit rate.

3.5.6 Signal to Interference and Noise Ratio (SINR)

The ratio of signal power to MAI and noise power can be expressed as:

$$\begin{aligned} SINR(\xi) &= \frac{P_s}{P_{MAI} + \sigma_n^2} \\ &= \frac{\alpha^2 2PN_c^2 \times (\mu_{11})^2}{(J-1)\alpha^2 2PN_c^2 \times |\mu_{ij}|^2 \times \frac{1}{G_p} + \sigma_n^2} \\ &= \frac{\alpha^2 2 \times SNR \times N_c^2 \times (\mu_{11})^2}{(J-1)\alpha^2 2 \times SNR \times N_c^2 \times |\mu_{ij}|^2 \times \frac{1}{G_p} + BT \times \frac{N_m}{N_o}} \end{aligned}$$

(3.22)

where $P = SNR$,

$$\sigma_n^2 = BT \times \frac{N_m}{N_o}$$

3.5.7 Bit Error Rate (BER) of the Receiver

The bit error rate of the coherent PSK receiver can be obtained as :

$$BER = 0.5 \times \text{erfc} \left(\sqrt{SINR/2} \right) \quad (3.23)$$

where, erfc is the complementary error function.

3.6 System Analysis with Diversity

3.6.1 Receiver Model with Diversity (Rake Receiver)

The functional block diagram of the MC DS-CDMA receiver with rake is shown in Fig. 3-4 below:

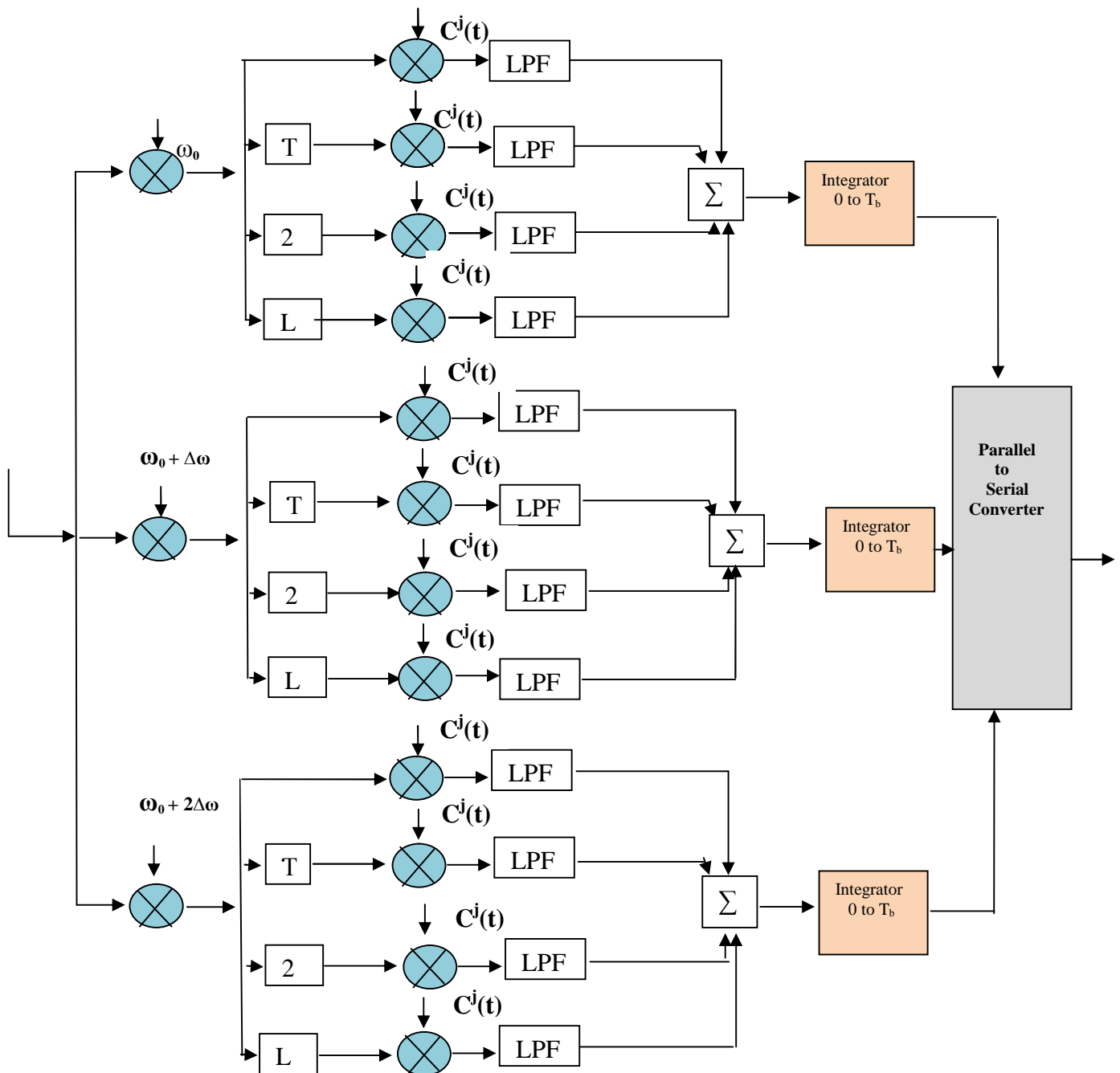


Fig. 3-4 Block diagram of MC DS-CDMA receiver with diversity

Let us consider there are rake receivers in each subcarrier channel which have L no of fingers and they are considered for maximal ratio combining. If $\xi_1 \dots \dots \xi_L$ be the instantaneous bit SINR for different branches , then the conditioned probability of bit error at the output of SSSDR conditioned on a given value of ξ , is given by :

$$P_b(\xi) = \frac{1}{2^{2L-1}} e^{-\gamma} \sum_{k=0}^{L-1} w_k \xi^k \quad (3.24)$$

where,

$$w_k = \frac{1}{k!} \sum_{n=0}^{L-1-k} \binom{2L-1}{n}$$

So, the average bit error probability can be obtained by averaging the conditional bit error rate over the probability density function (pdf) of the instantaneous SINR, ξ :

$$P_b = \int_0^{\infty} P_b(\xi) \cdot f(\xi) d\xi \quad (3.25)$$

where, the pdf of ξ is given as :

$$f(\xi) = \frac{d}{d\gamma} F(\xi) = L \left[\sum_{k=0}^{L-1} \Psi_k (1 - e^{-\frac{\xi}{\Lambda_k}}) \right]^{L-1} \sum_{k=0}^{L-1} \frac{\Psi_k}{\Lambda_k} e^{-\frac{\xi}{\Lambda_k}} \quad (3.26)$$

CHAPTER-4

RESULTS AND DISCUSSIONS

4.1 Introduction

This chapter provides the results obtained by numerical computation following the theoretical analysis of a power line communication system with MC DS-CDMA described in chapter-3. Results are evaluated numerically without diversity and with diversity using a rake receiver. Performance results are shown graphically for several system and channel parameters. Finally, optimum system parameters are determined from the BER performance curves.

4.2 Performance of Power Line Communication System with Varying Channel Parameters

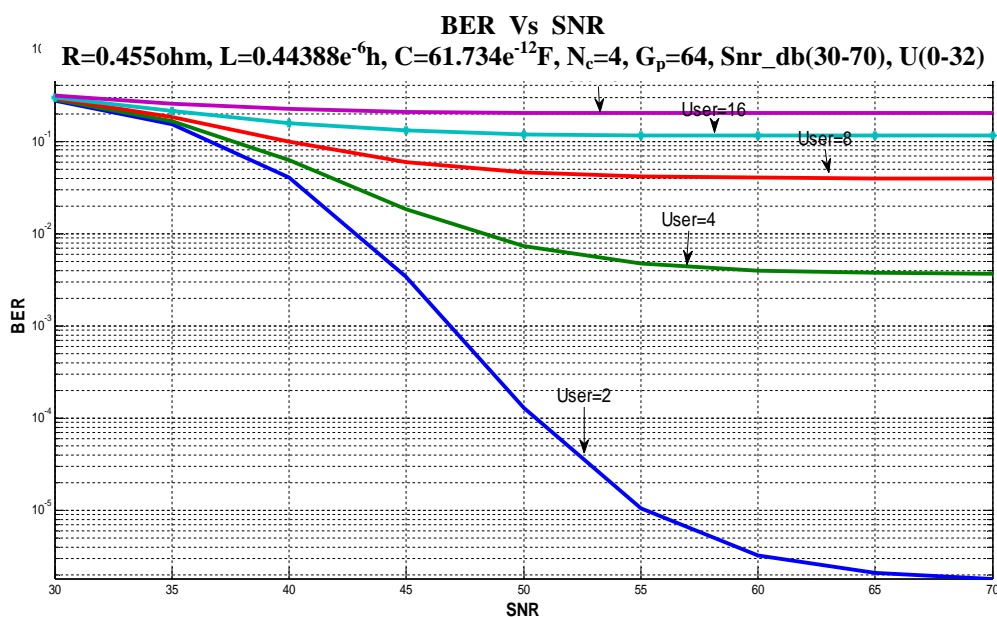
Following the analysis presented in chapter-3, we evaluate the BER performance of a power line communication system and results are presented in Fig. 4-1 to Fig. 4-3. Here, the aim of the analysis is to evaluate the BER performance of the system at certain values of channel parameters. The power line channel described in section 2.5, chapter-2 is considered here. The values and list of parameters are shown in Table 4-1. We consider a given code sequence and found the signal at the output of receiver. From the sampled signal and interference values, μ_{11} and μ_{ij} are numerically evaluated for different code length, number of subcarriers and PLC system parameters.

Table 4-1: List of channel and system parameters

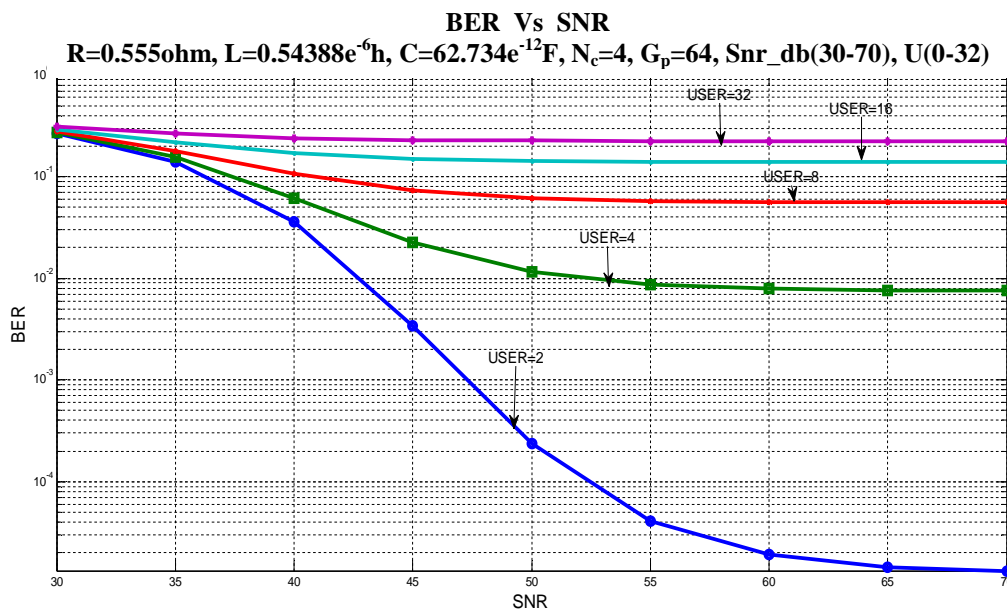
	Parameter	Value
Channel parameters	Resistance (R)	0.455 - 0.755ohm/m
	Inductance (L)	$0.443e^{-6}$ - $0.743 e^{-6}$ h/m
	Capacitance (C)	$61.734 e^{-12}$ - $64.734 e^{-12}$ F/m
	Number of branch	04
	Branch length	10-25m, 15-30m, 23-38m, 20-35m
	Source impedance (Z_s)	70-85 ohm
System parameters	Number of subcarriers (N_c)	04
	Processing gain (G_p)	64
	SNR(dB)	30-70 dB
	User	2-32
	Δf	10 KHz
	Band Width	1-20 MHz
	Bit rate (R_b)	40 kbps

4.2.1 BER Vs SNR for Different Line Impedances (Values of R,L and C varying)

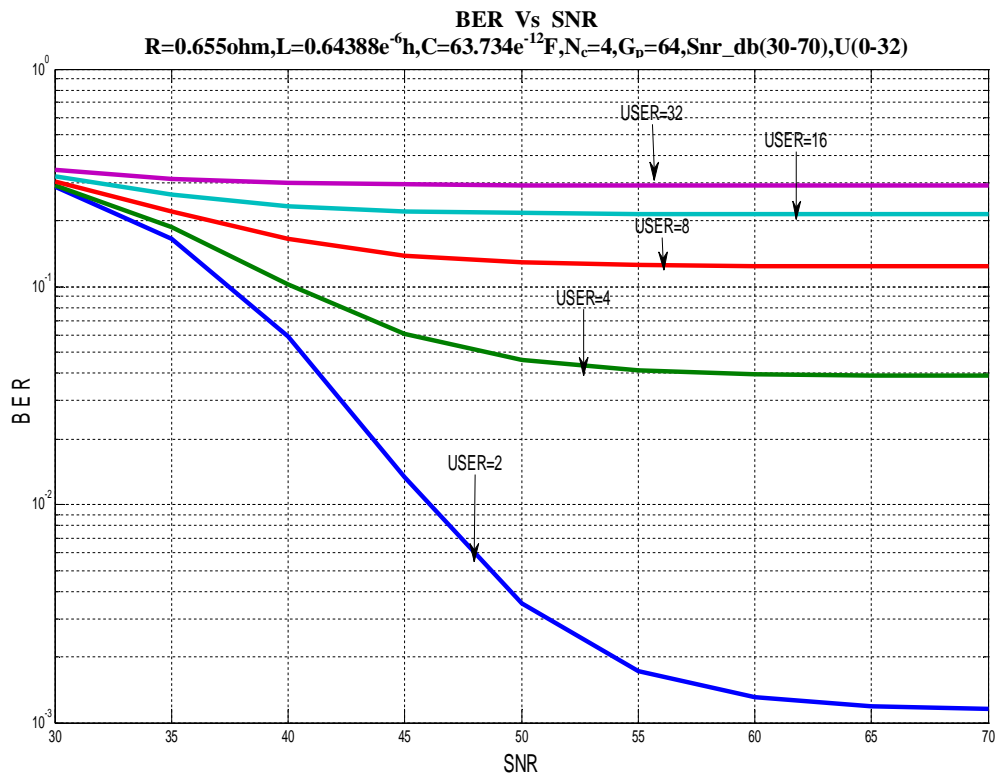
The plots of BER of a MC DS-CDMA power line communication system are shown in Fig 4.1(a) through 4.1(d) as a function of SNR with number of user as a parameter. The value of other parameters are $G_p=64$, number of subcarrier, $N_c=4$ and several values of RLC line components. It is noticed from the curves that the BER decreases with SNR upto certain value of SNR and then BER floor occurs. The BER floor occurs at a higher value of BER with increase in the number of simultaneous user. As noted from the figures, as the line impedance increases, the BER performance deteriorates and BER floor occurs at higher value of BER with increase in line impedance. For some values of line parameters, BER floor occurs at or above 10^{-2}



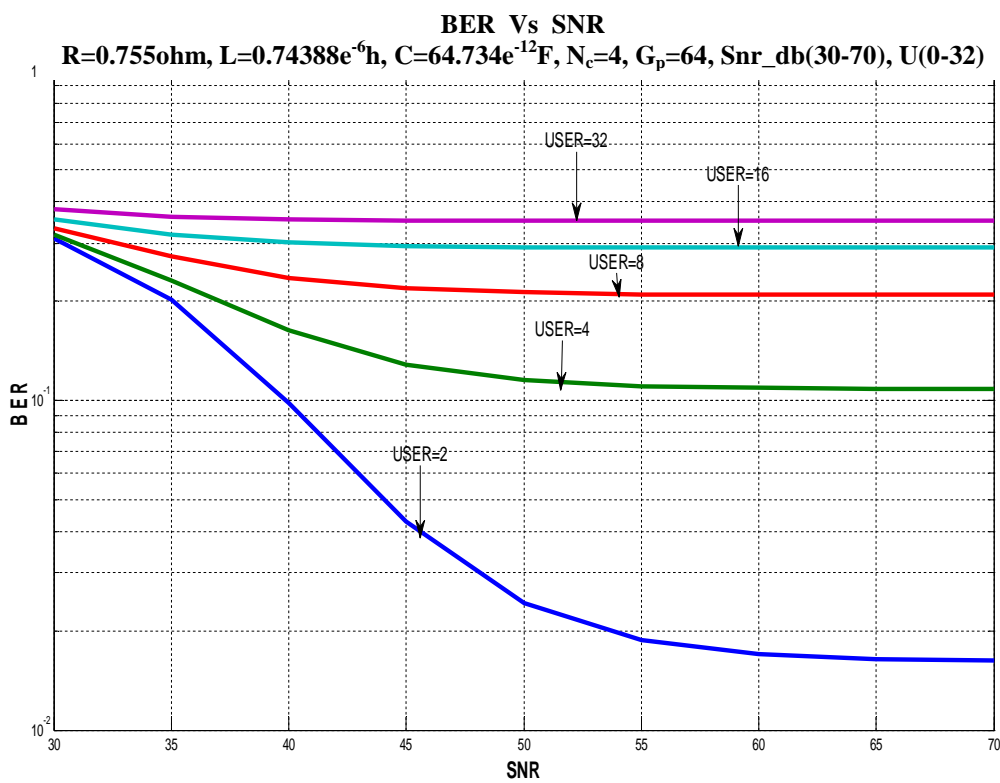
(a)



(b)



(c)

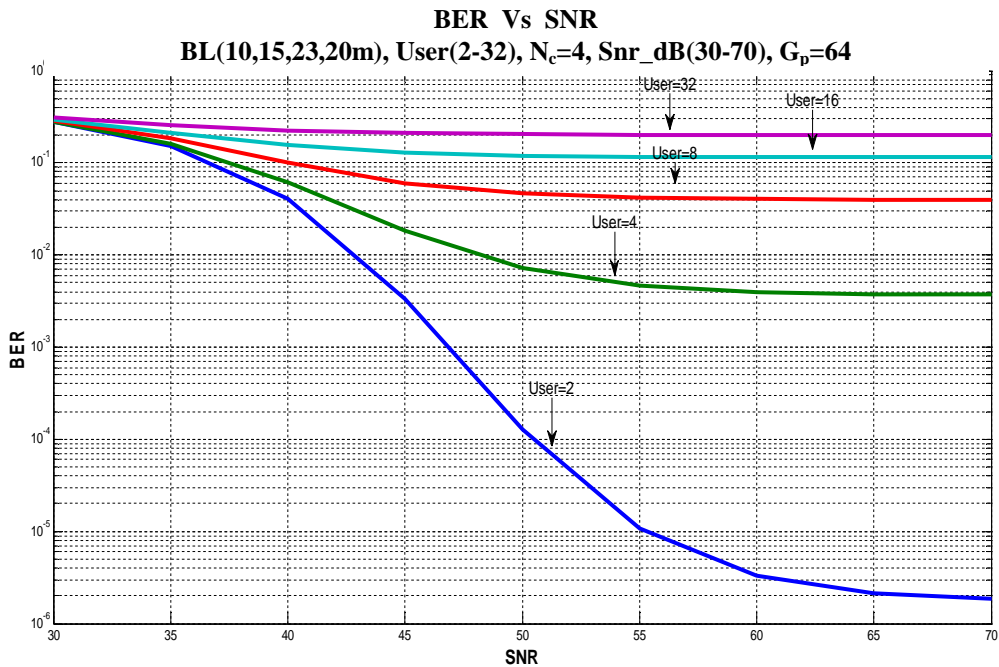


(d)

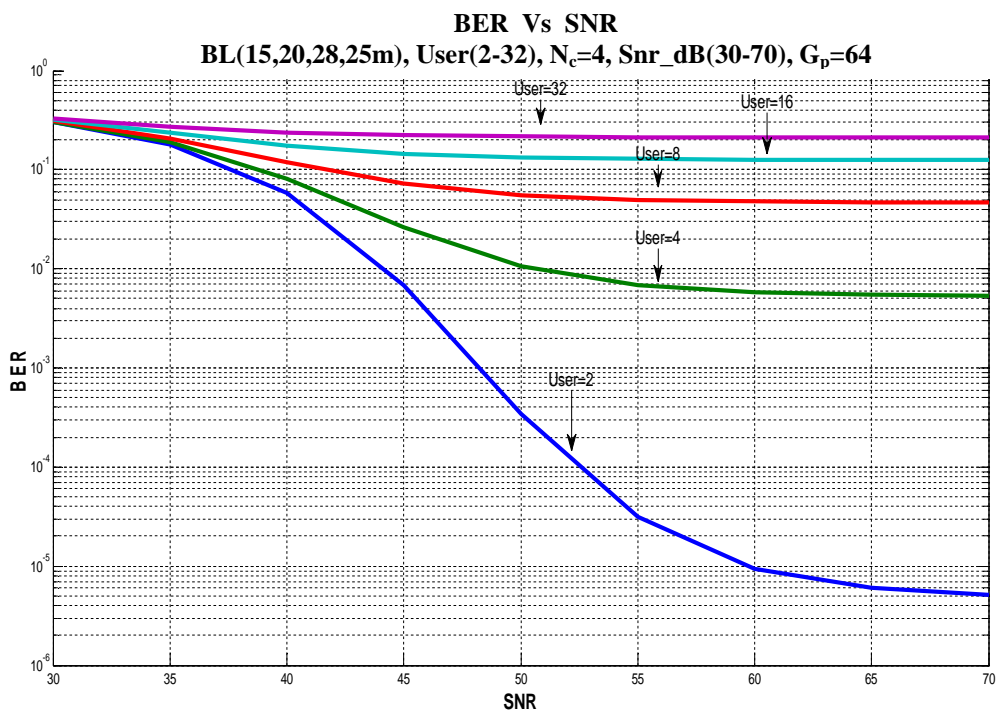
Fig. 4-1 Plots of BER Vs SNR for different line impedances (values of R,Land C varying)

4.2.2 BER Vs SNR for Different Branch Lengths

The plots of BER versus SNR for different branch lengths are depicted in Fig 4-2(a) through 4-2(d). It is noticed that for a given value of load impedance, as the number of branch lengths are increased, the BER floor occurs at higher values. For $BER \leq 10^{-2}$, the number of users that can be supported is less than 4.



(a)



(b)

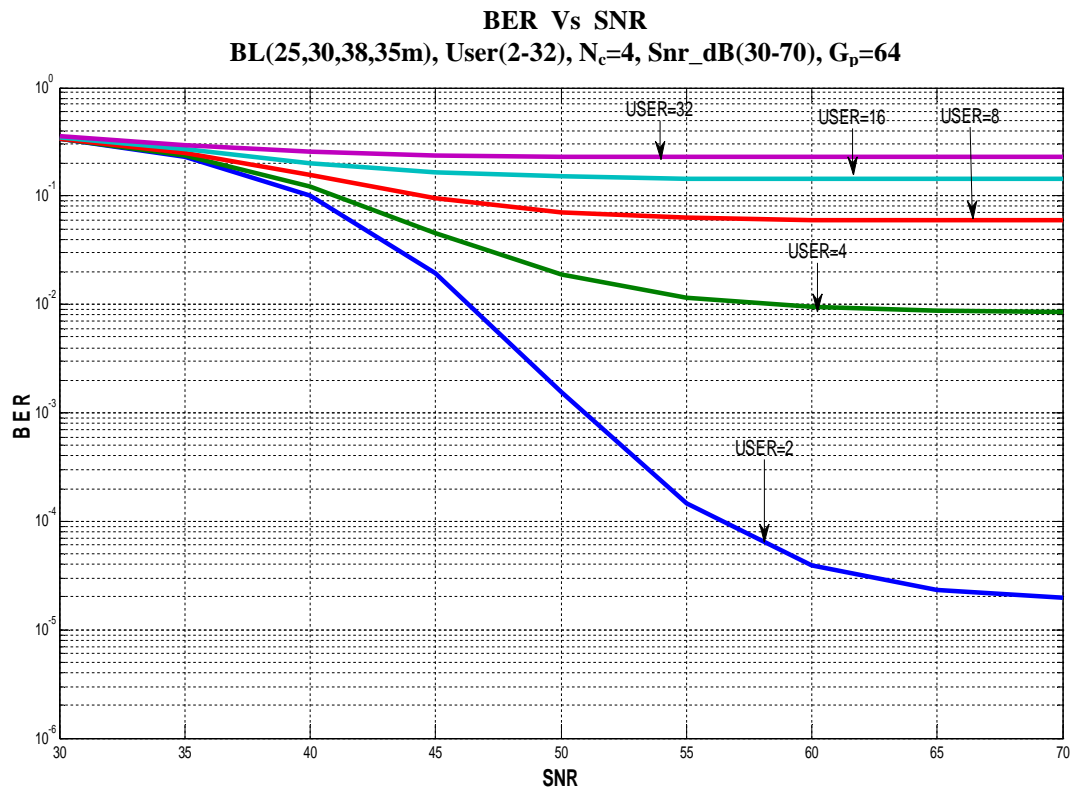
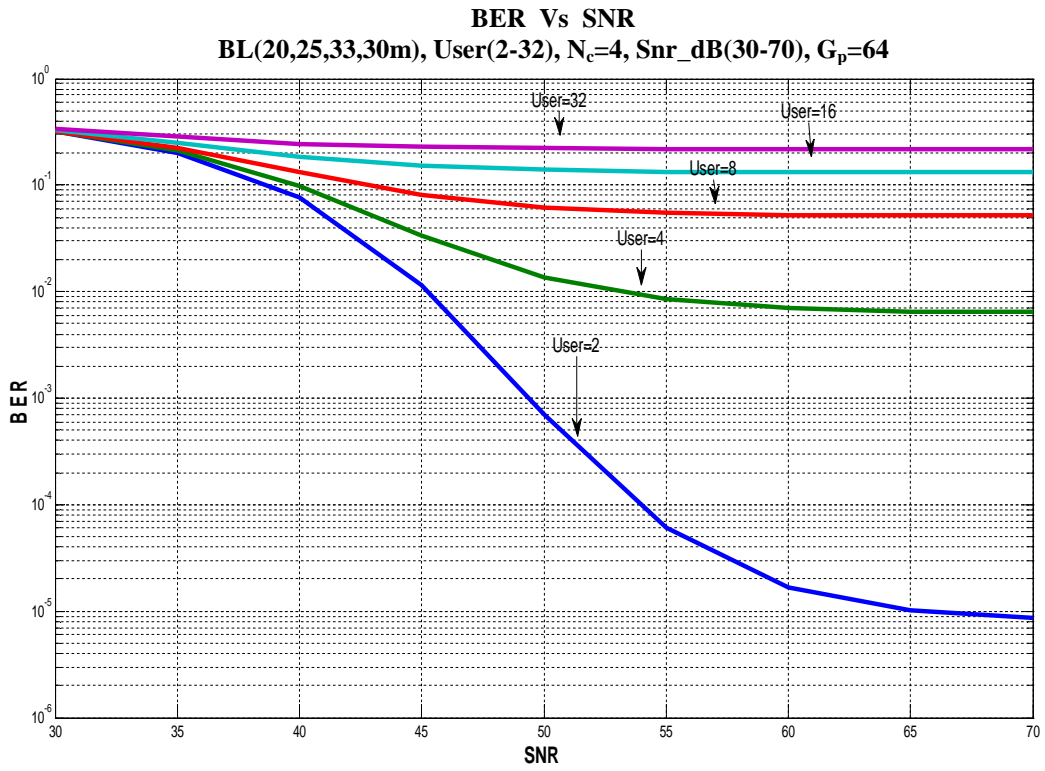
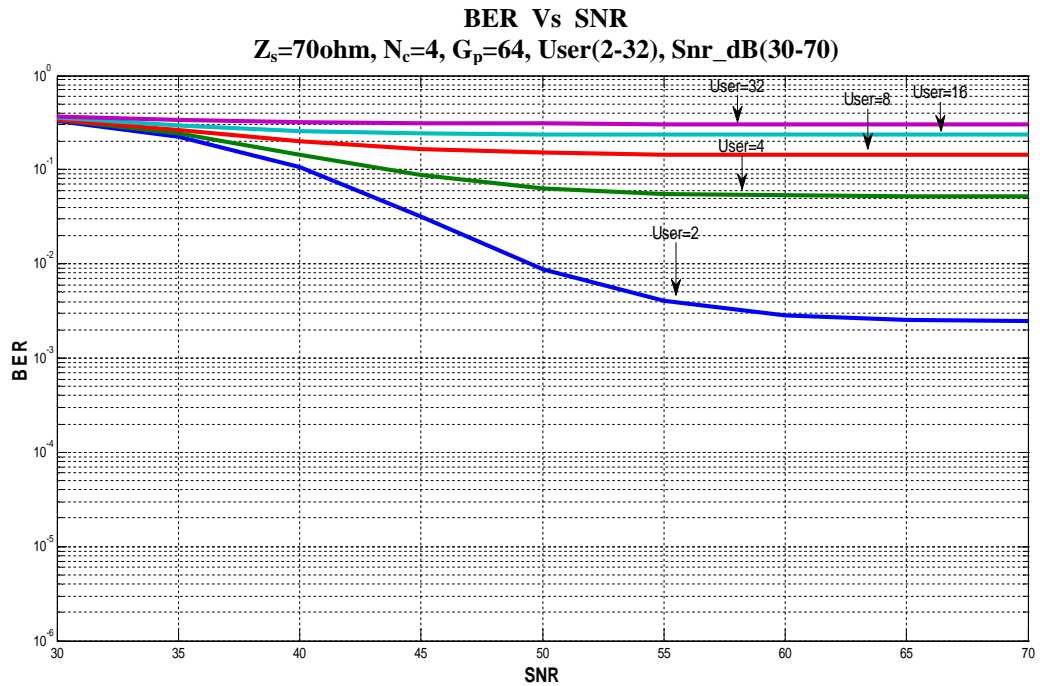


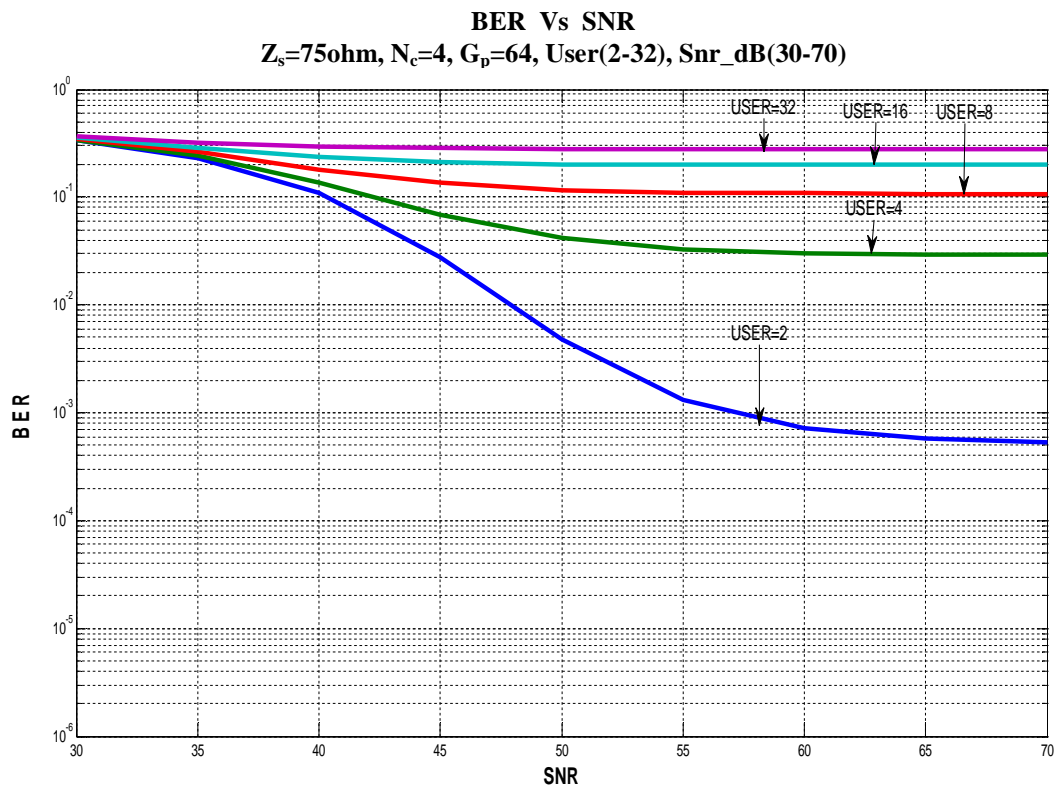
Fig. 4-2 Plots of BER Vs SNR for different branch lengths

4.2.3 BER Vs SNR for Different Source Impedances

The plots of BER versus SNR with various source impedances and number of user as a parameter are shown in Fig. 4-3(a) through Fig. 4-3(d) with other parameters as before. It is found that as the source impedance is increased, there are improvements in BER performance.



(a)



(b)
34

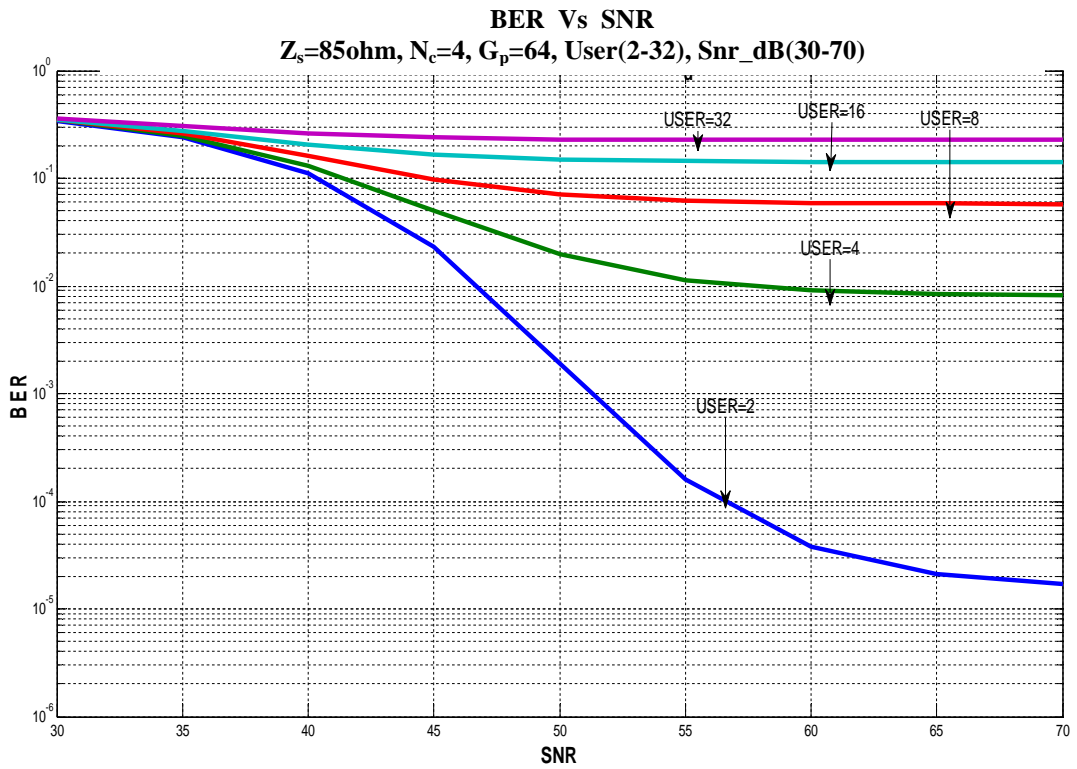
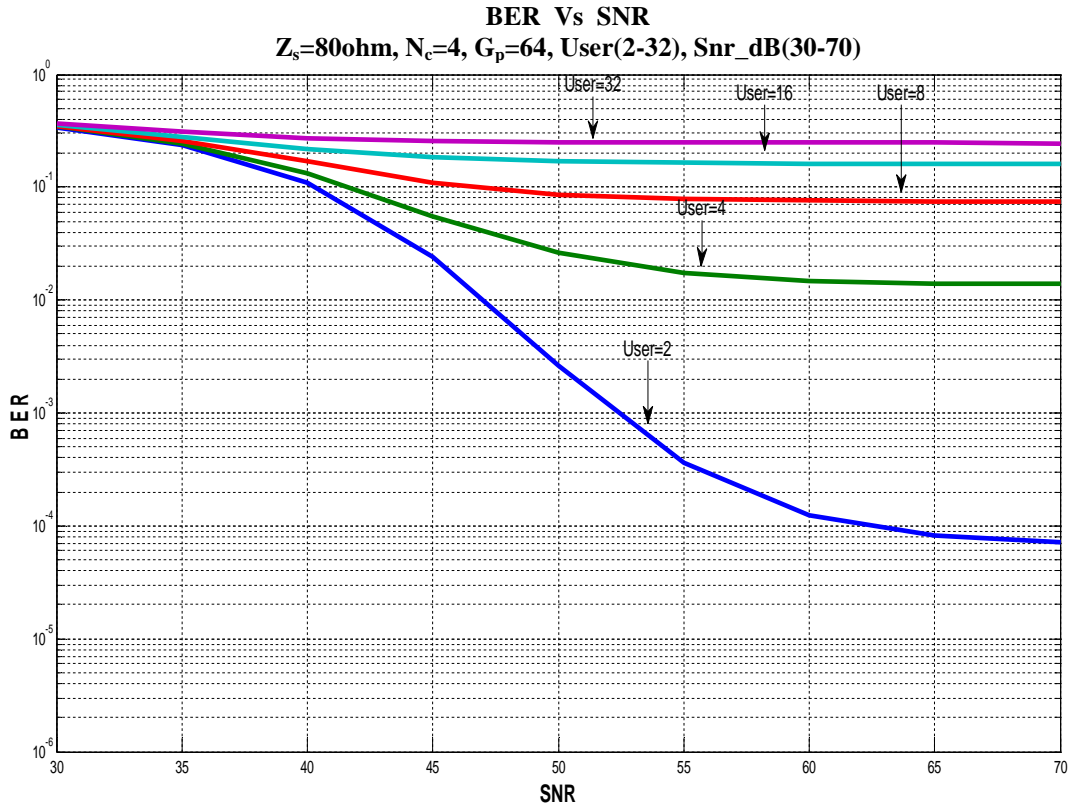


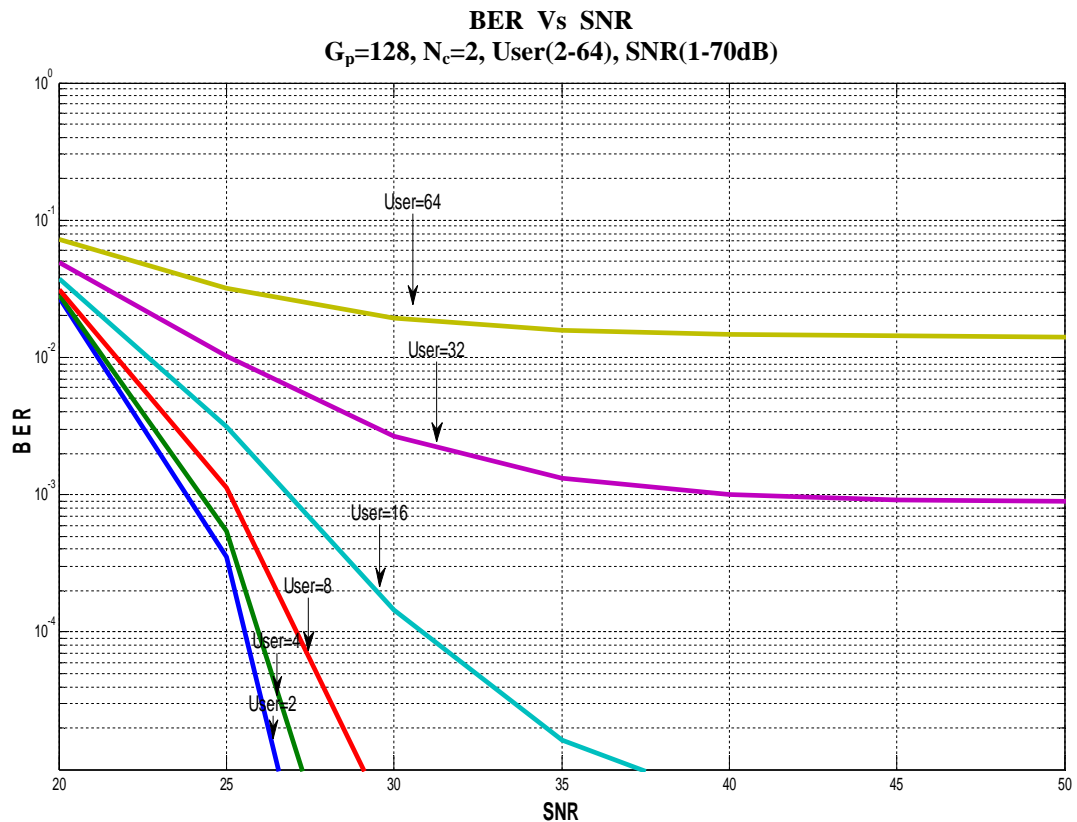
Fig. 4-3 Plots of BER Vs SNR for different source impedances

4.3 Performance of Power Line Communication System with Varying System Parameters (Without Diversity)

Following the analysis presented in chapter-3, we evaluate the BER performance of a power line communication system and results are presented in Fig. 4-4 to Fig. 4-6. Here, the aim of the analysis is to evaluate the BER performance of the system at certain values of system parameters.

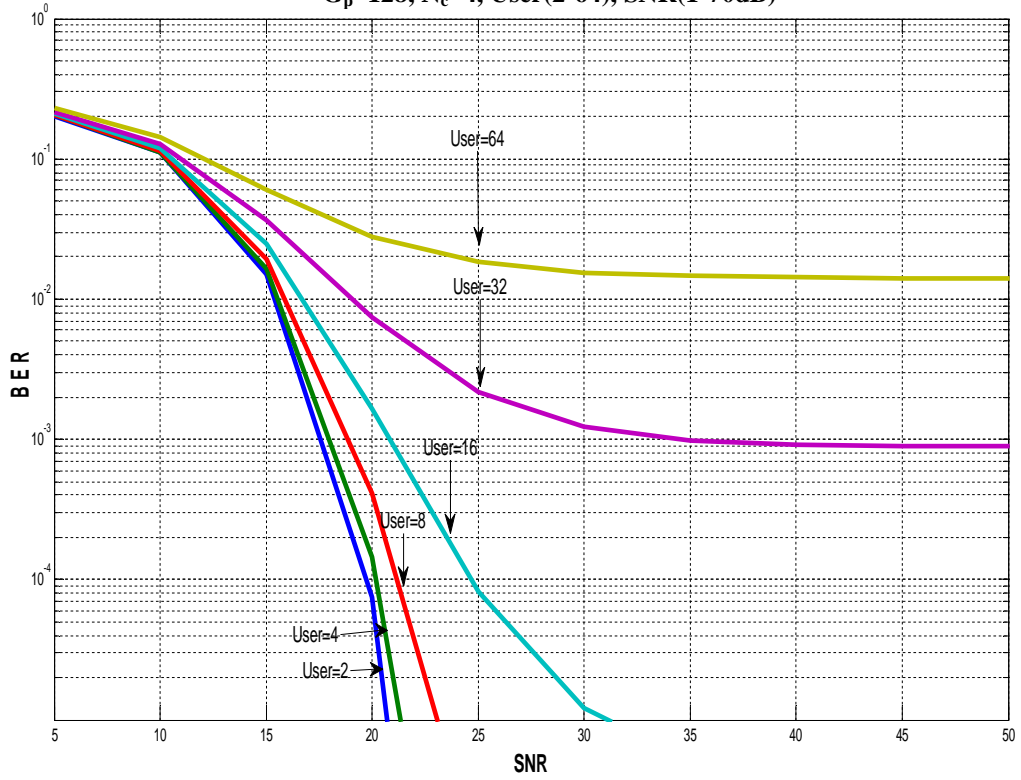
4.3.1 BER Vs SNR for Different Number of Subcarriers at Fixed Processing Gain ($G_p=128$)

The plots of BER versus SNR are shown in Fig. 4-4(a) through 4-4(d) for number of subcarriers, $N_c=2,4,8,16$ and $G_p=128$, with other parameters remaining fixed. It is noticed that, compared to Fig. 4-1 corresponding to $G_p=64$, the BER performance improves for $G_p=128$ and number of user that is supported is around 16. Comparison of Fig. 4-4(a) through Fig. 4-4(d), it is revealed that performance improves with increase in the number of subcarriers, N_c from 2 to 16 as the BER floor goes down with increase in N_c . Further, the number of user that can be supported increased with increase in N_c . Also the required SNR to achieve $BER \leq 10^{-3}$ is found to be 27 dB, 21 dB, 14.5 dB and 8 dB for $N_c= 2,4,8,16$ respectively.



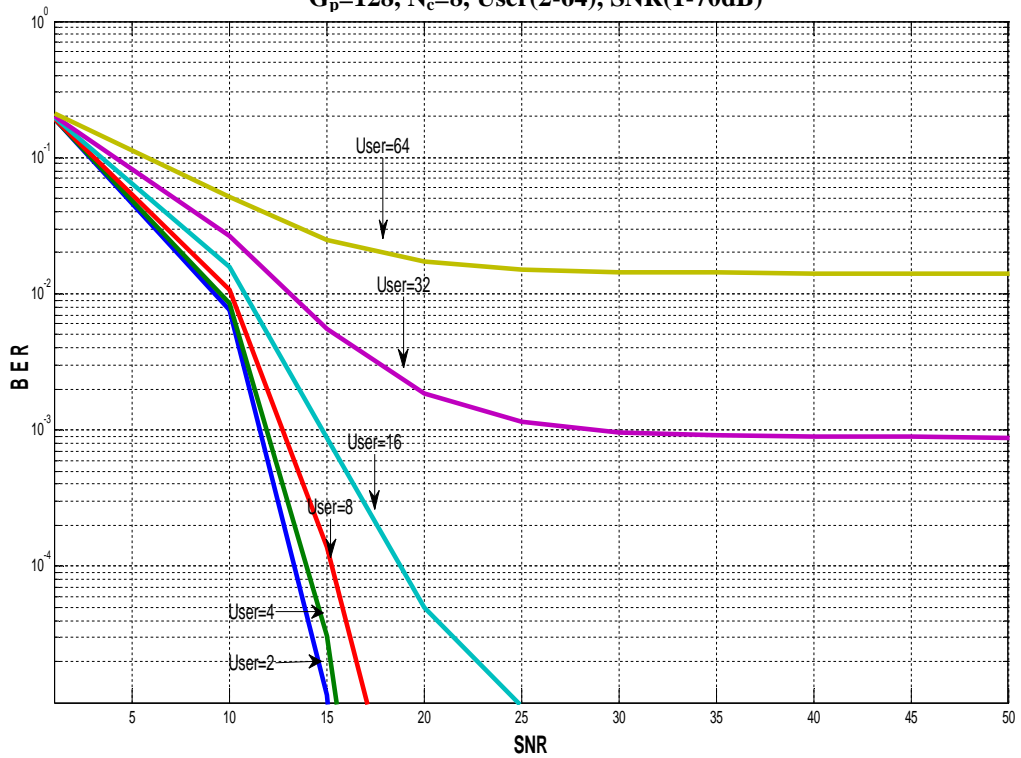
(a)

BER Vs SNR
 $G_p=128, N_c=4, \text{User}(2-64), \text{SNR}(1-70\text{dB})$

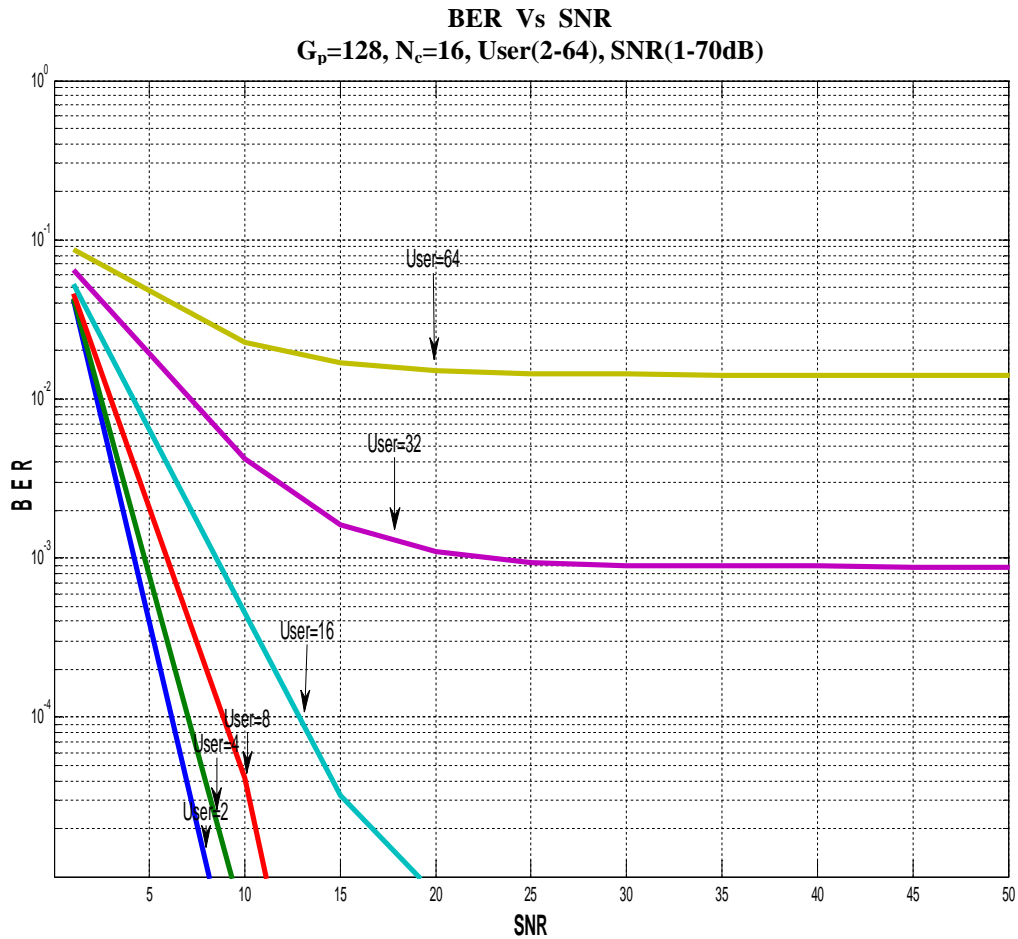


(b)

BER Vs SNR
 $G_p=128, N_c=8, \text{User}(2-64), \text{SNR}(1-70\text{dB})$



(c)



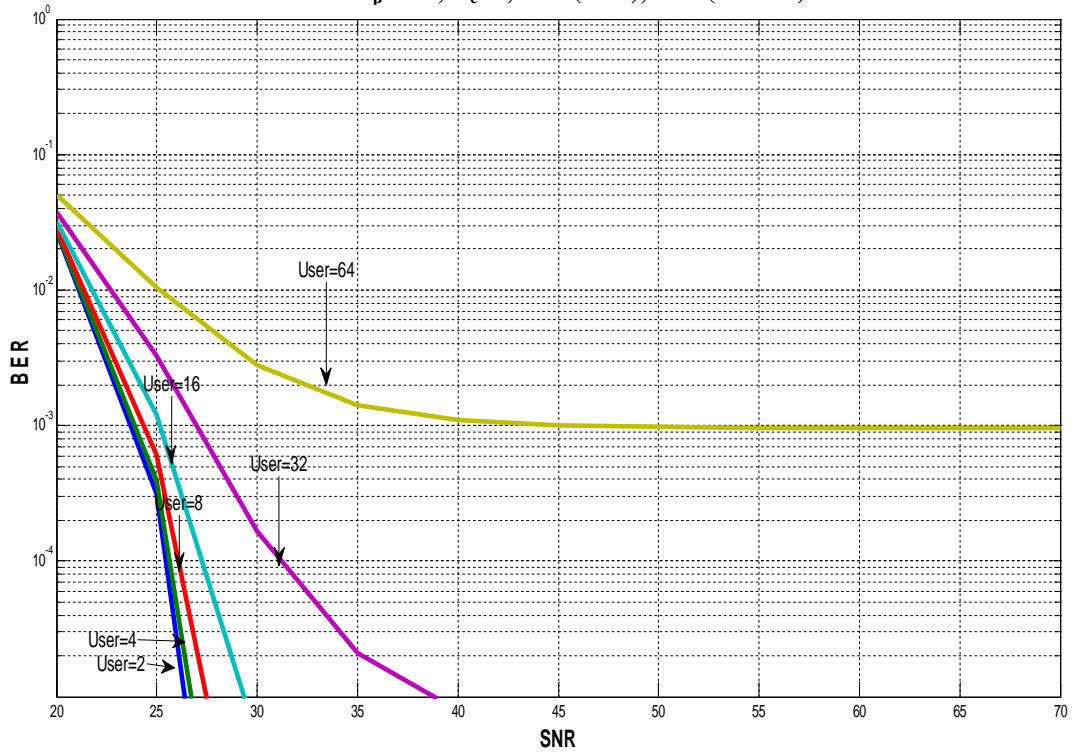
(d)

Fig. 4-4 Plots of BER Vs SNR for different number of subcarriers at fixed processing gain ($G_p=128$)

4.3.2 BER Vs SNR for Different Number of Subcarriers at Fixed Processing Gain ($G_p=256$)

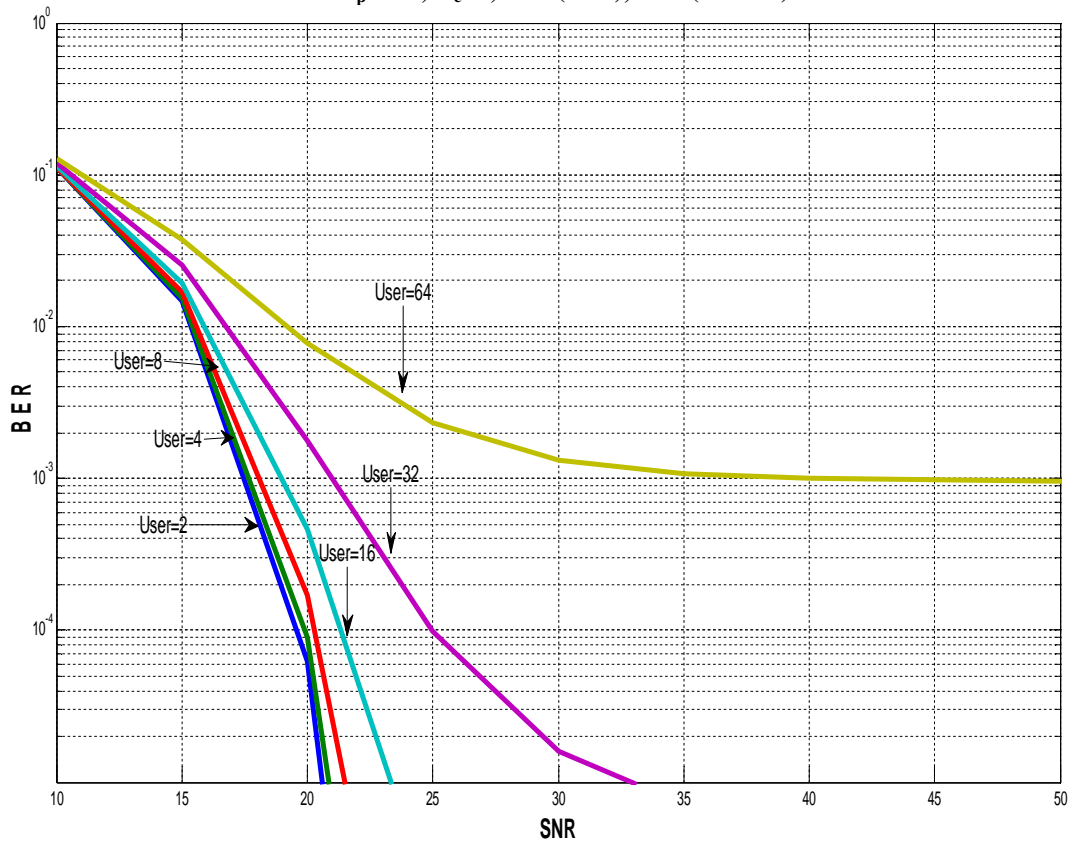
Similar results of BER versus SNR with different values of N_c are depicted in Fig. 4-5(a) through Fig. 4-5(d) for $G_p=256$. It is noticed that there is significant improvement in receiver sensitivity at a given BER compared to $G_p=128$ and 64, and the BER floors are found to occur at lower BER values. It is noticed that the maximum number of user is around 64 for $N_c=2,4,8,16$.

BER Vs SNR
 $G_p=256, N_c=2, \text{User}(2-64), \text{SNR}(1-70\text{dB})$



(a)

BER Vs SNR
 $G_p=256, N_c=4, \text{User}(2-64), \text{SNR}(1-70\text{dB})$



(b)

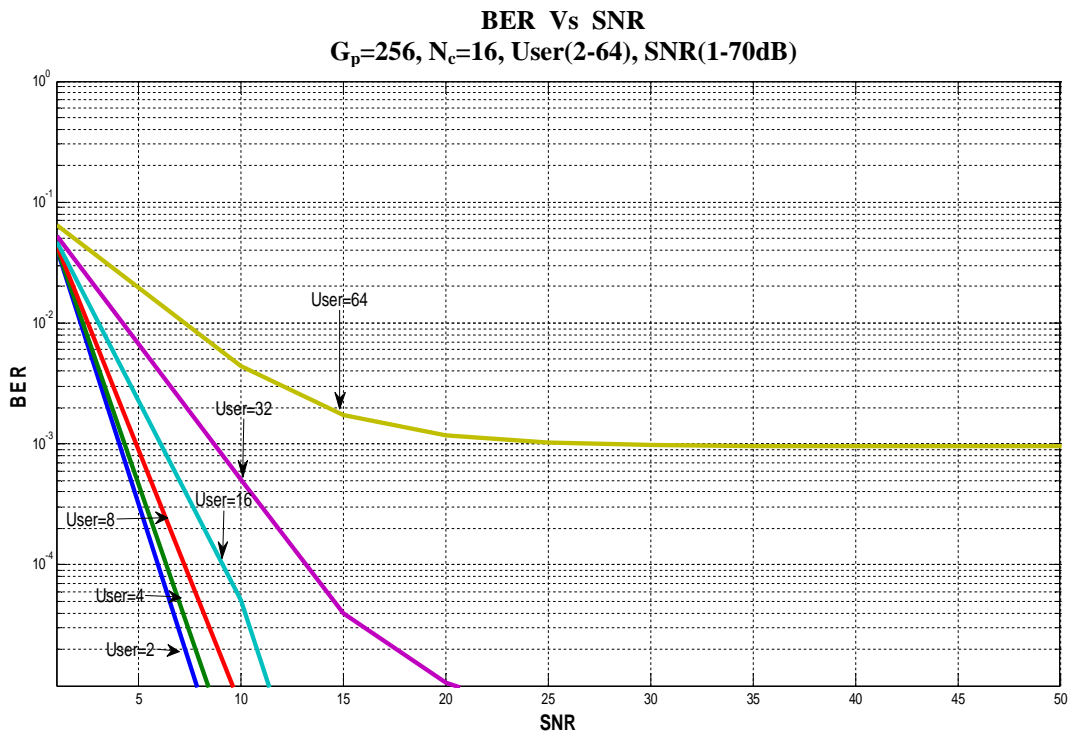
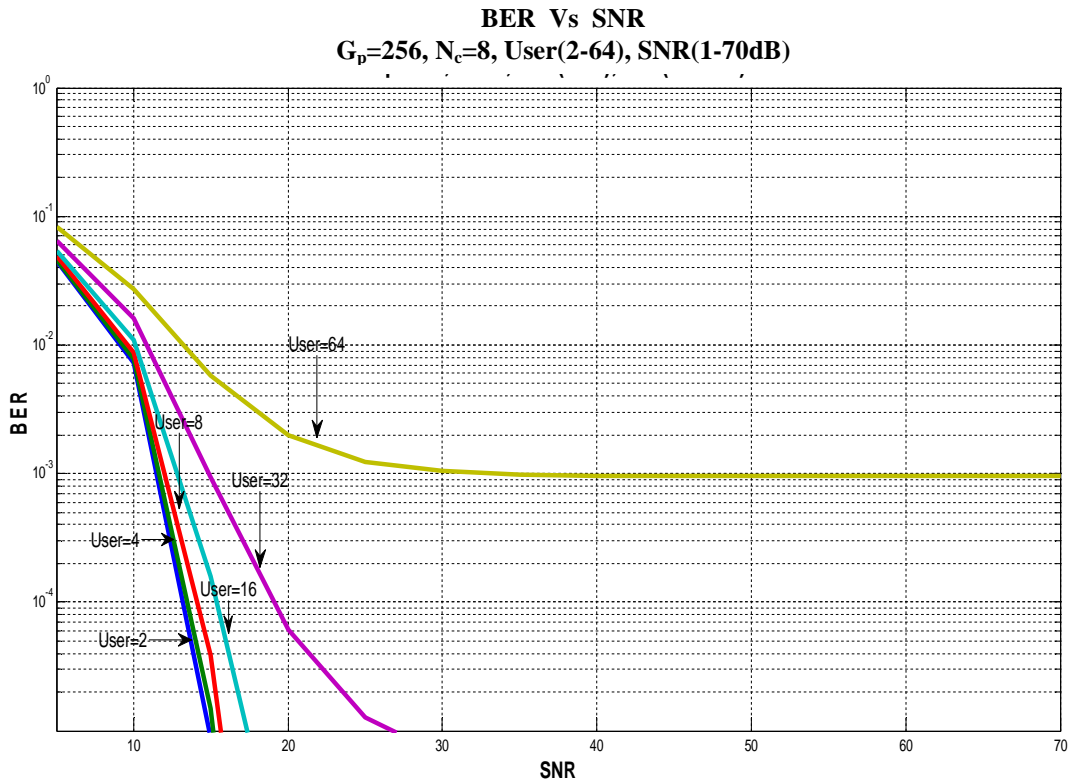
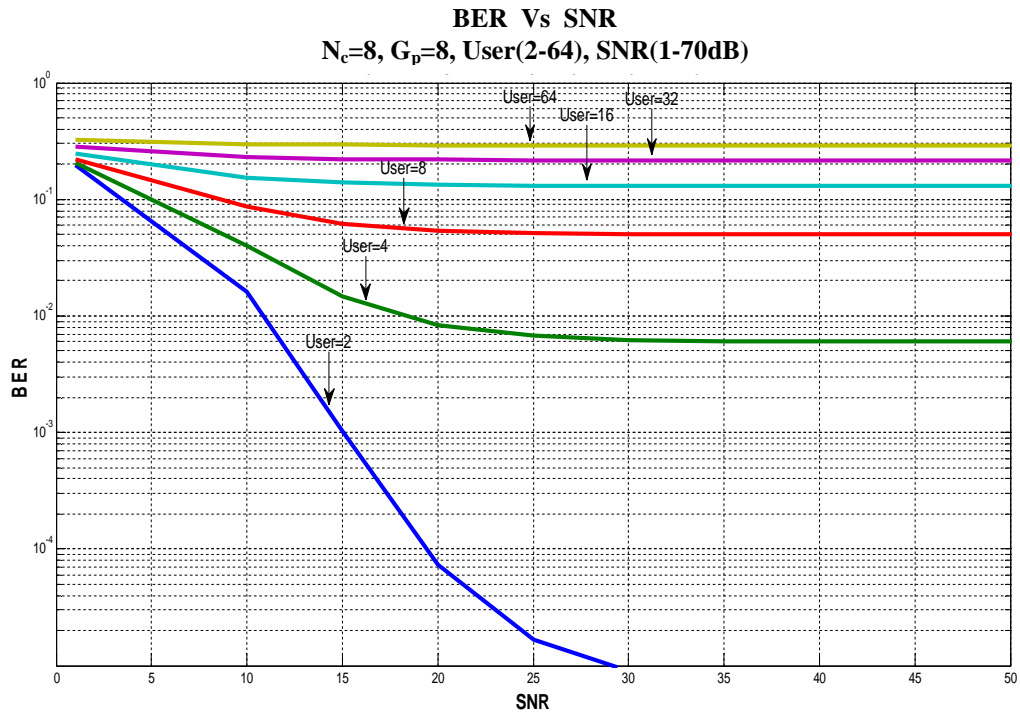


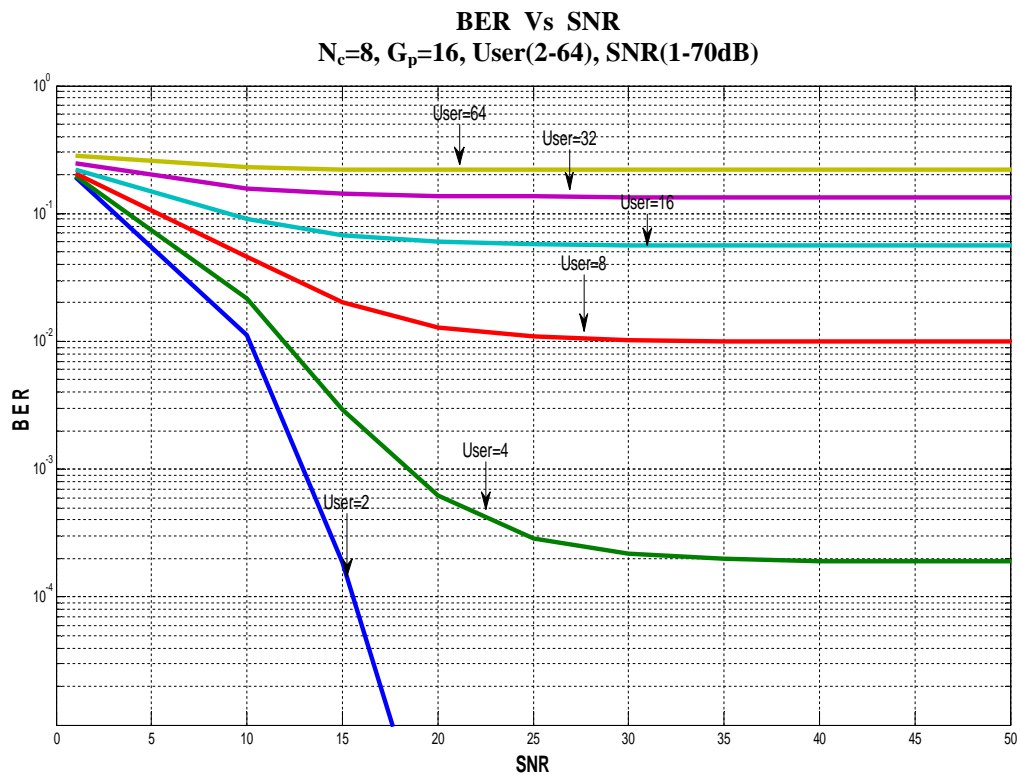
Fig. 4-5 Plots of BER Vs SNR for different number of subcarriers at fixed processing gain ($G_p=256$)

4.3.3 BER Vs SNR for Different Processing Gains at Fixed Number of Subcarriers ($N_c=8$)

The BER performance results for a given value $N_c=8$ and various values of $G_p=8$ to 256 are depicted in Fig. 4-6(a) through Fig. 4-6(f). The plots reveal that there is improvement in receiver sensitivity at a given BER as well as the capacity of the CDMA system with increasing value of G_p .

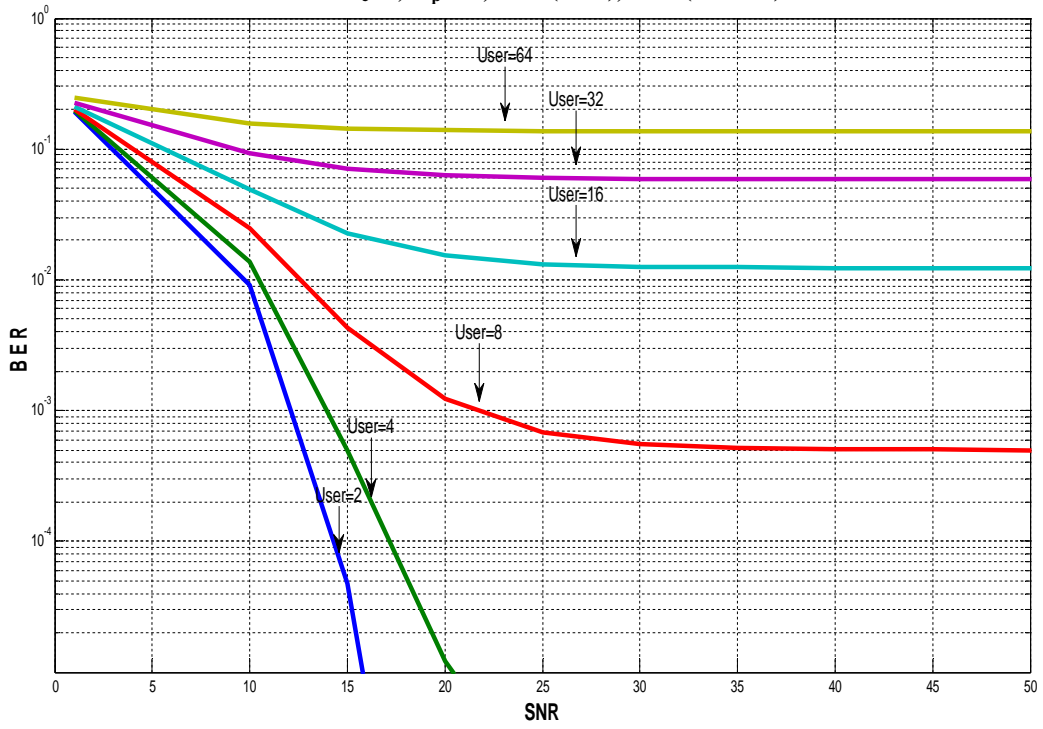


(a)



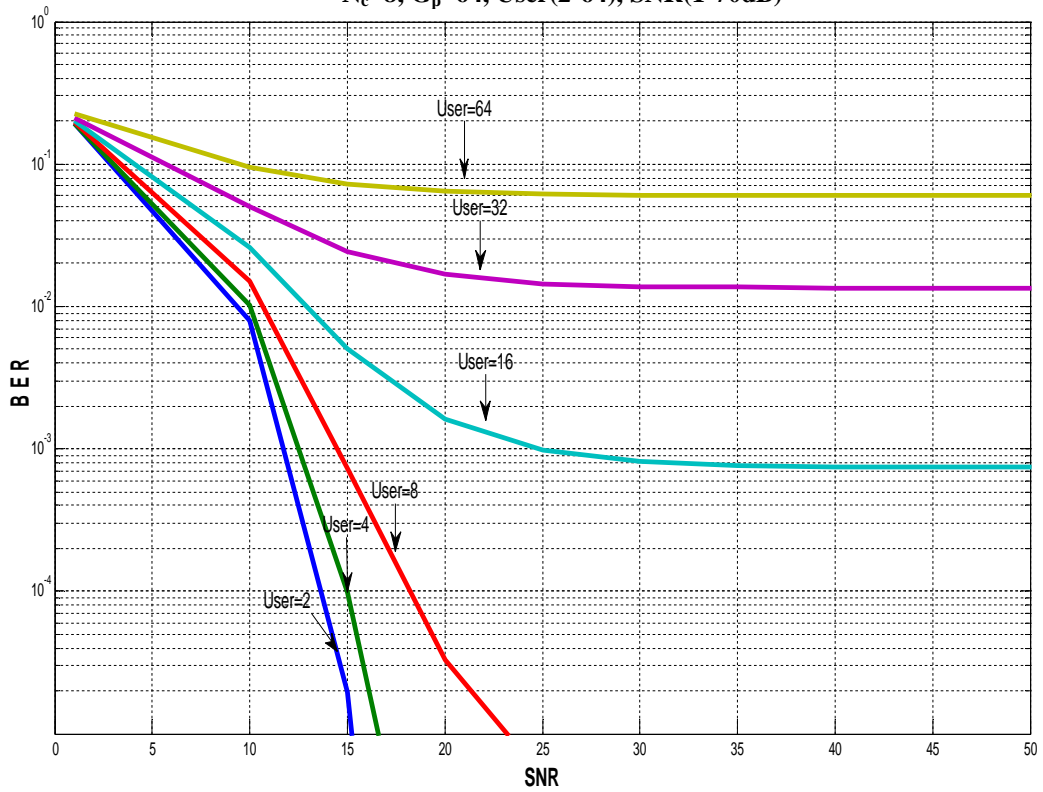
(b)

BER Vs SNR
 $N_c=8, G_p=32, \text{User}(2-64), \text{SNR}(1-70\text{dB})$



(c)

BER Vs SNR
 $N_c=8, G_p=64, \text{User}(2-64), \text{SNR}(1-70\text{dB})$



(d)

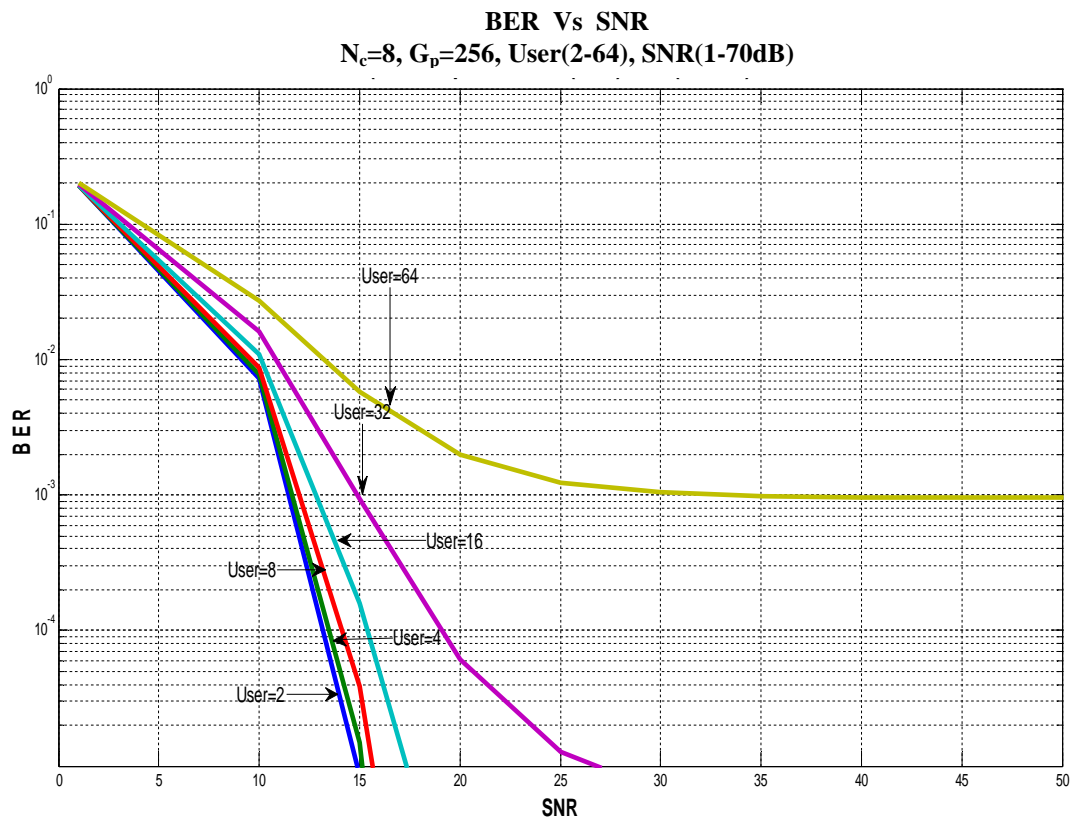
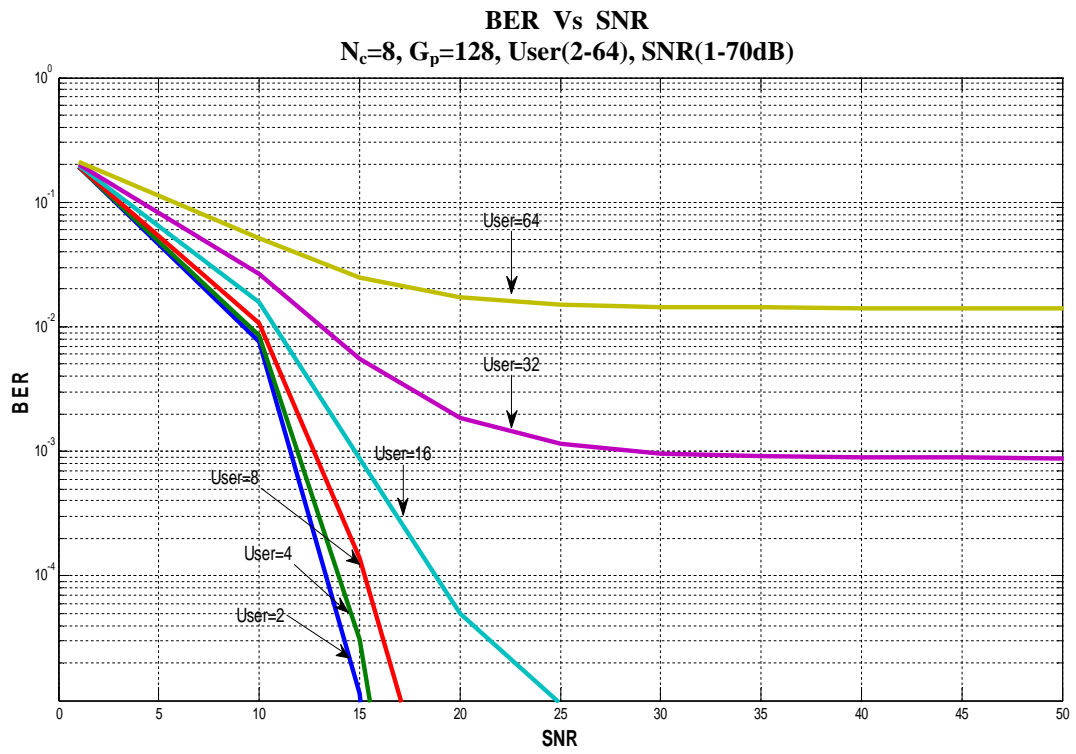


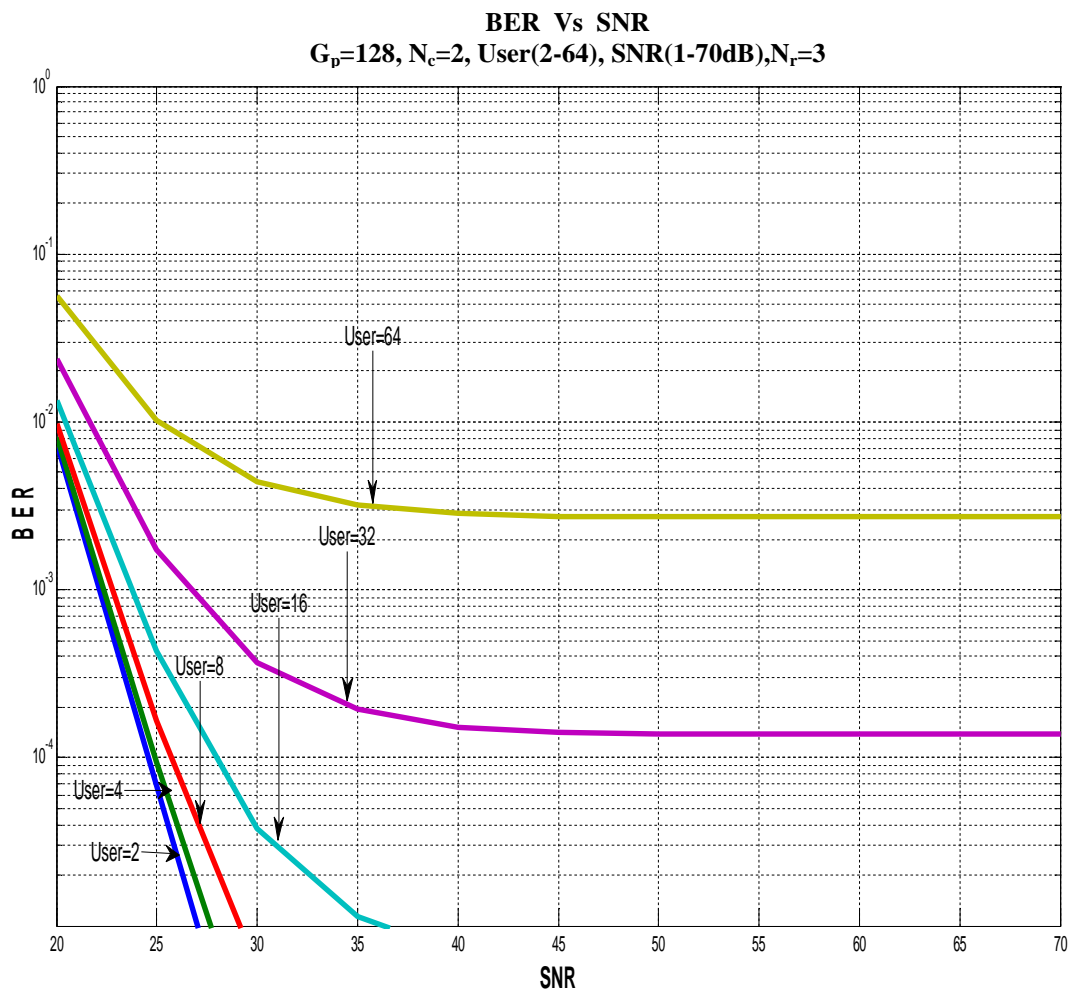
Fig. 4-6 Plots of BER Vs SNR for different processing gains at fixed number of subcarriers ($N_c=8$)

4.4 Performance of Power Line Communication System with Varying System Parameters (With Diversity using a Rake Receiver)

The BER performance results with diversity using a rake receiver are depicted in Fig. 4-7 through Fig. 4-12 as discussed below.

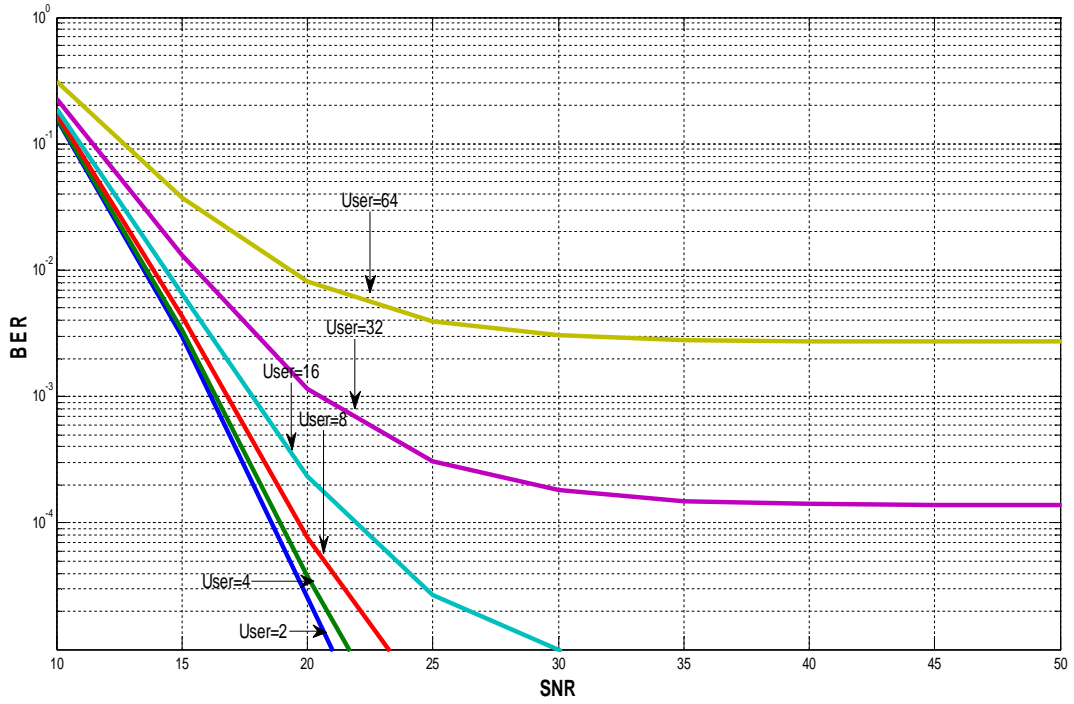
4.4.1 BER Vs SNR for Different Number of Subcarriers at Fixed Processing Gain ($G_p=128$) with a Rake Receiver having Number of Rake Fingers, $N_r=3$

Fig. 4-7(a) through Fig. 4-7(e) depict the plots of BER versus SNR of MC DS-CDMA PLC system with a rake receiver with number of rake fingers, $N_r=3$, $G_p=128$ for number of subcarriers, $N_c=2,4,8,16,32$. From comparison of Fig. 4-7 with Fig. 4-4, it is noticed that compared to the BER performance without path-diversity, the system with rake receiver provides a significant improvement in receiver sensitivity for the same value of G_p and other parameters. As evident from the plots it is also noticed that at given SNR, more number of users can be supported.



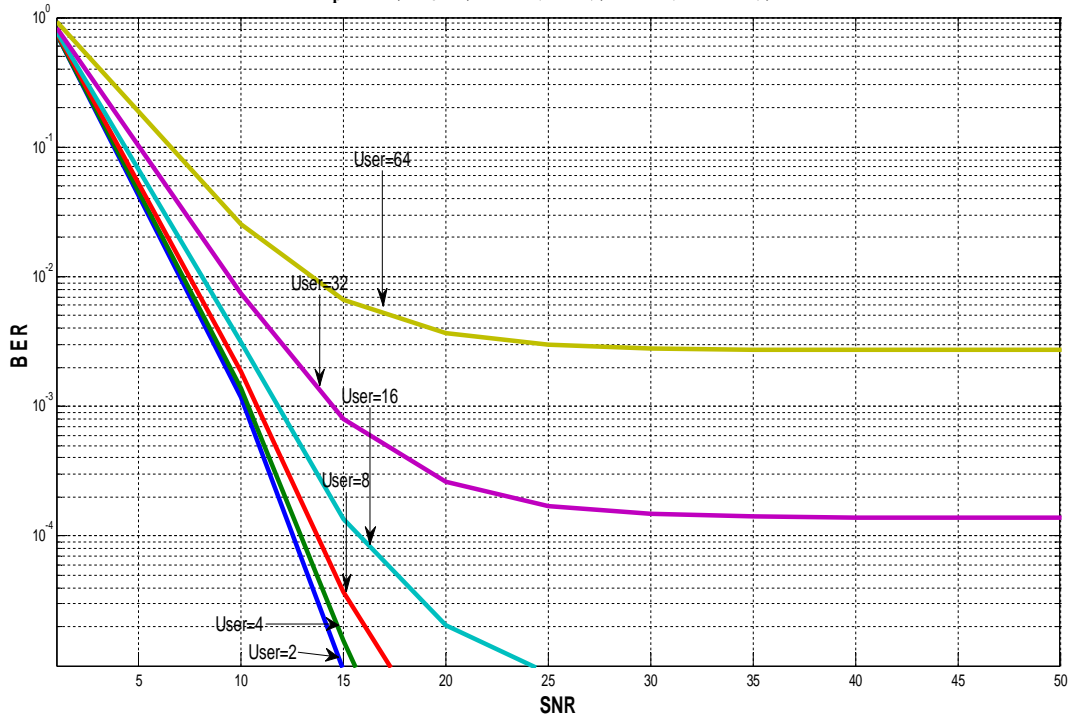
(a)

BER Vs SNR
 $G_p=128, N_c=4, \text{User}(2-64), \text{SNR}(1-70\text{dB}), N_r=3$

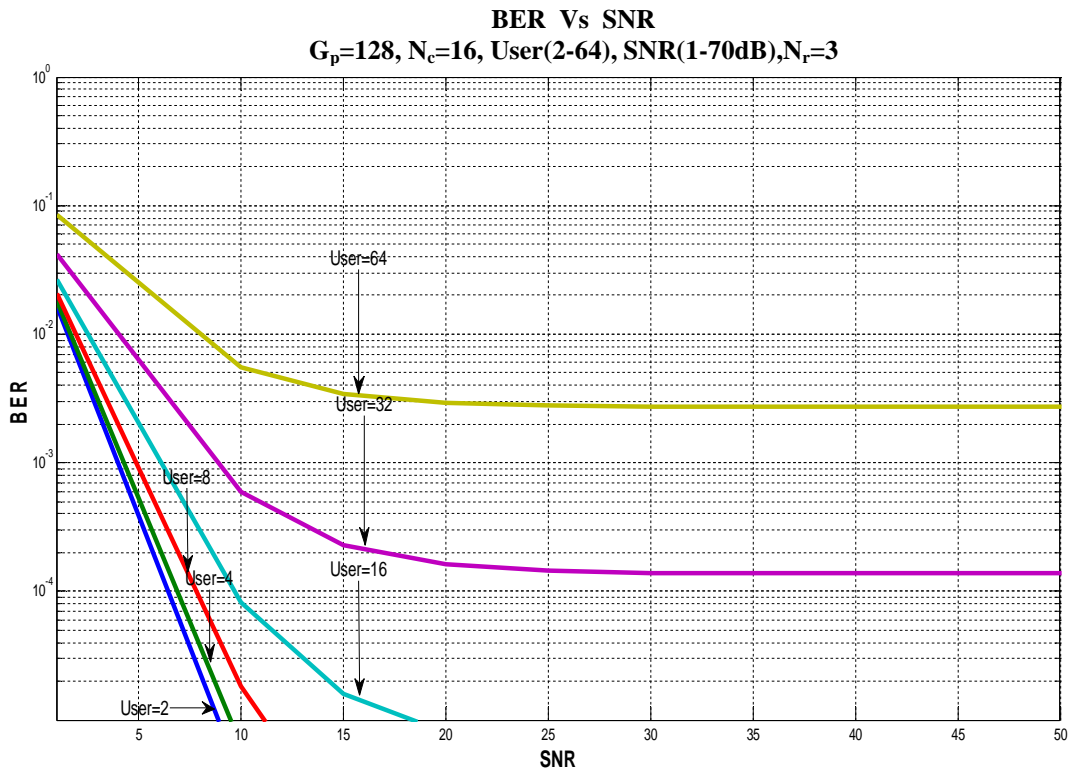


(b)

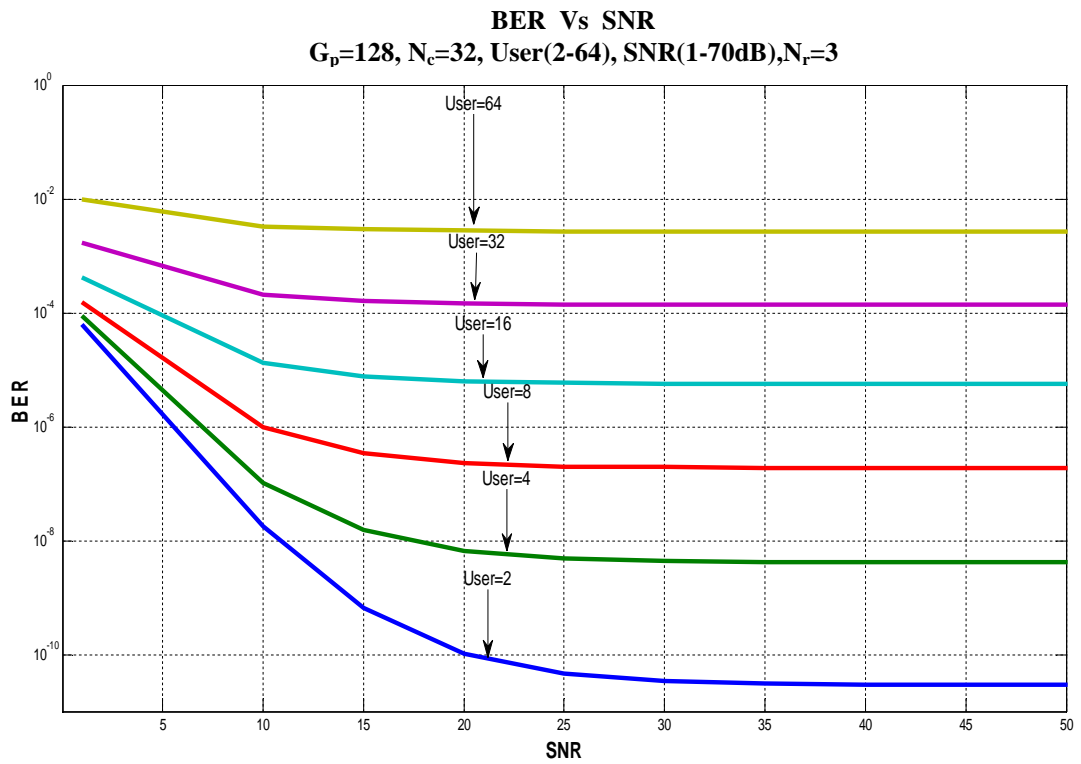
BER Vs SNR
 $G_p=128, N_c=8, \text{User}(2-64), \text{SNR}(1-70\text{dB}), N_r=3$



(c)



(d)

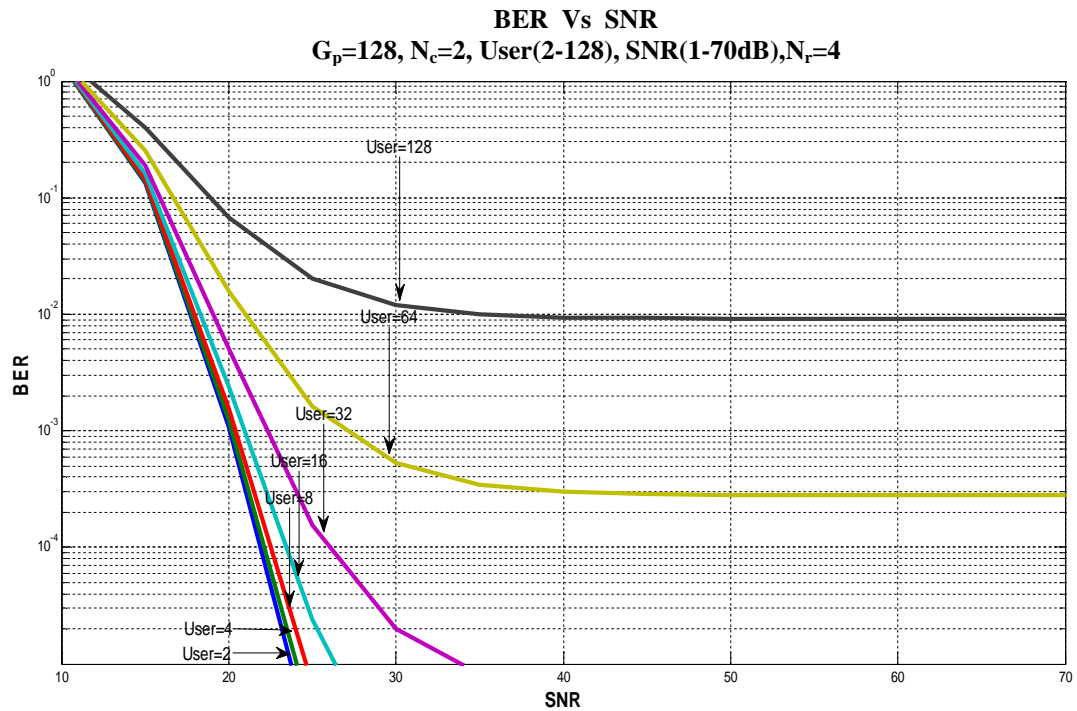


(e)

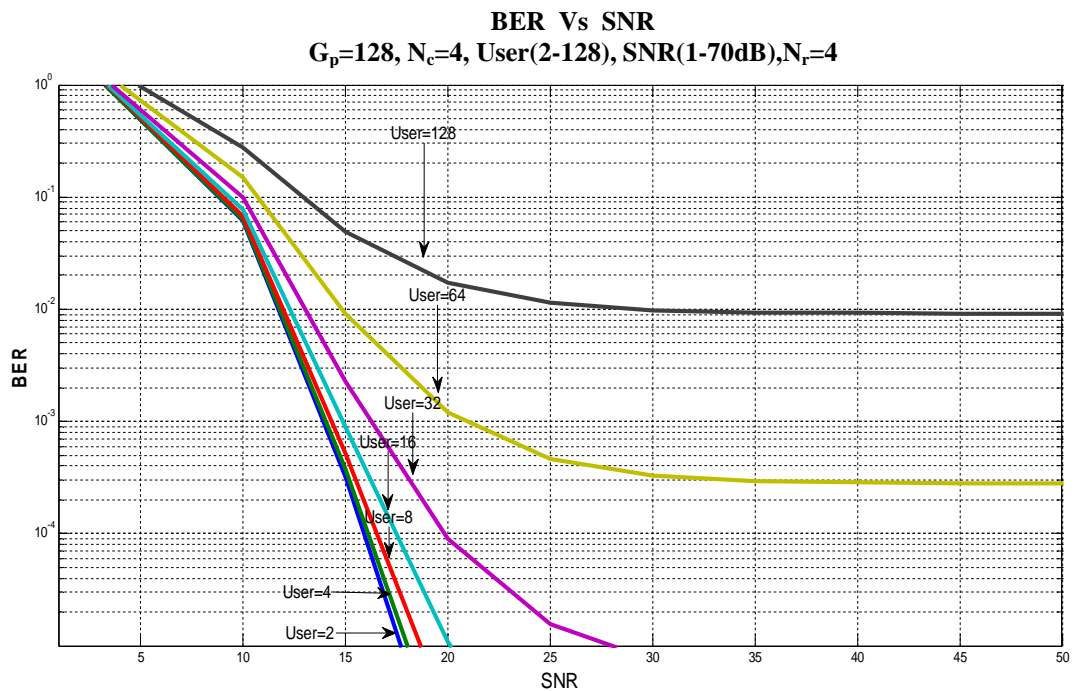
Fig. 4-7 Plots of BER Vs SNR for different number of subcarriers at fixed processing gain ($G_p=128$) with a rake receiver having number of rake fingers, $N_r=3$

4.4.2 BER Vs SNR for Different Number of Subcarriers at Fixed Processing Gain ($G_p=128$) with a Rake Receiver having Number of Rake Fingers, $N_r=4$

Similar results for $N_r=4$ and $G_p=128$ are shown in Fig. 4-8 with number of user and several values of N_c as a parameter. Fig. 4-9 depicts similar results for $N_r=3$ and $G_p=256$ and Fig. 4-10 for $N_r=4$ and $G_p=256$ respectively. It is found that there are significant improvement in system performance at a given BER in terms of SNR and number of simultaneous user, with increase in the number of rake fingers and G_p .

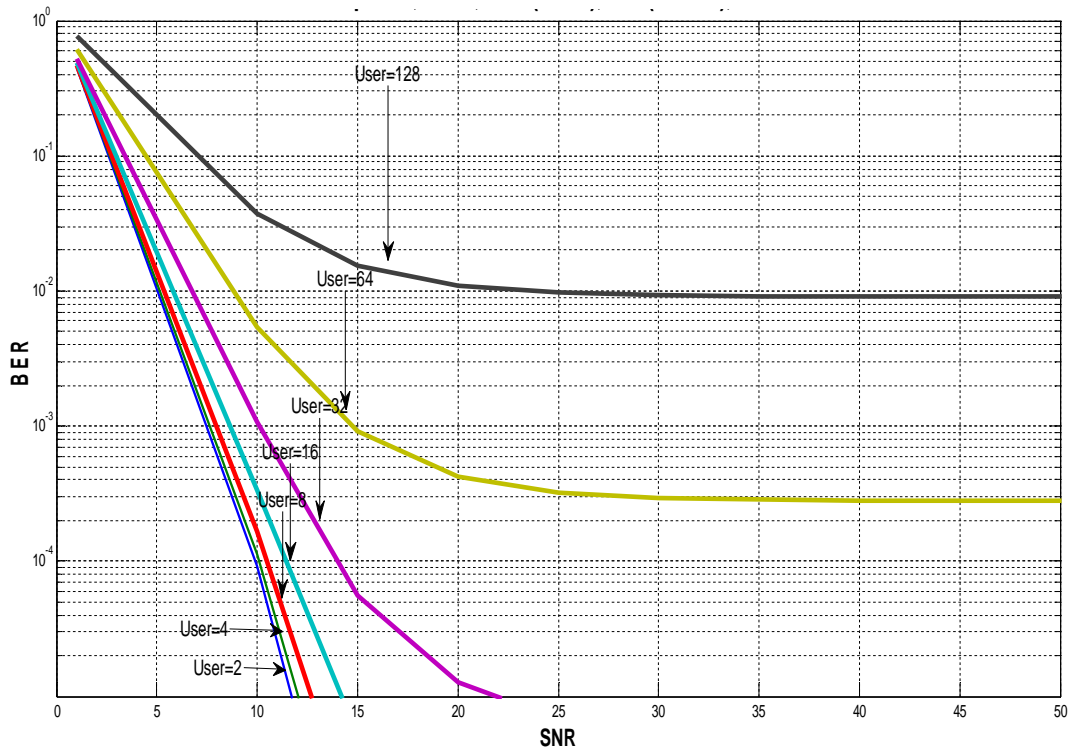


(a)



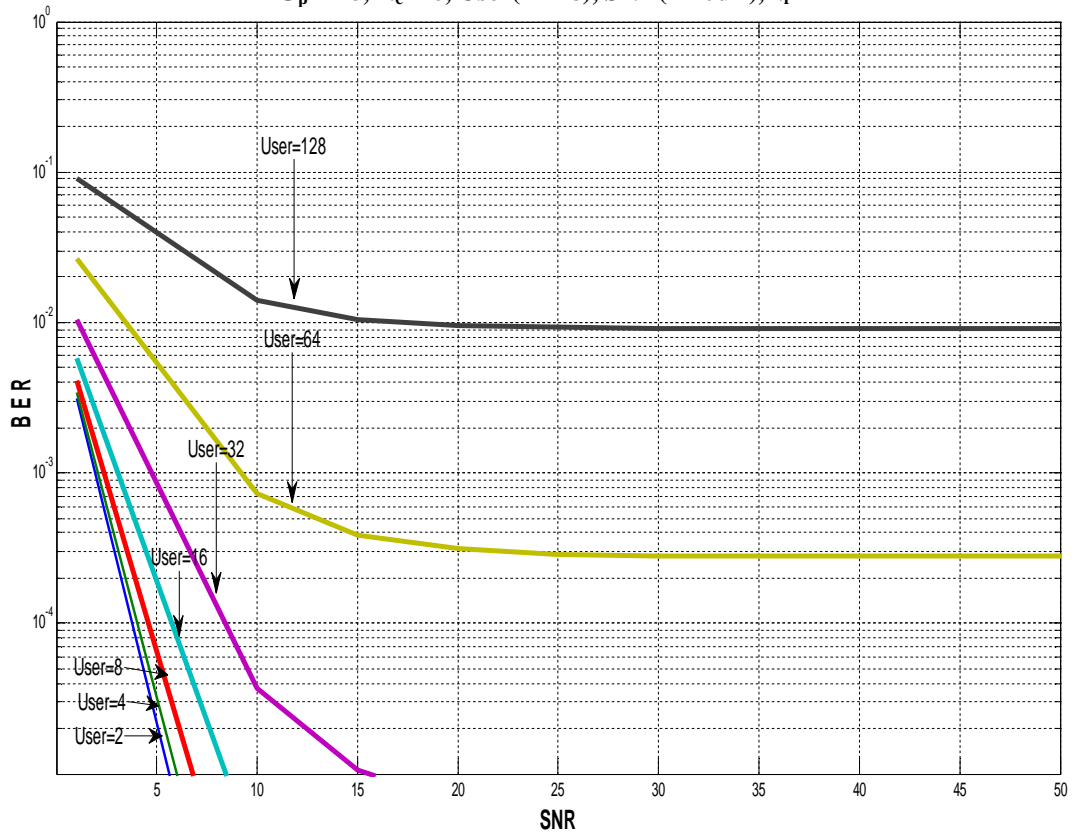
(b)

BER Vs SNR
 $G_p=128, N_c=8, \text{User}(2-128), \text{SNR}(1-70\text{dB}), N_r=4$

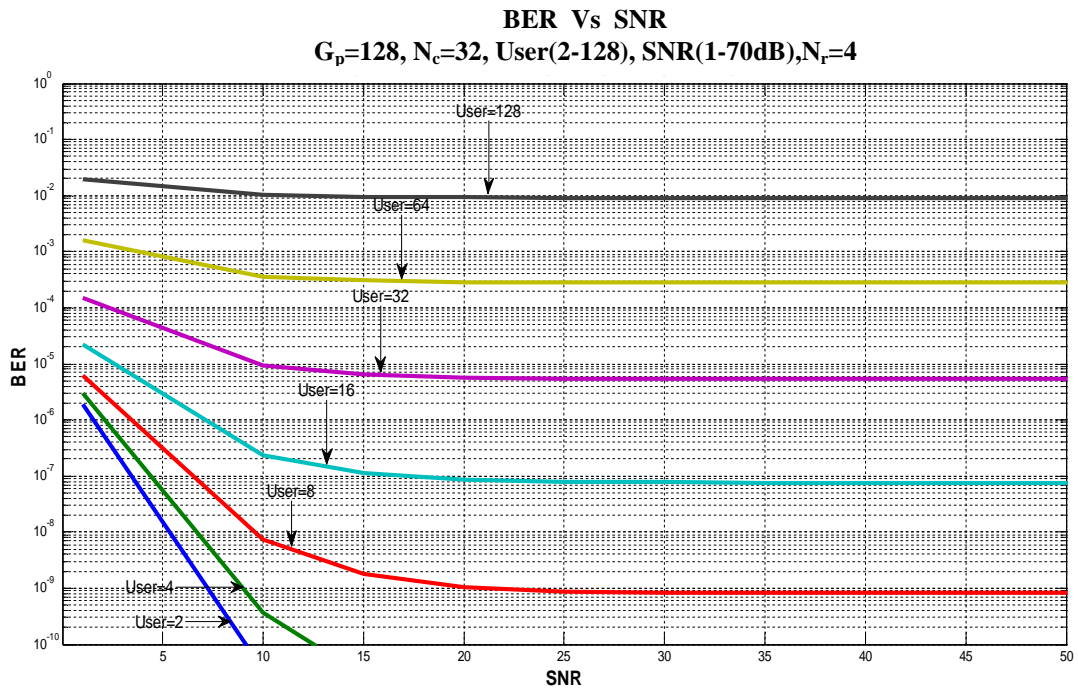


(c)

BER Vs SNR
 $G_p=128, N_c=16, \text{User}(2-128), \text{SNR}(1-70\text{dB}), N_r=4$



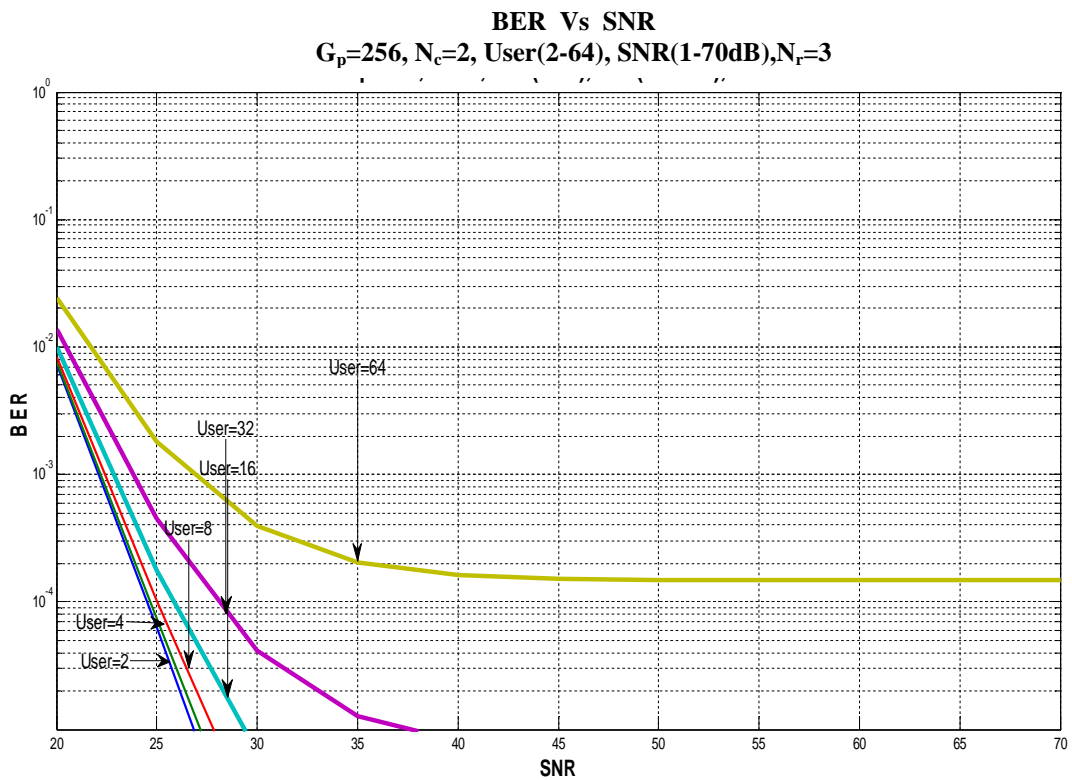
(d)



(e)

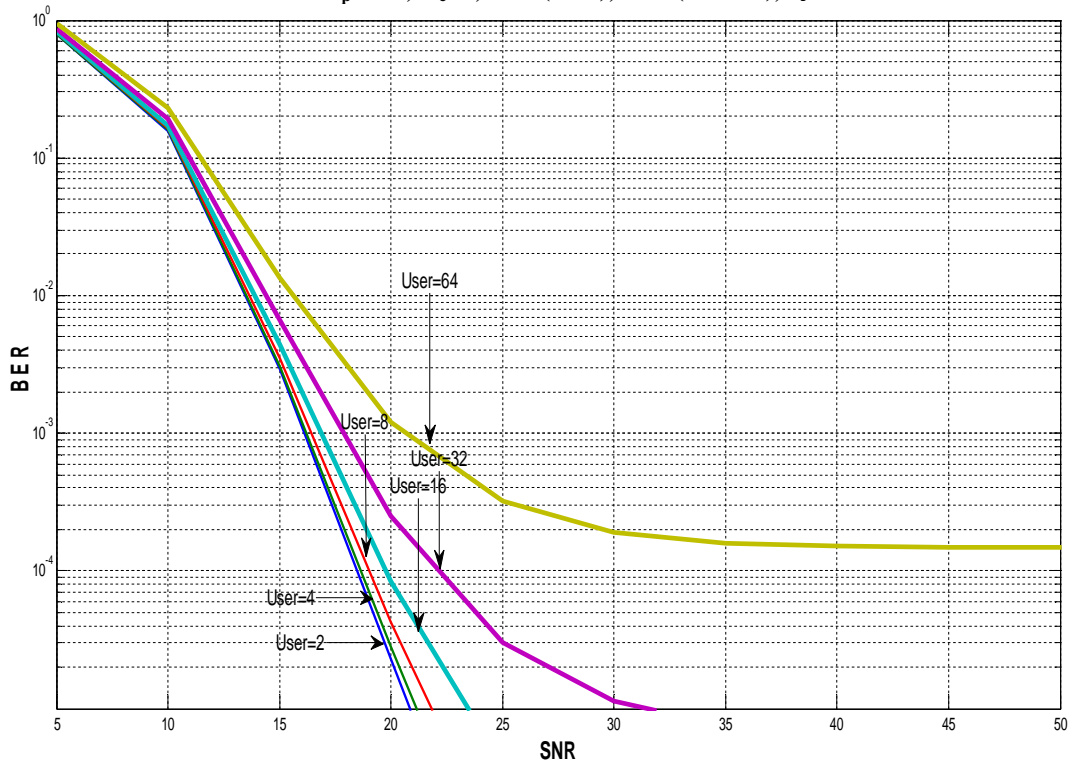
Fig. 4-8 Plots of BER Vs SNR for different number of subcarriers at fixed processing gain ($G_p=128$) with a rake receiver having number of rake fingers, $N_r=4$

4.4.3 BER Vs SNR for Different Number of Subcarriers at Fixed Processing Gain ($G_p=256$) with a Rake Receiver having Number of Rake Fingers, $N_r=3$



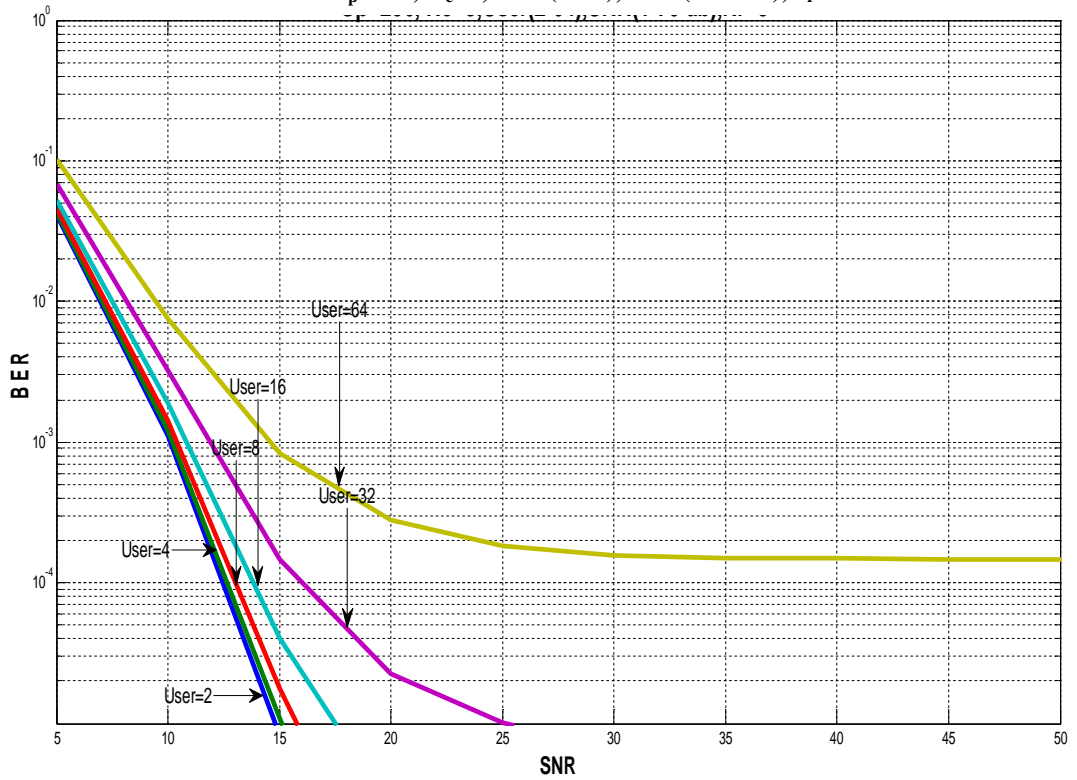
(a)

BER Vs SNR
 $G_p=256, N_c=4, \text{User}(2-64), \text{SNR}(1-70\text{dB}), N_r=3$



(b)

BER Vs SNR
 $G_p=256, N_c=8, \text{User}(2-64), \text{SNR}(1-70\text{dB}), N_r=3$



(c)

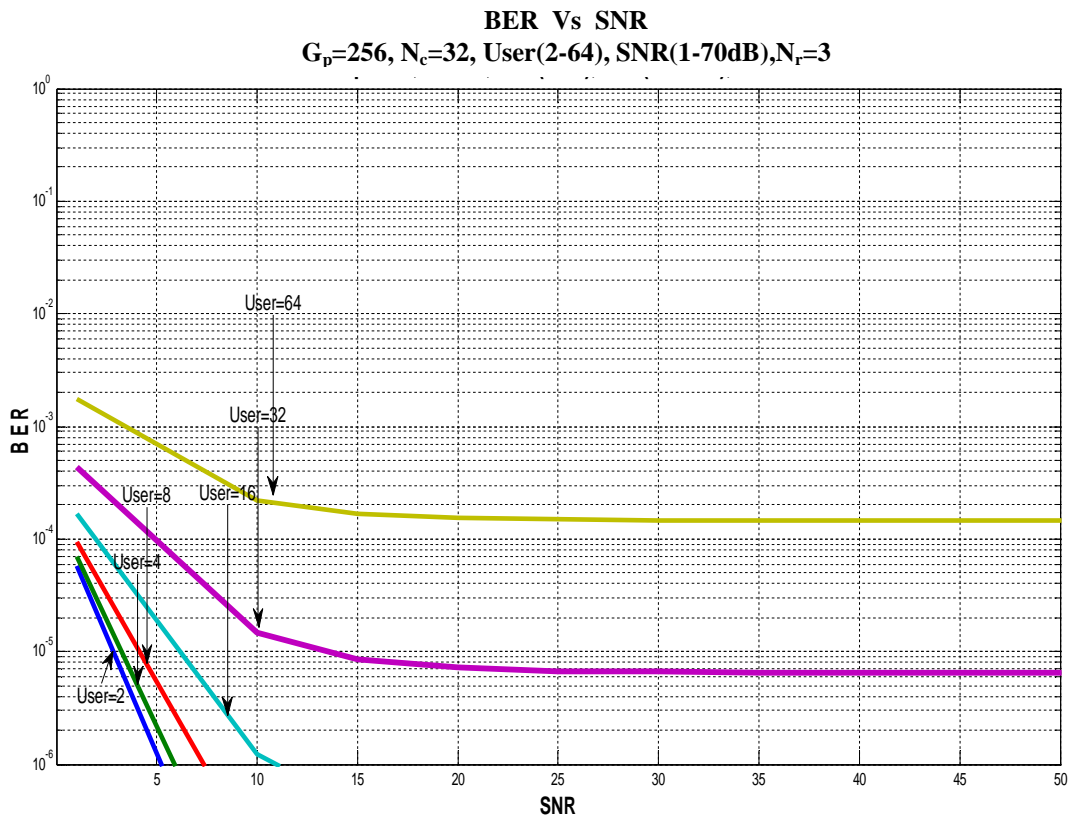
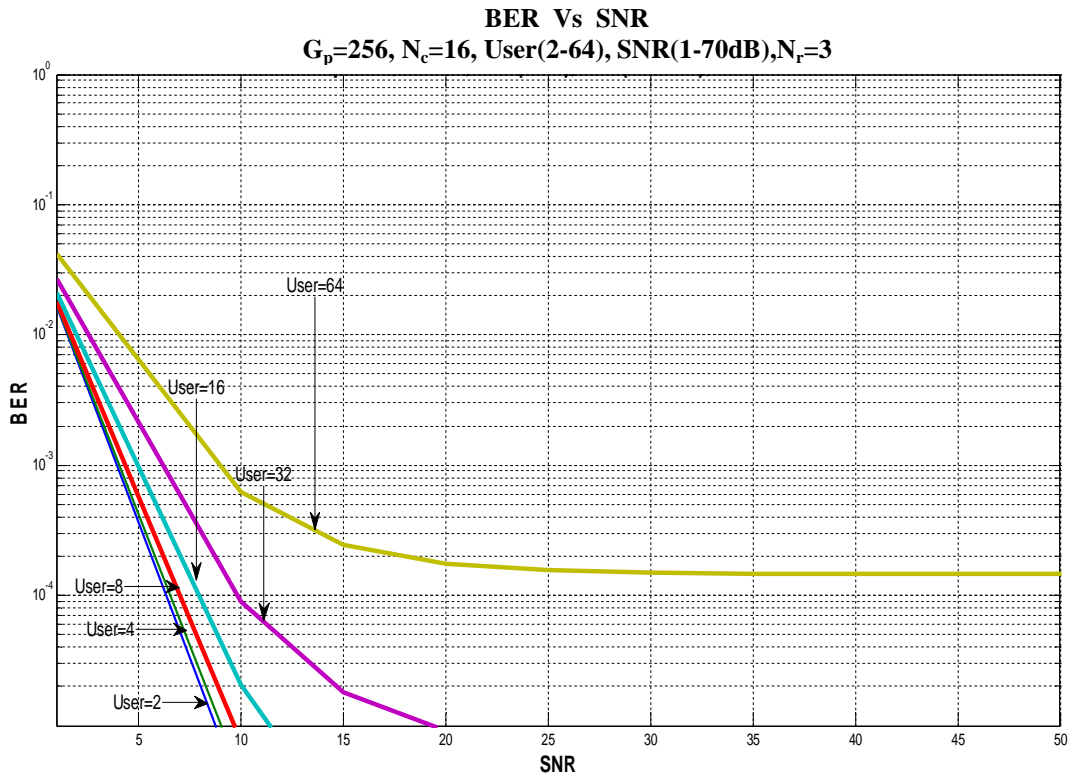
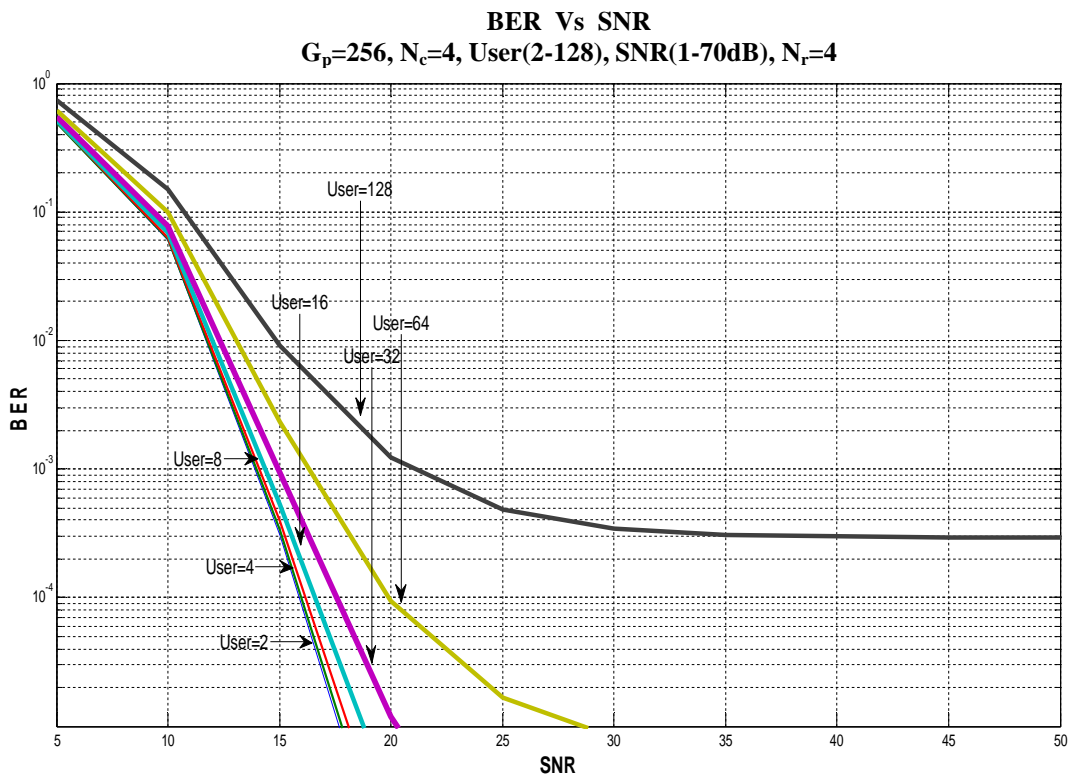
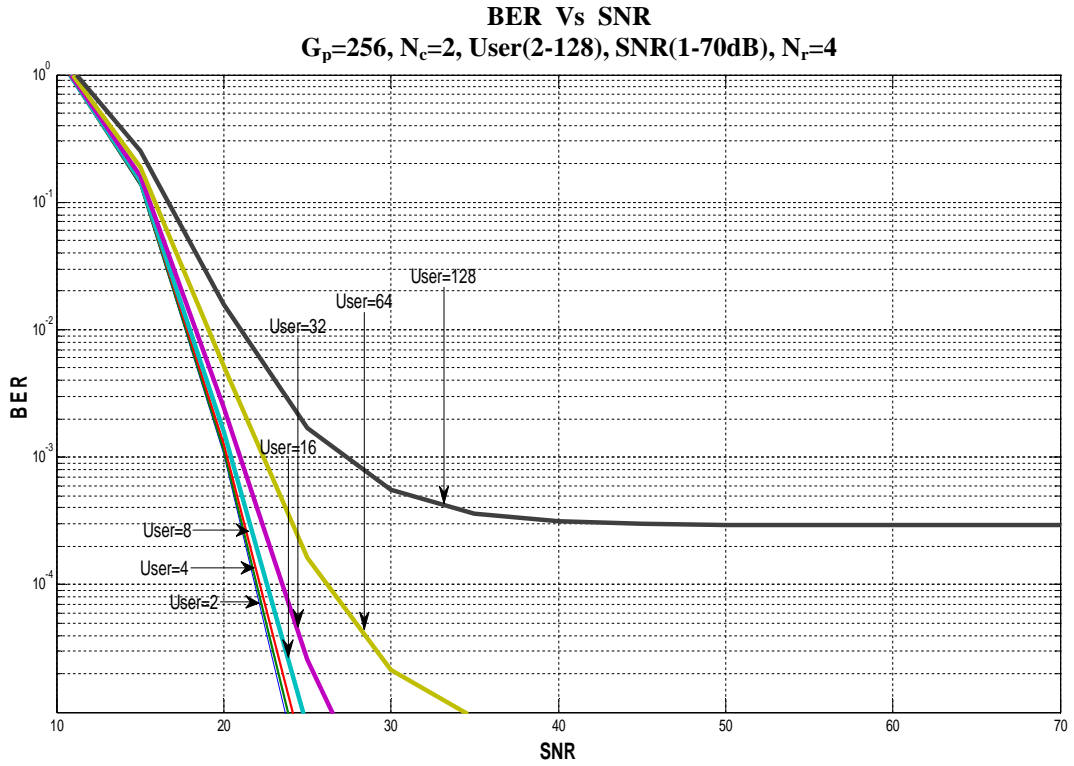
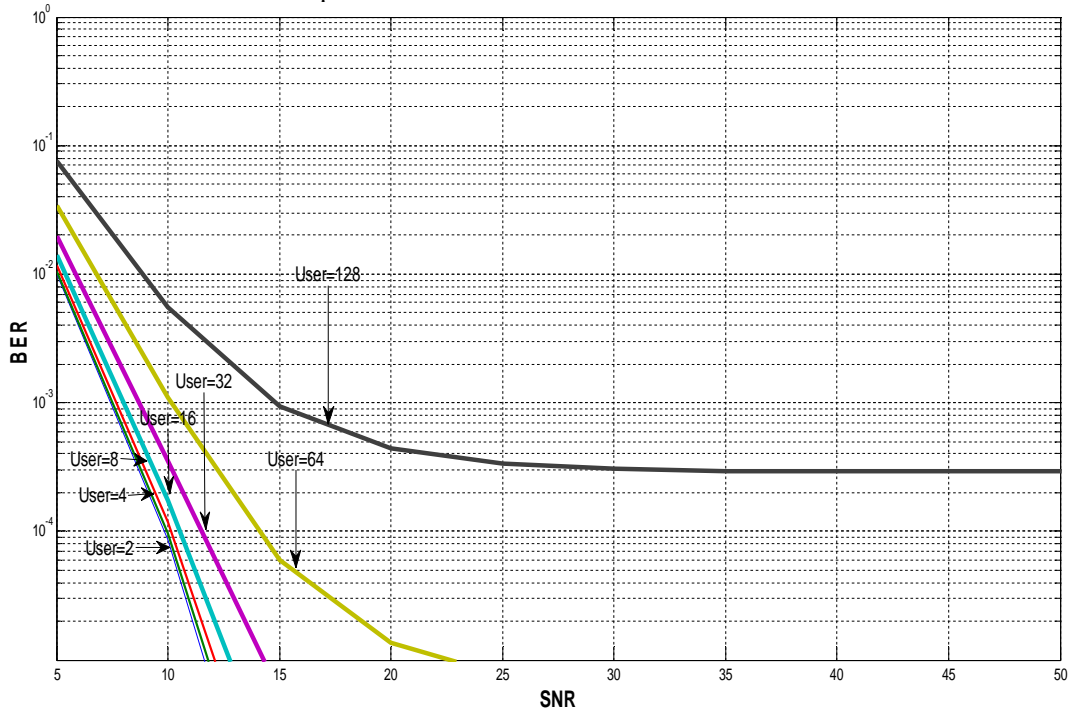


Fig. 4-9 Plots of BER Vs SNR for different number of subcarriers at fixed processing gain ($G_p=256$) with a rake receiver having number of rake fingers, $N_r=3$

4.4.4 BER Vs SNR for Different Number of Subcarriers at Fixed Processing Gain ($G_p=256$) with a Rake Receiver having Number of Rake Fingers, $N_r=4$

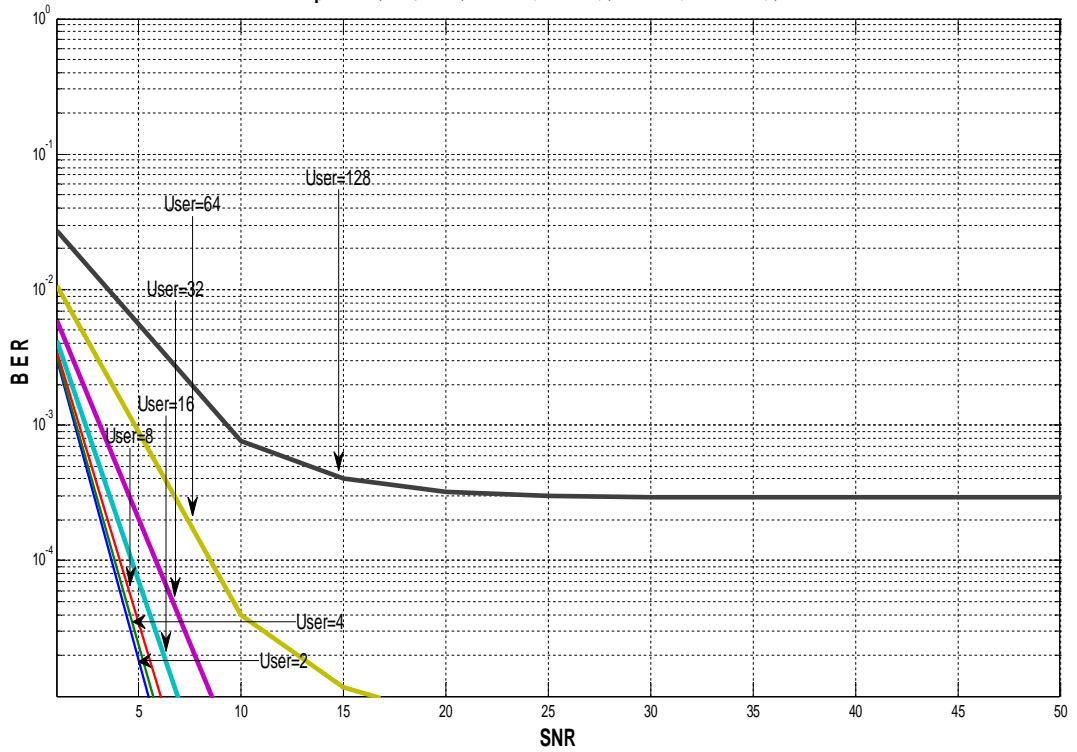


BER Vs SNR
 $G_p=256, N_c=8, \text{User}(2-128), \text{SNR}(1-70\text{dB}), N_r=4$

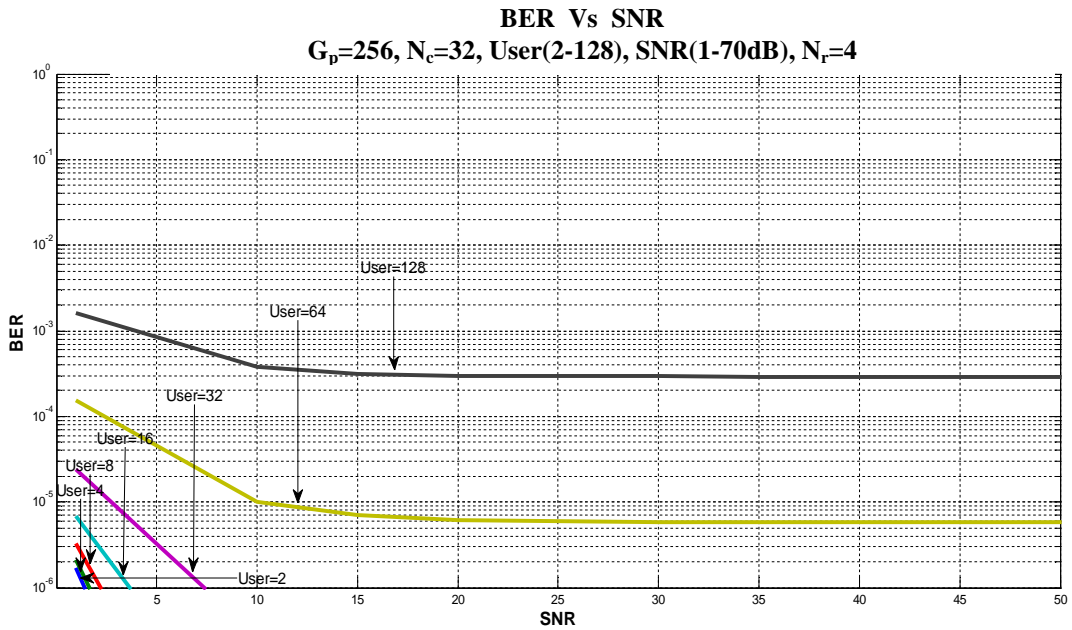


(c)

BER Vs SNR
 $G_p=256, N_c=16, \text{User}(2-128), \text{SNR}(1-70\text{dB}), N_r=4$



(d)

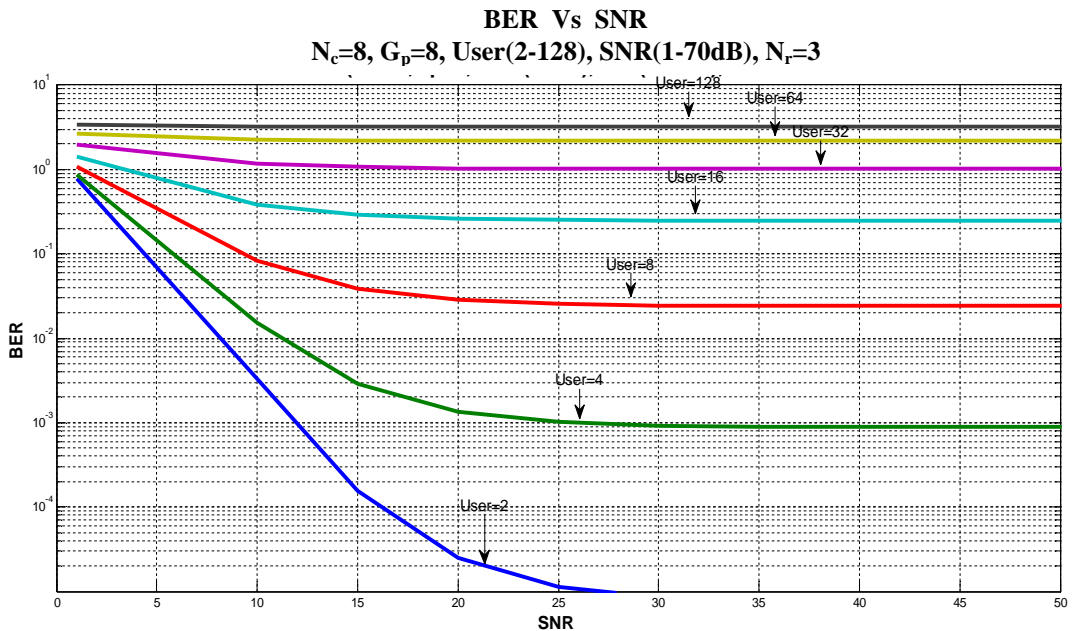


(e)

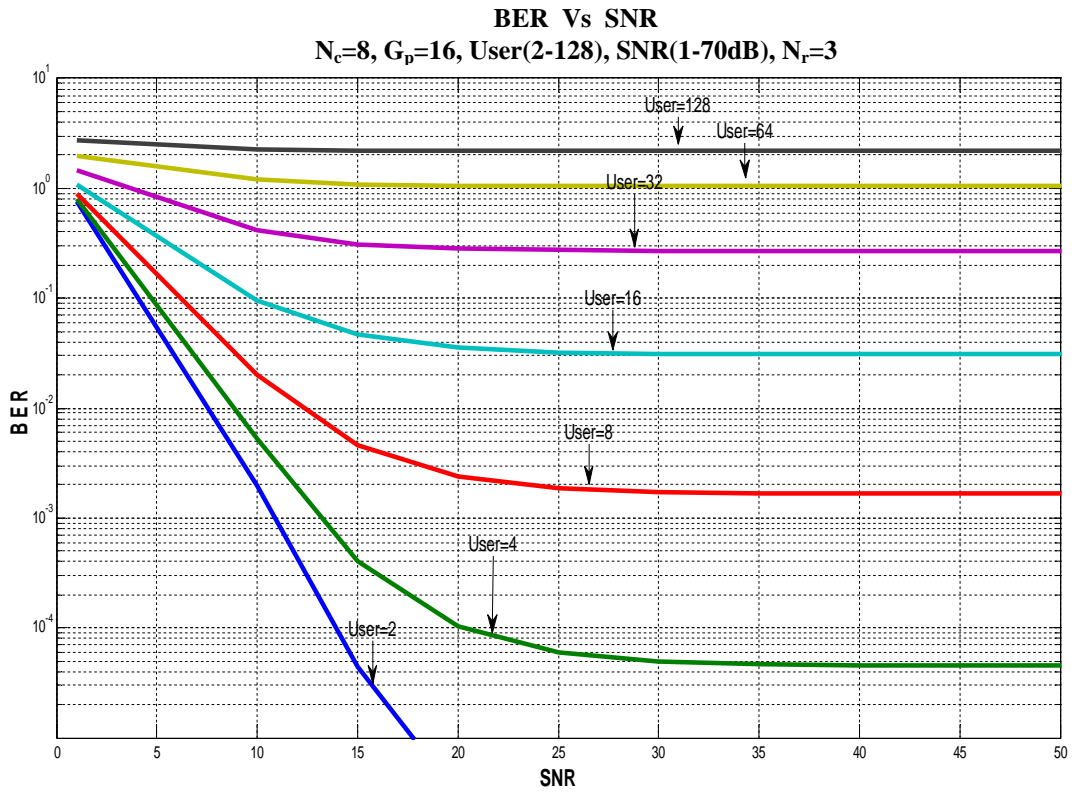
Fig. 4-10 Plots of BER Vs SNR for different number of subcarriers at fixed processing gain ($G_p=256$) with a rake receiver having number of rake fingers, $N_r=4$

4.4.5 BER Vs SNR for Different Processing Gains at Fixed Number of Subcarriers ($N_c=8$) with a Rake Receiver having Number of Rake Fingers, $N_r=3$

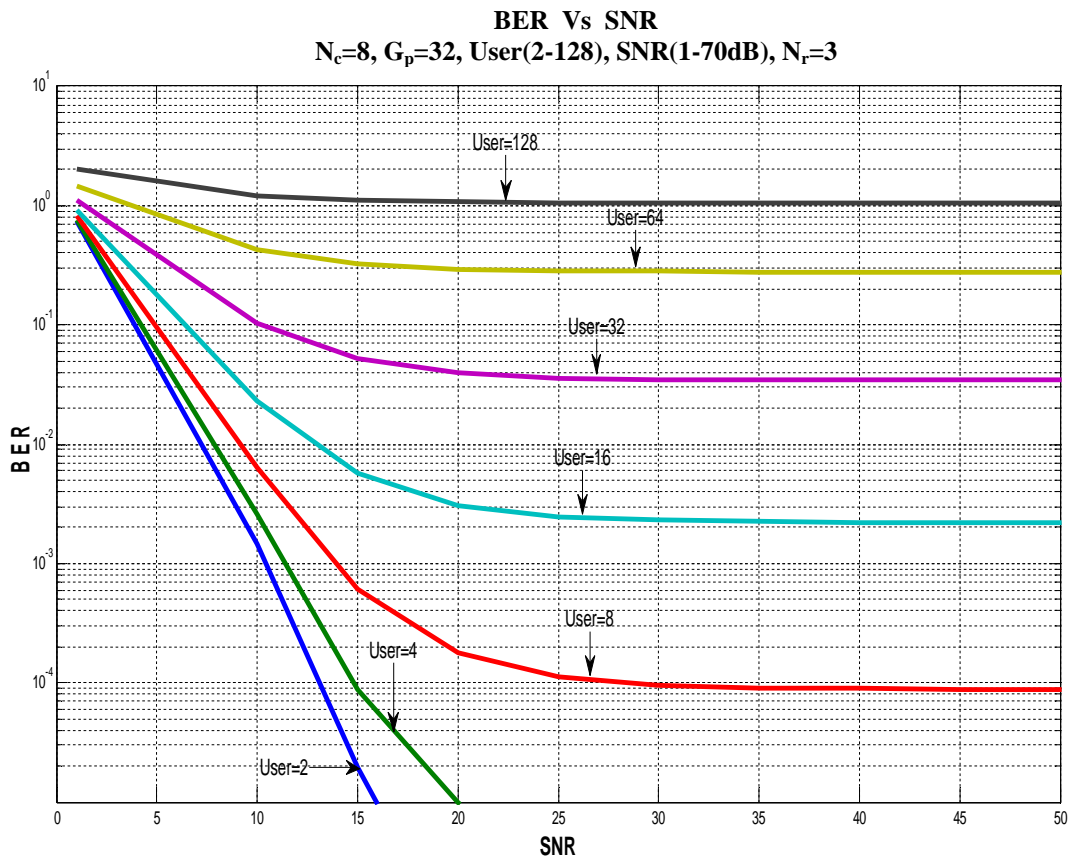
Results of BER versus SNR for a given value of N_c and N_r are shown in Fig. 4-11 for $N_r=3, N_c=8$ and in Fig. 4-12 for $N_r=4, N_c=8$ with G_p as a parameter ranging from 8 to 256. It is observed that there are improvement in system capacity at a given value of BER with increase in G_p as well as N_r . Achievable number of simultaneous user is found to be around 128 for $N_r=3, G_p=256$ and 256 corresponding to $N_r=4, G_p=256$ respectively.



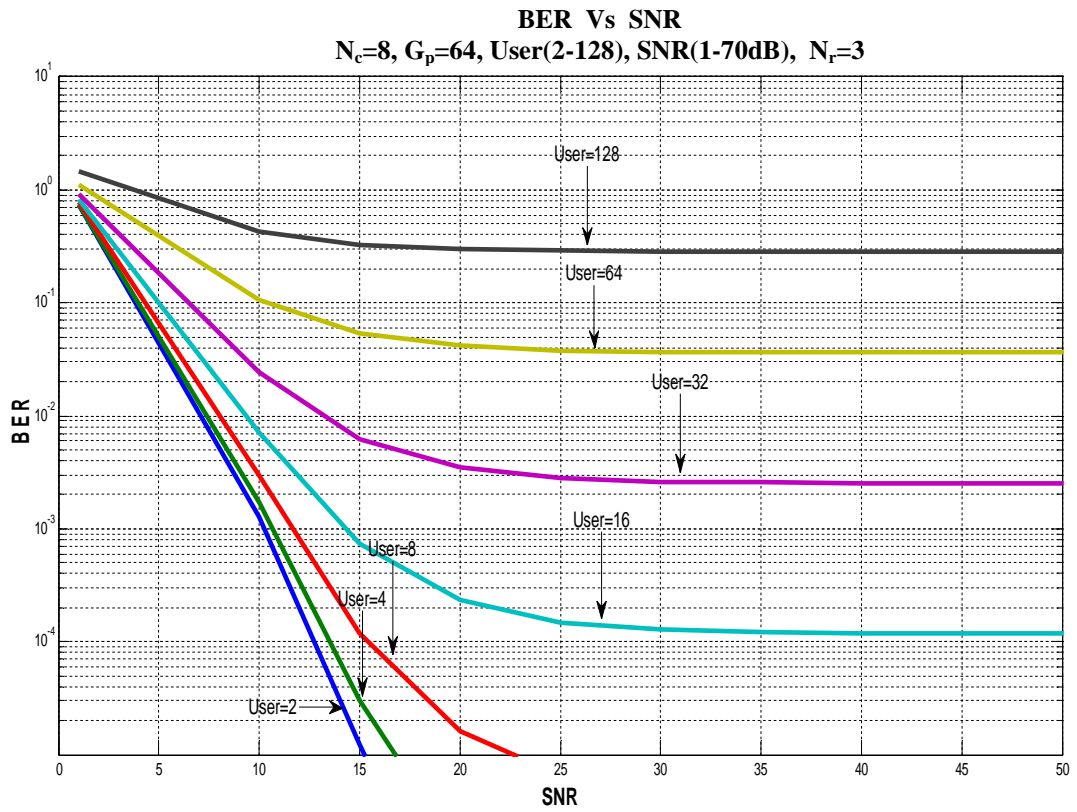
(a)



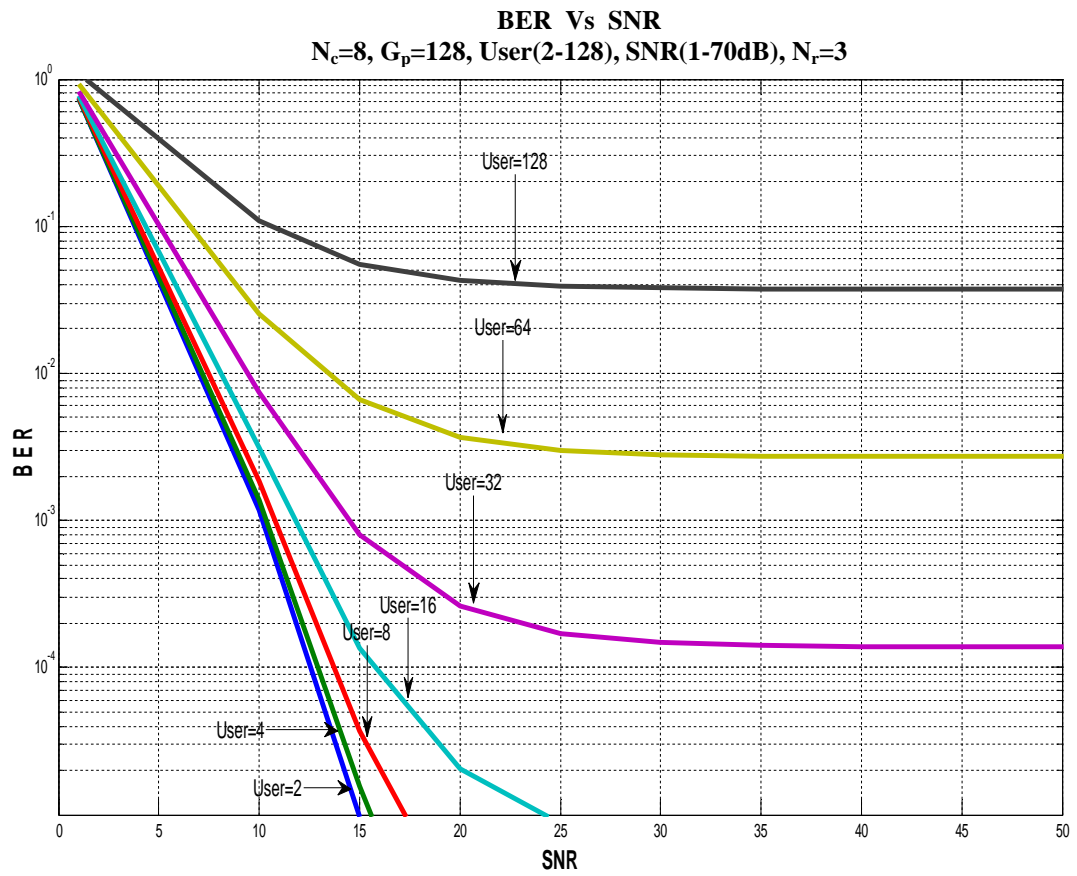
(b)



(c)



(d)



(e)

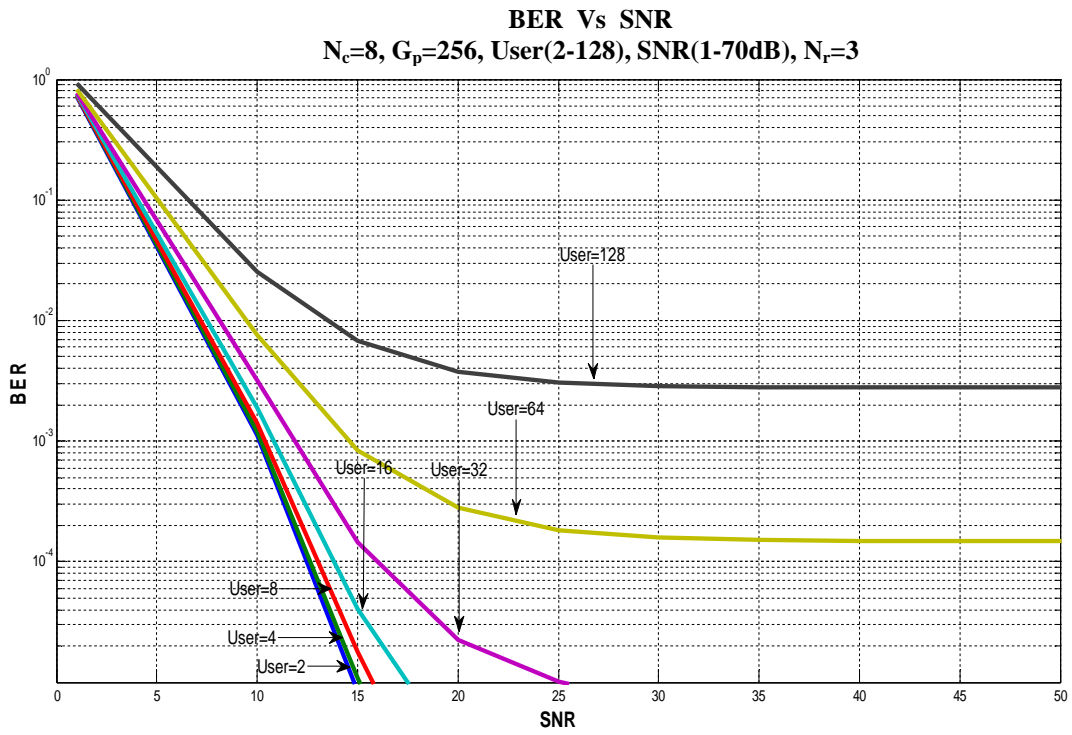
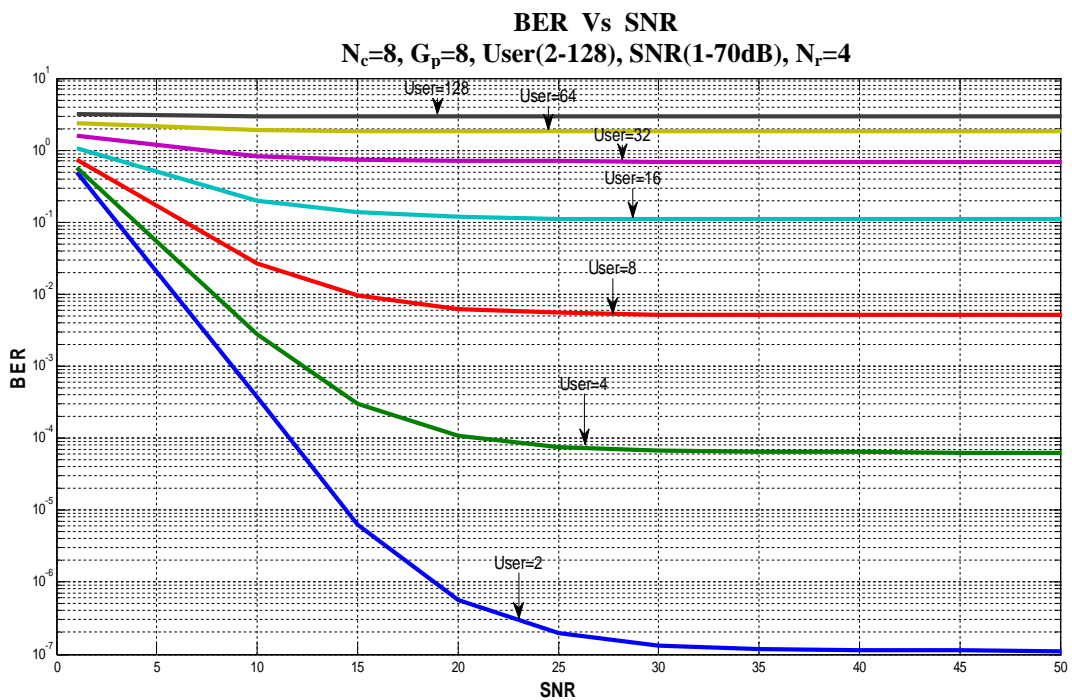
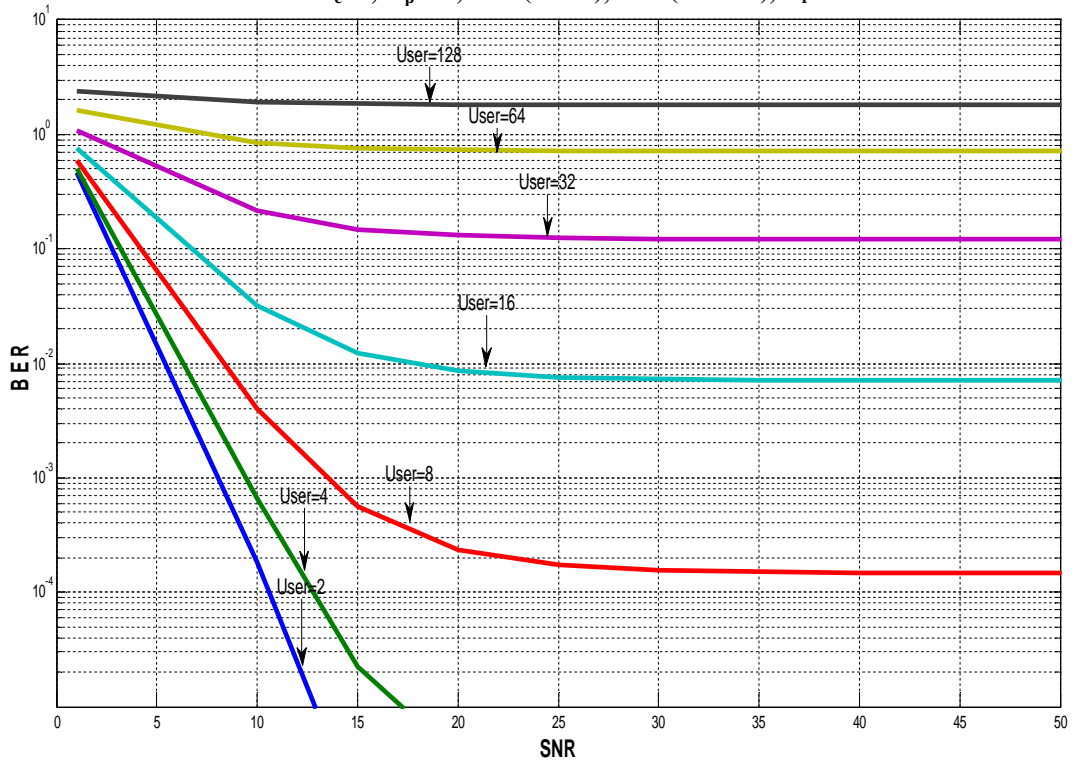


Fig. 4-11 Plots of BER Vs SNR for different processing gains at fixed number of subcarriers ($N_c=8$) with a rake receiver having number of rake fingers, $N_r=3$

4.4.6 BER Vs SNR for Different Processing Gains at Fixed Number of Subcarriers ($N_c=8$) with a Rake Receiver having Number of Rake Fingers, $N_r=4$

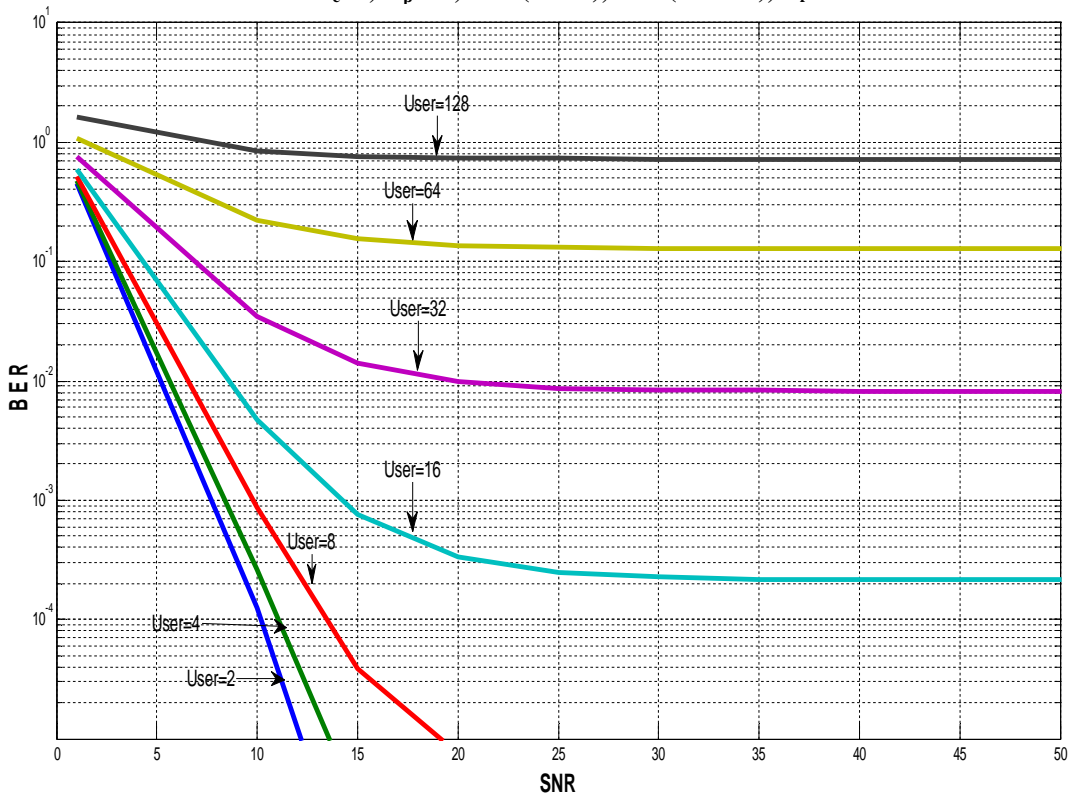


BER Vs SNR
 $N_c=8, G_p=16, \text{User}(2-128), \text{SNR}(1-70\text{dB}), N_r=4$



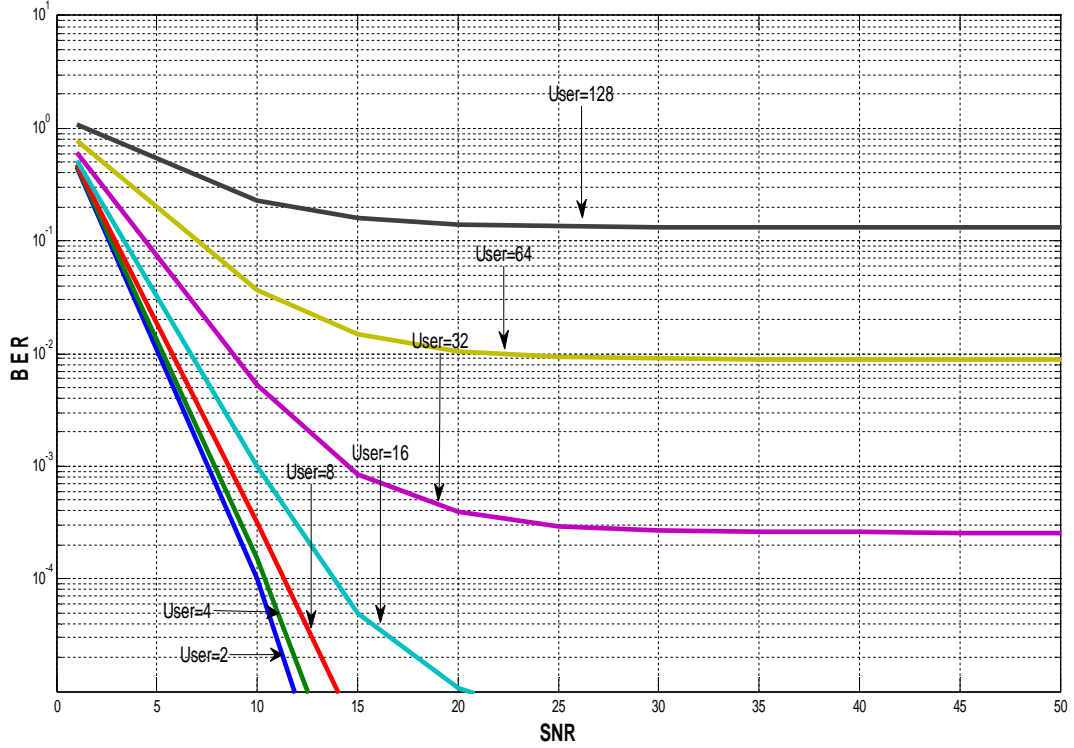
(b)

BER Vs SNR
 $N_c=8, G_p=32, \text{User}(2-128), \text{SNR}(1-70\text{dB}), N_r=4$



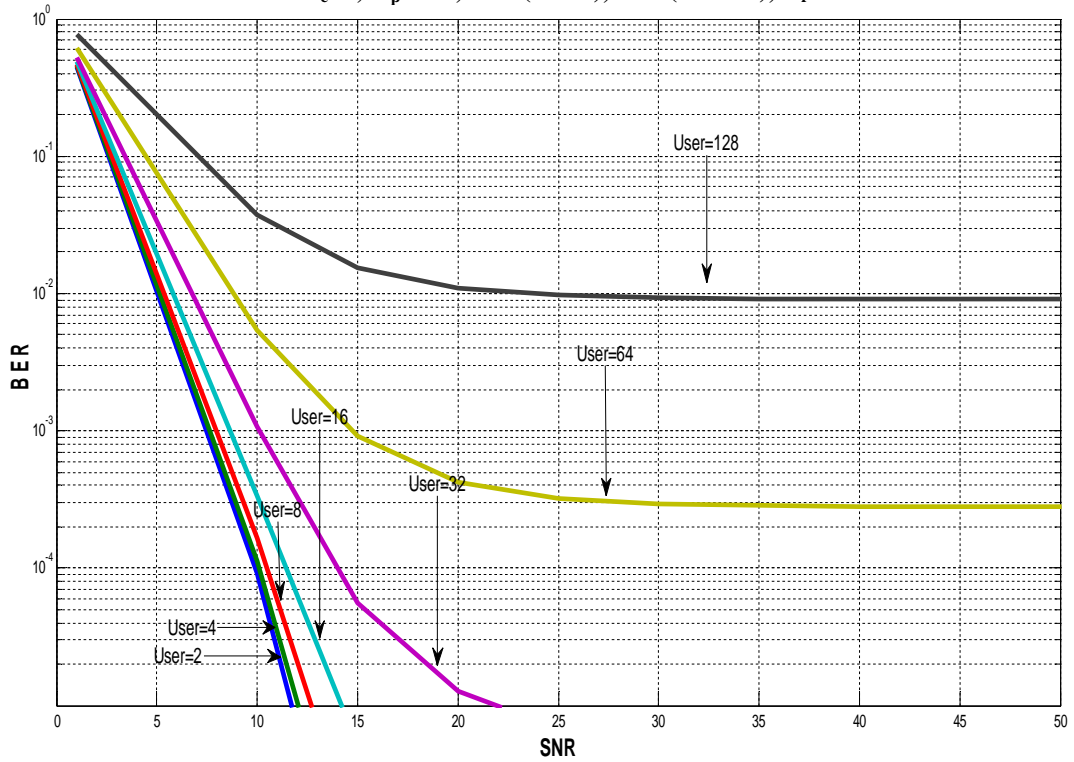
(c)

BER Vs SNR
 $N_c=8, G_p=64, \text{User}(2-128), \text{SNR}(1-70\text{dB}), N_r=4$



(d)

BER Vs SNR
 $N_c=8, G_p=128, \text{User}(2-128), \text{SNR}(1-70\text{dB}), N_r=4$



(e)

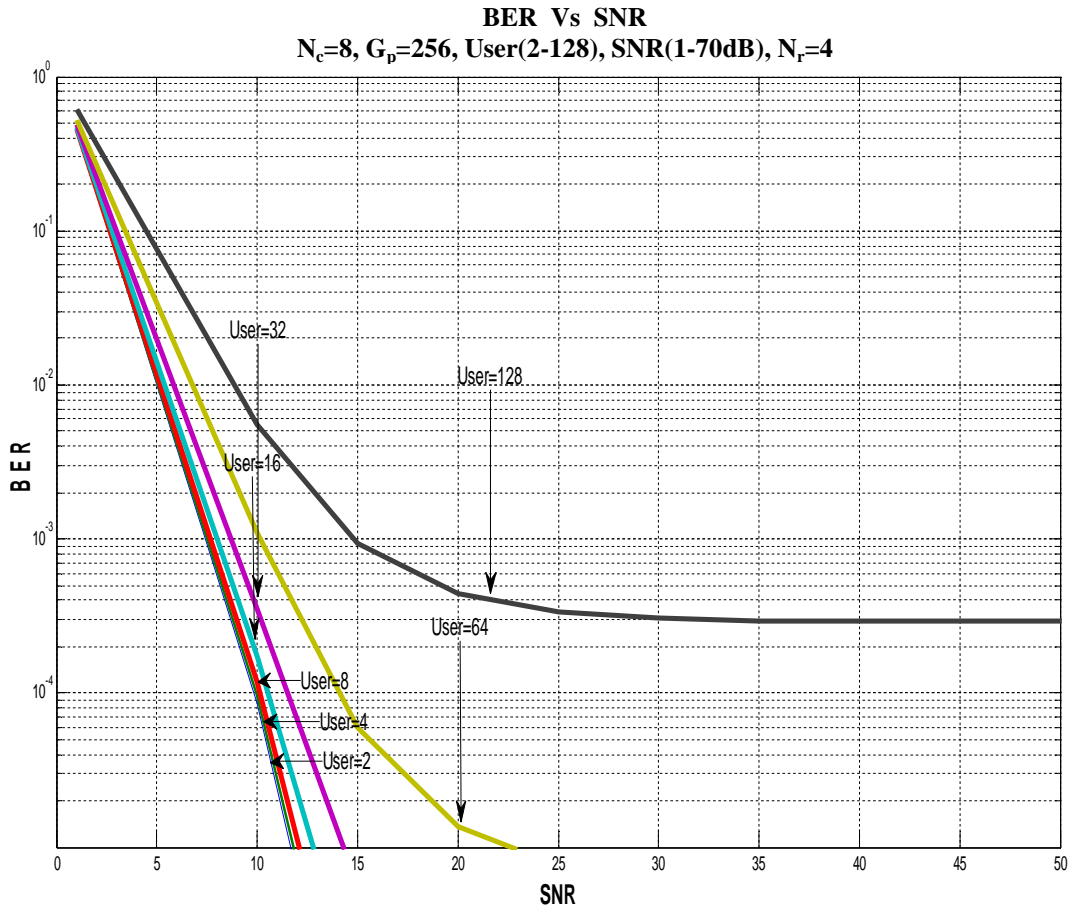


Fig. 4-12 Plots of BER Vs SNR for different processing gains at fixed number of subcarriers ($N_c=8$) with a rake receiver having number of rake fingers, $N_r=4$

4.5 Optimum System Parameters

Considering different system parameters, based on the BER performance curves shown in section 4.3 and 4.4, various relationships between system parameters have been computed to determine optimum system parameters. In this case, we consider BER performance level at 10^{-3} .

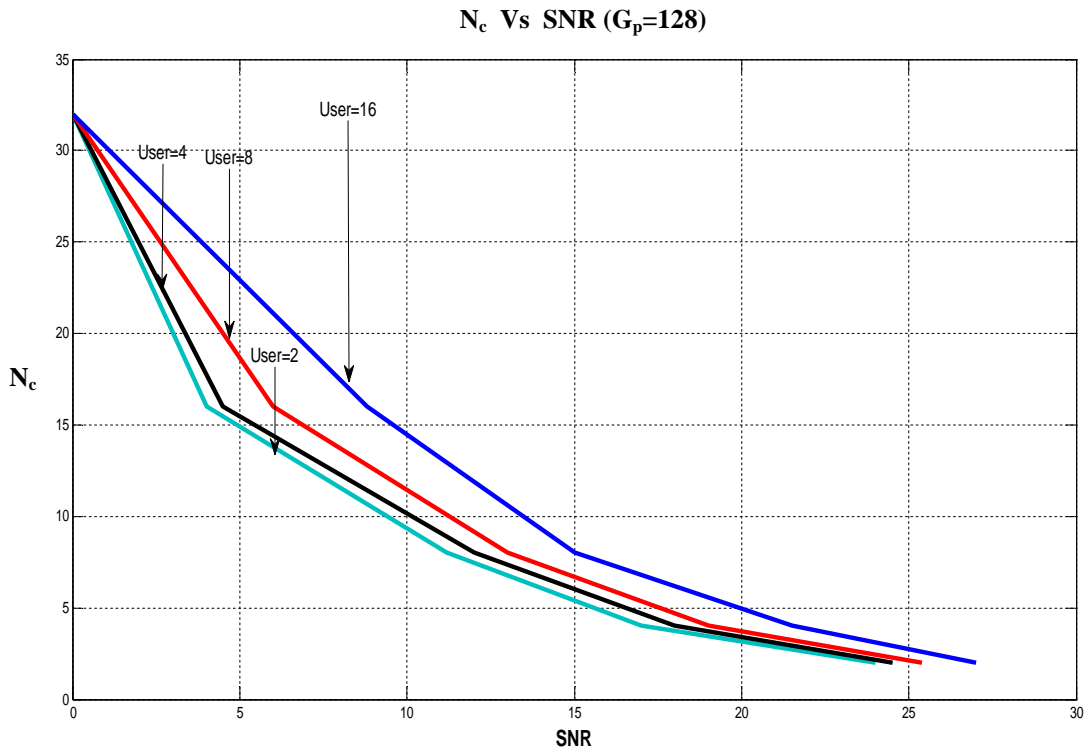
4.5.1 N_c (Subcarrier) Vs SNR for Different Users at G_p (Processing Gain)=128

The required receiver sensitivity to achieve a given $\text{BER}=10^{-3}$, for various combinations of number of subcarriers and number of users are depicted in Table 4-2 for the system with $G_p=128$ without diversity and with path diversity employing rake receiver with number of rake fingers, $N_r=3,4$.

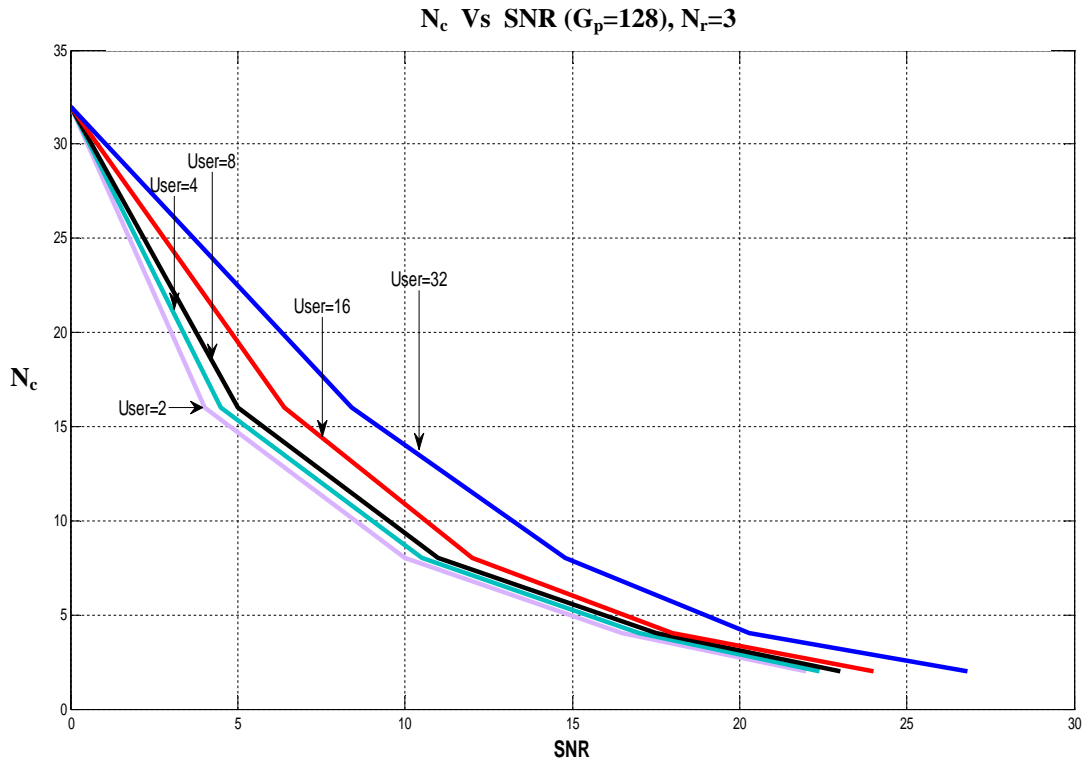
Table 4-2: Values of SNR(dB) corresponding to BER= 10⁻³, G_p=128

At BER=10 ⁻³																
N _c ↓	Without diversity					With diversity										
	Number of User →					Number of User with N _r =3 →					Number of User with N _r =4 →					
	2	4	8	16	32	2	4	8	16	32	2	4	8	16	32	64
2	24	24.5	25.4	27	40.2	22	22.4	23	24	26.8	20	20.5	21	21.4	22.2	24.2
4	17	18	19	21.5	34.8	16.5	17	17.5	18	20.3	13	13.2	14	15	16.3	20.5
8	11.2	12	13	15	28	10	10.5	11	12	14.8	7	7.4	8	9	10.5	14.5
16	4	4.5	6	8.8	23.8	4	4.5	5	6.4	8.4	2	2.2	3	4	4.9	9

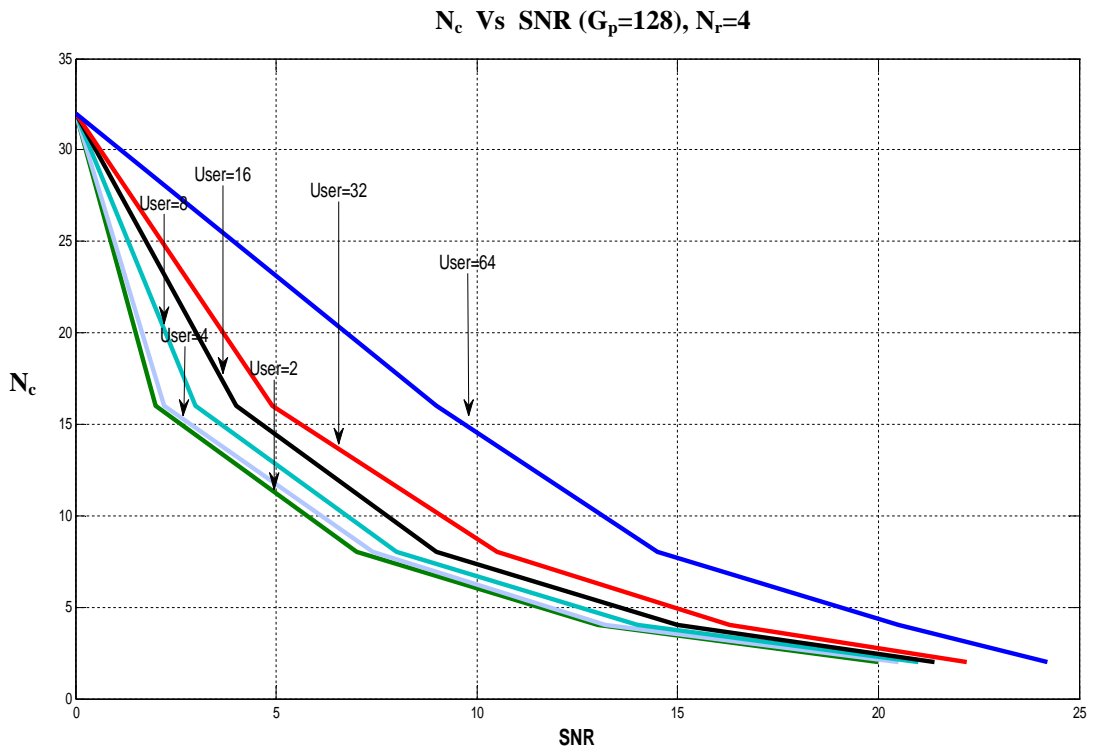
The results are also depicted in terms of plots of N_c versus required SNR(dB) in Fig. 4-13(a) through Fig. 4-13(c) for given G_p=128 and N_r=1,3,4 respectively for BER=10⁻³. It is noticed that at BER=10⁻³ the required SNR(dB) is drastically less at higher values of N_c for a given number of users. Further, at given BER=10⁻³, and at a given SNR(dB), more user can be supported by increasing the number of subcarriers, N_c. Diversity provides further improvement in the number of simultaneous user. For example, without diversity, the number of user that can be supported is about 4 for N_c=10 and is 16 for N_c=15. With diversity, for N_r=3, the above number of user is around 32 and for N_r=4, it is around 64.



(a)



(b)

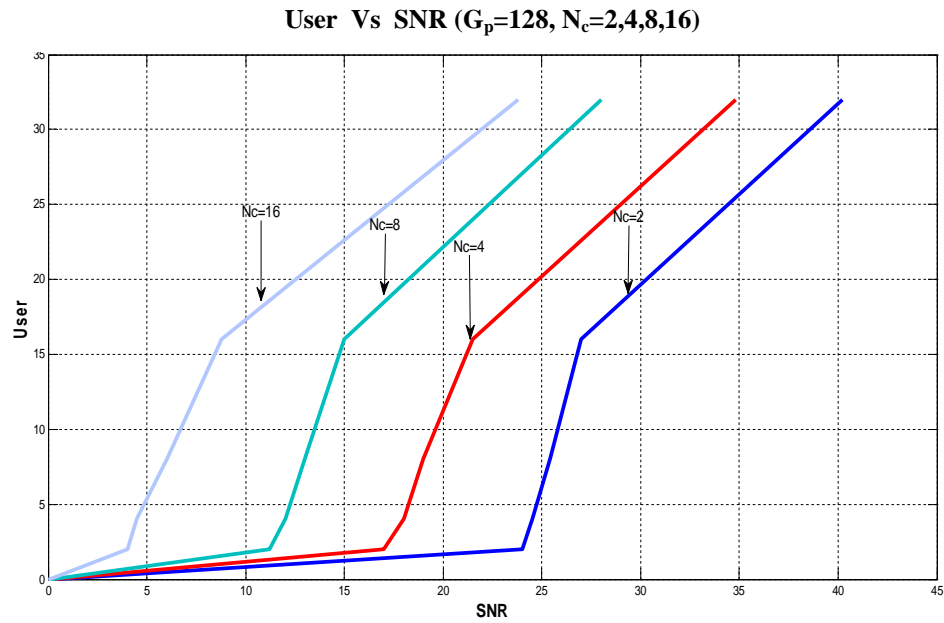


(c)

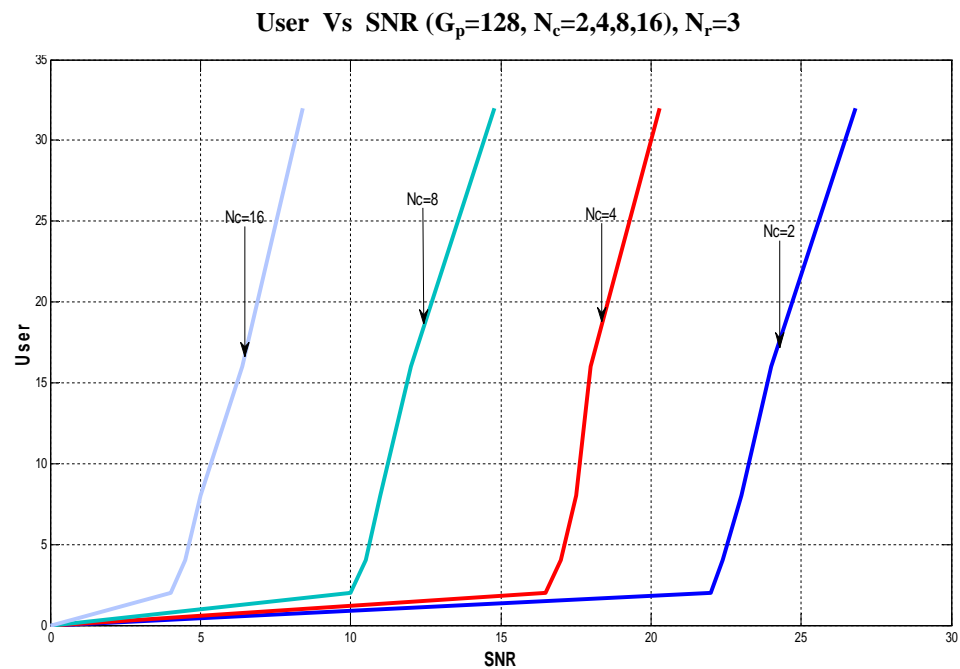
Fig. 4-13 N_c (Subcarrier) Vs SNR for different users at G_p (Processing gain)=128

4.5.2 User Vs SNR for Different Number of Subcarriers (N_c) at $G_p=128$

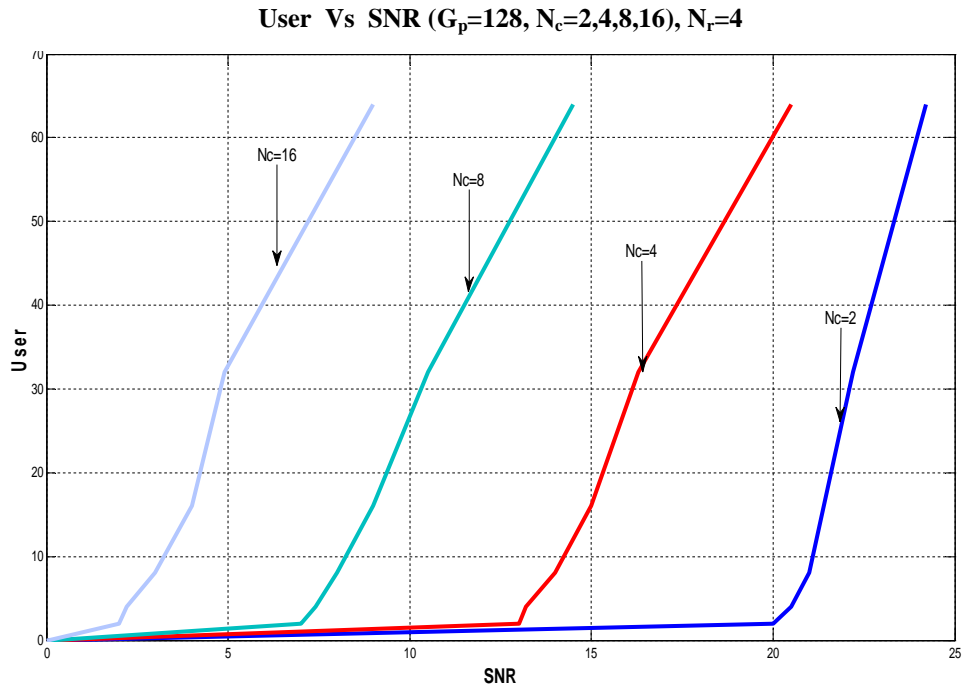
The achievable number of simultaneous users in a MC DS-CDMA PLC system at a given $BER=10^{-3}$ are shown in Fig. 4-14(a) as a function of required receiver sensitivity SNR(dB) with number of subcarriers, N_c as a parameter corresponding to $G_p=128$. The similar results with rake receiver are shown in Fig. 4-14(b) and Fig. 4-14(c) for $N_r=3$ and 4 respectively. The results are very much useful for design a MC DS-CDMA system over a PL channel.



(a)



(b)



(c)

Fig. 4-14 User Vs SNR for different number of subcarriers (N_c) at $G_p=128$

4.5.3 Subcarrier (N_c) Vs User for a Certain SNR (15dB) at $G_p=128$

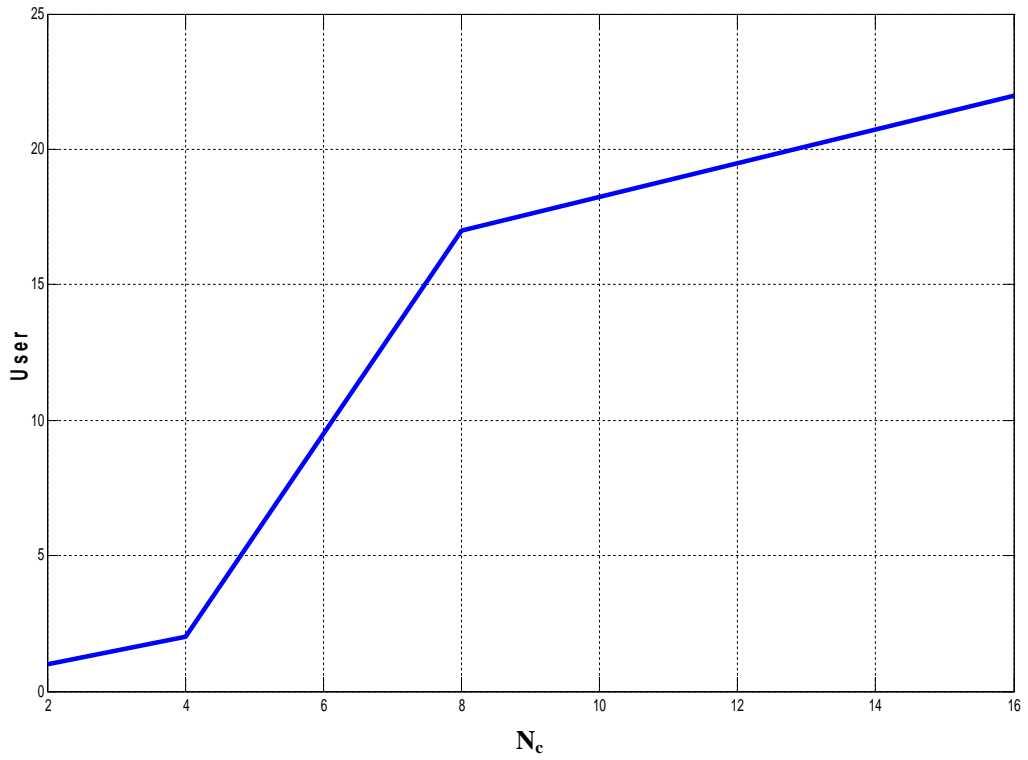
The variation of number of users with the number of subcarriers at a given SNR(dB) are depicted in Table 4-3 for SNR(dB)=15 without diversity and with diversity employing rake receiver with rake fingers, $N_r=3$ and 4.

Table 4-3: Number of users at different number of subcarriers (at SNR=15 dB), $G_p=128$

SNR (15 dB)			
N_c	Without diversity	With diversity	
	User	User with $N_r=3$	User with $N_r=4$
2	1	2	2
4	2	3	16
8	17	32	68
16	22	57	100

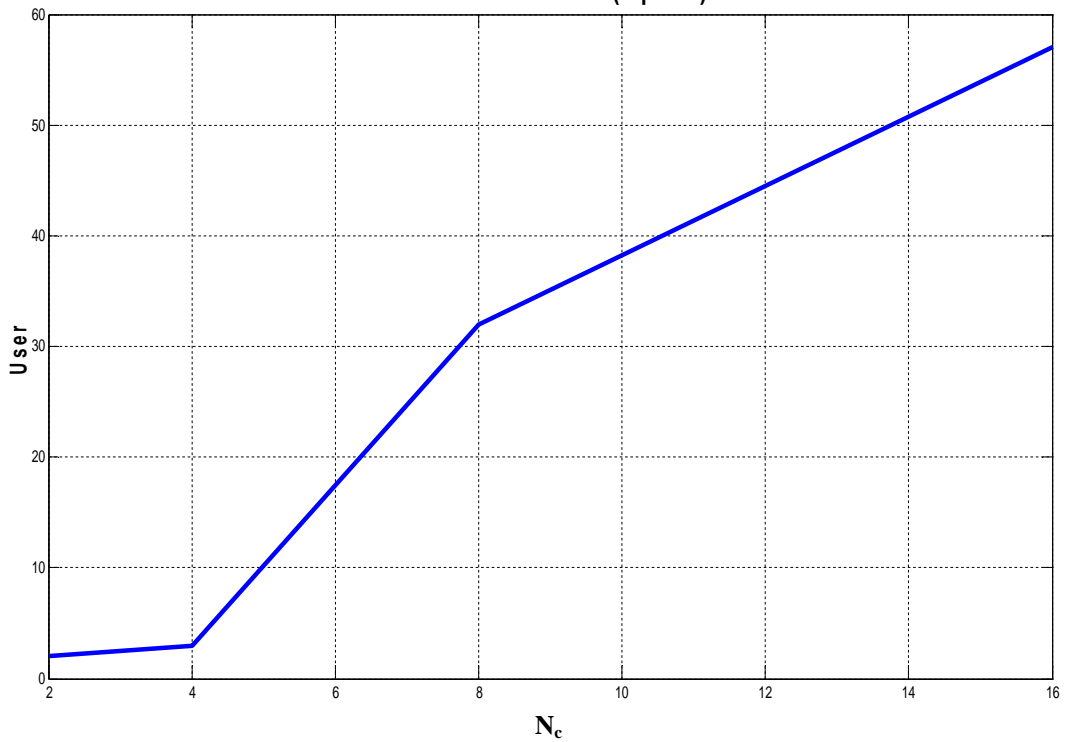
The results are also plotted in Fig. 4-15(a) through 4-15(c). The results verifying the improvements in system performance in terms of capacity due to diversity.

N_c Vs User at SNR=15dB ($G_p=128$)

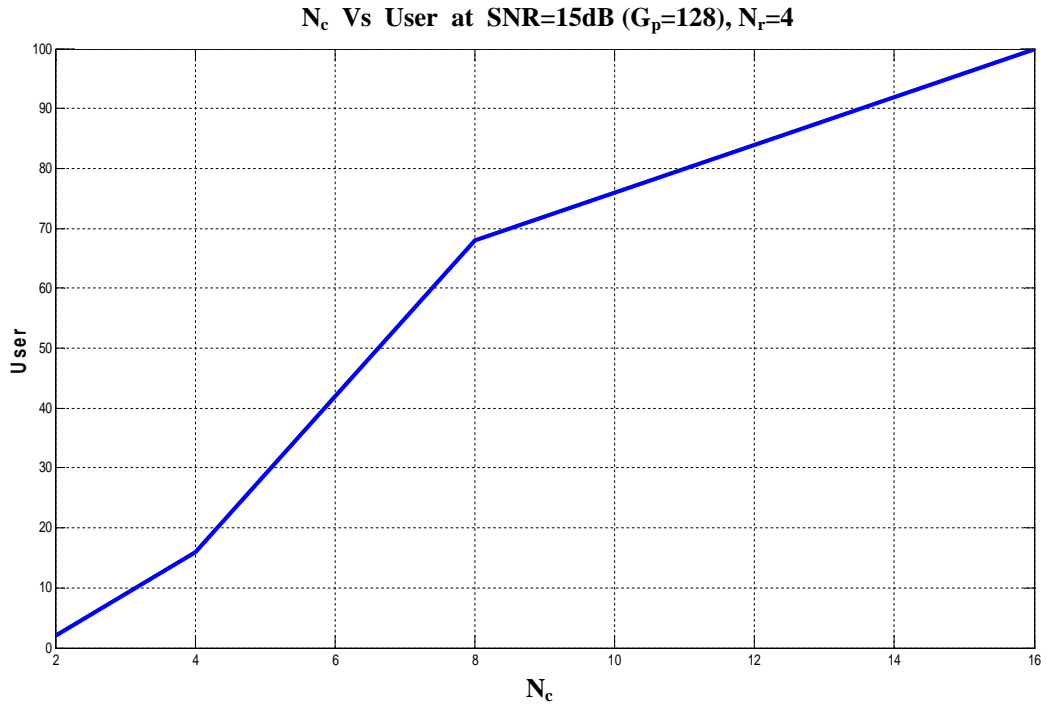


(a)

N_c Vs User at SNR=15dB ($G_p=128$), $N_r=3$



(b)



(c)

Fig. 4-15 Subcarrier (N_c) Vs User for a certain SNR (15dB) at $G_p=128$

4.5.4 N_c (Subcarrier) Vs SNR for Different Users at G_p (Processing Gain)=256

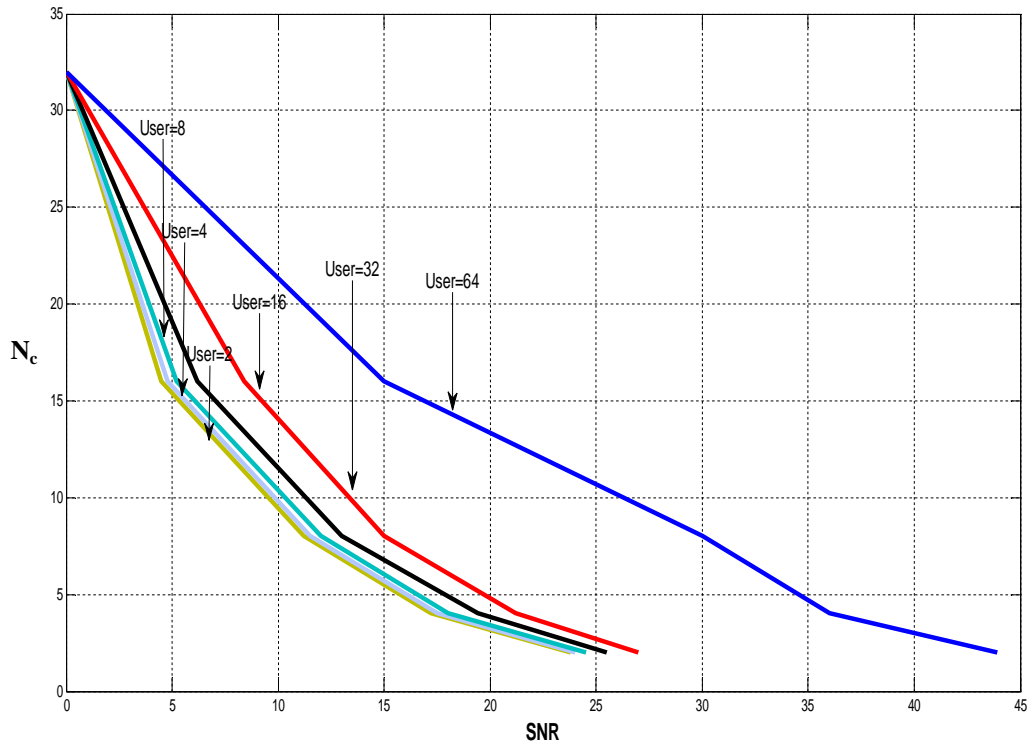
Similar results for the required receiver sensitivity to achieve a given $BER=10^{-3}$, for various combination of number of subcarriers and number of users are depicted in Table 4-4 for a system with $G_p=256$ without diversity and with path diversity employing rake receiver with number of rake fingers $N_r=3,4$.

Table 4-4: Values of SNR(dB) corresponding to $BER=10^{-3}$, $G_p=256$

N_c ↓	At $BER=10^{-3}$																		
	Without diversity						With diversity												
	Number of User →						Number of User with $N_r=3$ →						Number of User with $N_r=4$ →						
	2	4	8	16	32	64	2	4	8	16	32	64	2	4	8	16	32	64	128
2	23.8	24	24.5	25.5	27	43.9	21.5	21.7	22	22.5	23.9	26.5	19.9	20	20.3	20.5	21.2	23.0	26.2
4	14	15	16	17.2	20.2	36	13	13.2	14.5	16.5	18	20.8	12.8	13	14	14.2	15	16.8	20.5
8	10.2	10.5	11	12	14	29	9	9.2	9.5	10	11	13.8	6.2	6.4	6.8	7	8	9.4	13.9
16	4.5	4.8	5.2	6.2	8.4	15	2.5	3	3.4	4	5	9	1.5	1.8	2	2.4	3	5	9

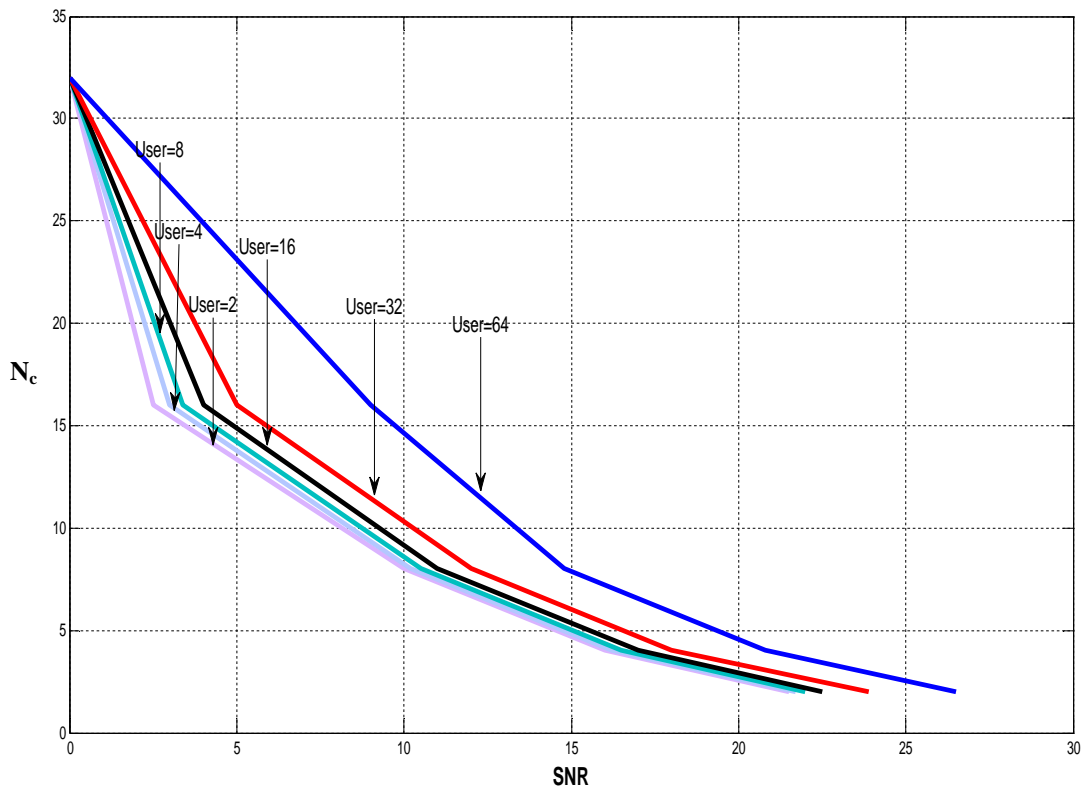
The results are also depicted in terms of plots of N_c versus required SNR(dB) in Fig. 4-16(a) through Fig. 4-16(c) for given $G_p=256$ and $N_r=1,3,4$ respectively for $BER=10^{-3}$. It is noticed that at $BER=10^{-3}$ in comparison to $G_p=128$, at a given SNR(dB), more user can be supported by increasing the number of subcarriers, N_c . Diversity provides further improvement in the number of simultaneous user.

N_c Vs SNR ($G_p=256$)



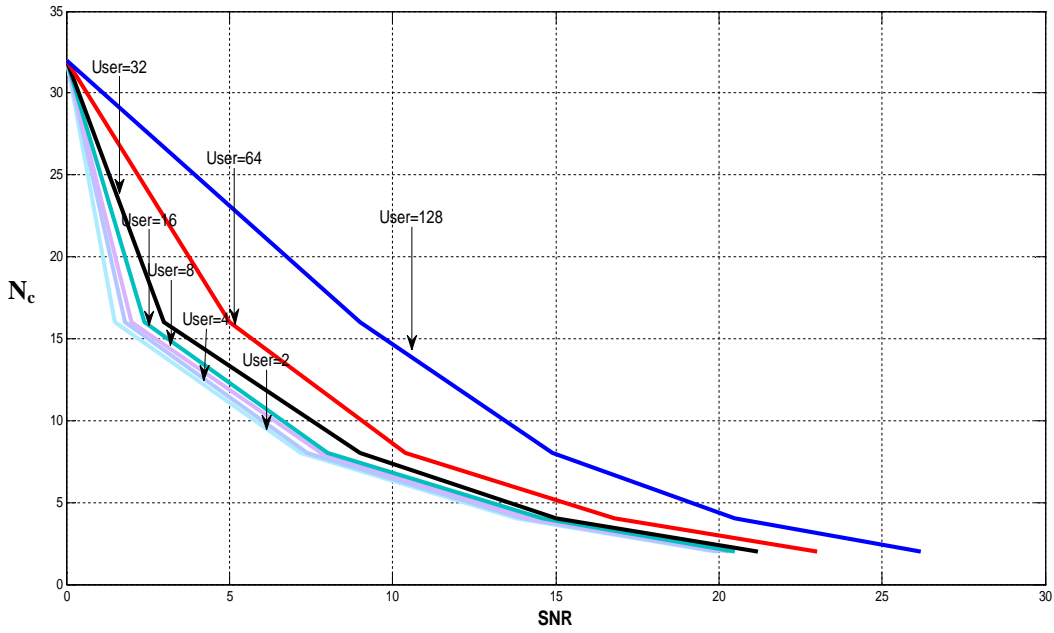
(a)

N_c Vs SNR ($G_p=256$, $N_r=3$)



(b)

N_c Vs SNR ($G_p=256$, $N_r=4$)



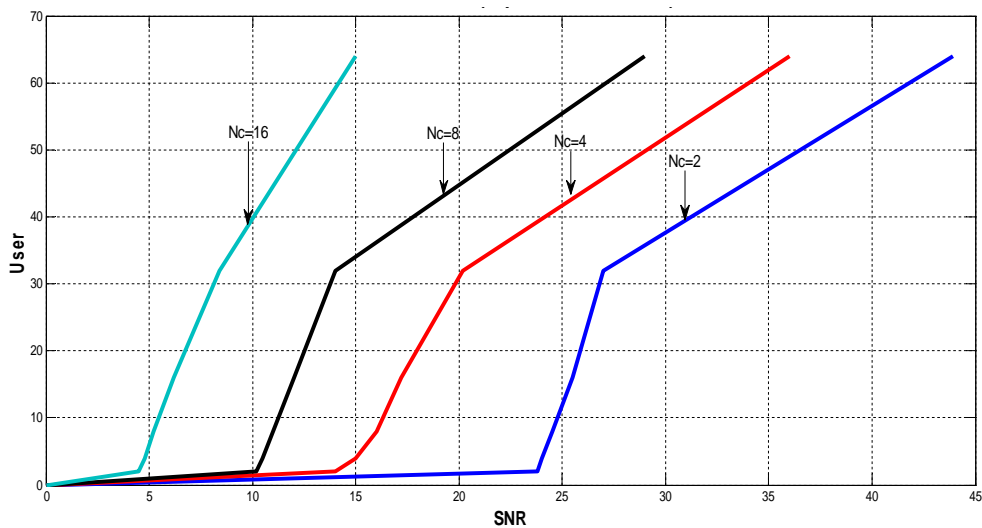
(c)

Fig. 4-16 N_c (Subcarrier) Vs SNR for different users at G_p (Processing gain)=256

4.5.5 User Vs SNR for Different Number of Subcarriers (N_c) at $G_p=256$

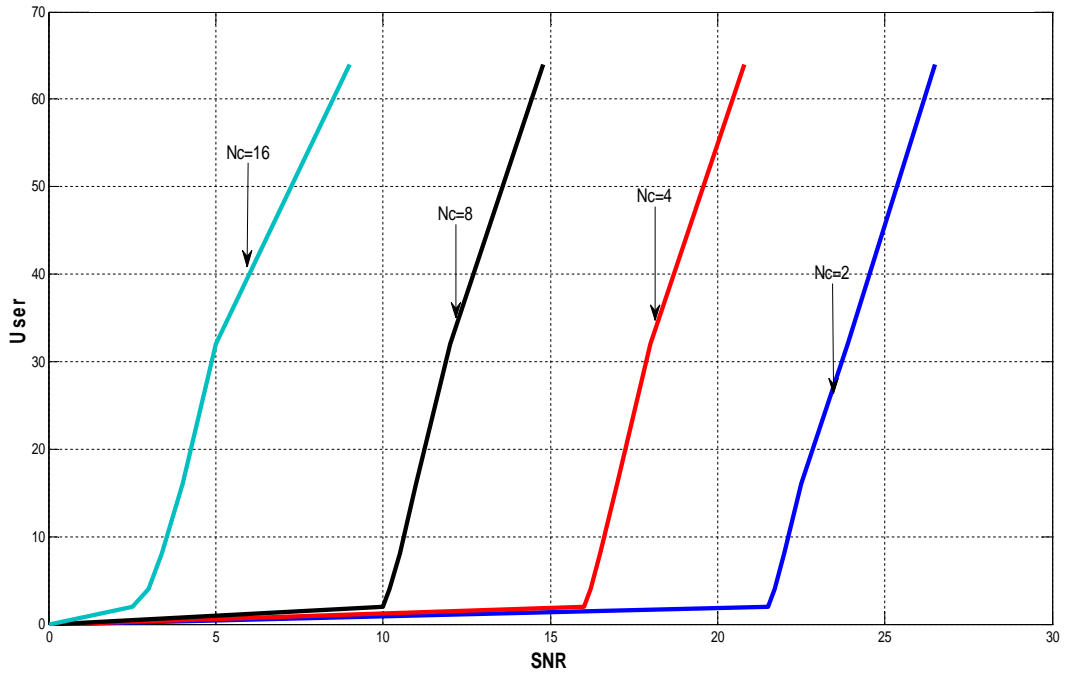
The achievable number of simultaneous users in a MC DS-CDMA PLC system at a given BER= 10^{-3} are shown in Fig. 4-17(a) as a function of required receiver sensitivity SNR(dB) with number of subcarriers, N_c as a parameter corresponding to $G_p=256$. The similar results with rake receiver are shown in Fig. 4-17(b) and Fig. 4-17(c) for $N_r=3$ and 4 respectively. In comparison to $G_p=128$, the system capacity significantly improves. The results are very much useful for design a MC DS-CDMA system over a PL channel.

User Vs SNR ($G_p=256$, $N_c=2,4,8,16$)



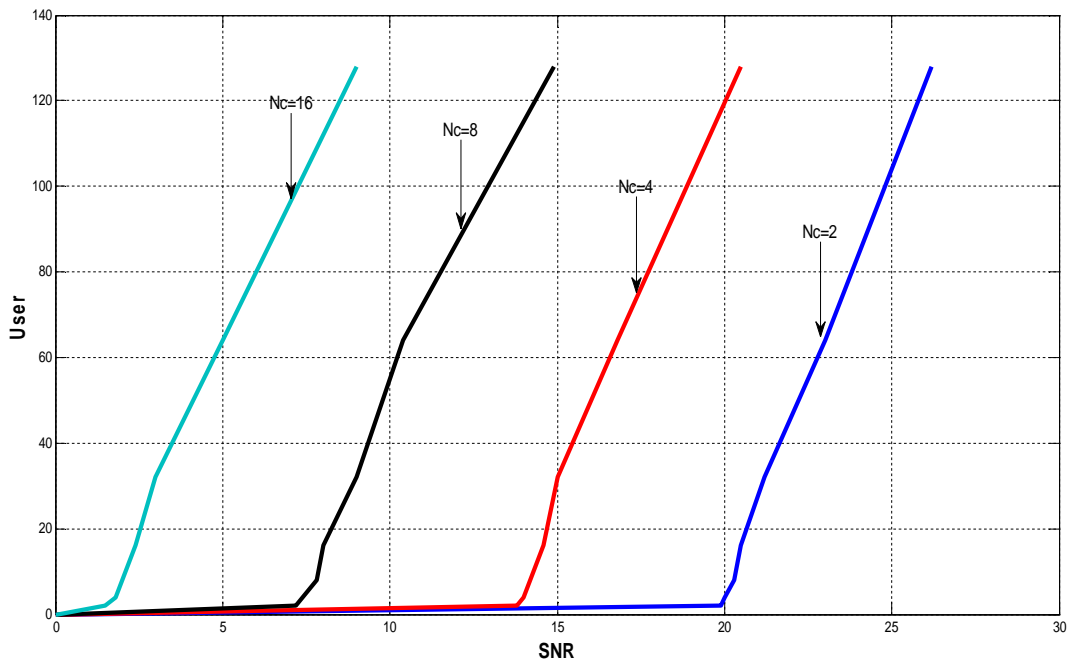
(a)

User Vs SNR ($G_p=256$, $N_c=2,4,8,16$), $N_t=3$



(b)

User Vs SNR ($G_p=256$, $N_c=2,4,8,16$), $N_t=4$



(c)

Fig. 4-17 User Vs SNR for different number of subcarriers (N_c) at $G_p=256$

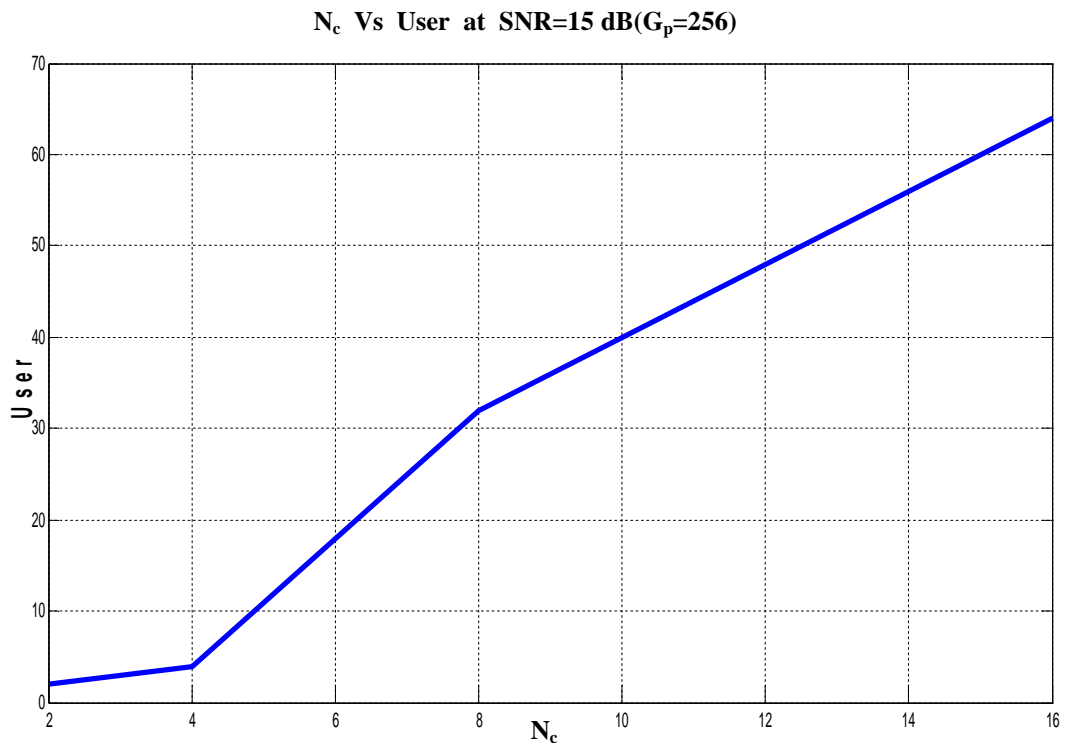
4.5.6 Subcarrier (N_c) Vs User for a Certain SNR (15dB) at $G_p=256$

The variation of number of user with the number of subcarrier at a given SNR(dB) are depicted in Table 4-5 for SNR(dB)=15 and $G_p=256$ without diversity and with diversity with rake fingers $N_r=3,4$.

Table 4-5: Number of users at different number of subcarriers (at SNR=15 dB), $G_p=256$

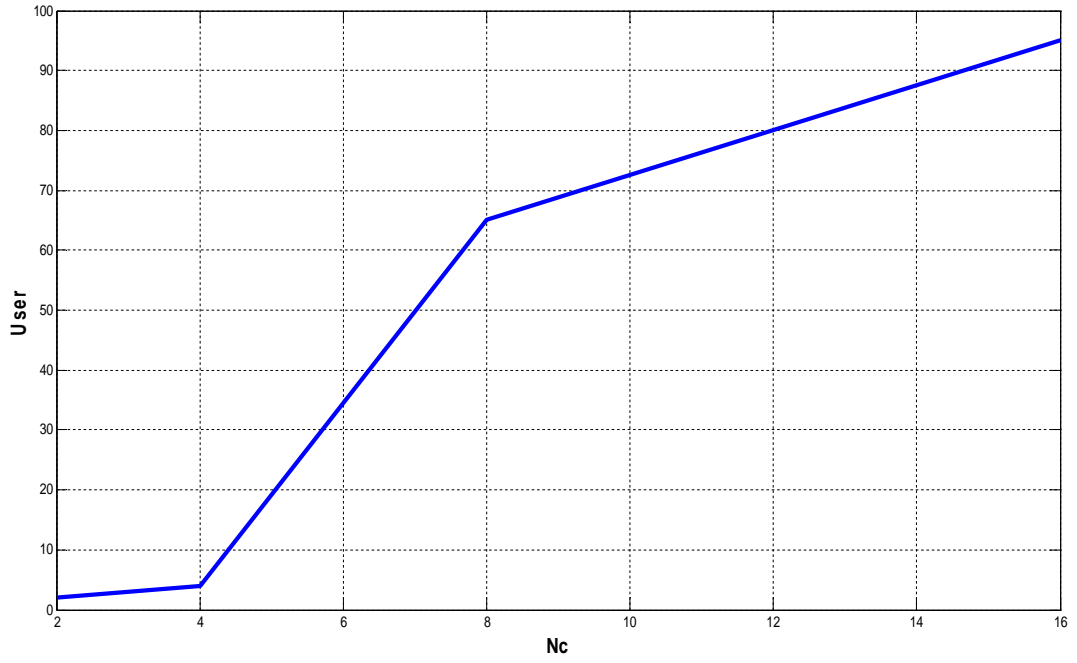
SNR (15 dB)			
N_c	Without diversity	With diversity	
	User	User with $N_r=3$	User with $N_r=4$
2	2	2	4
4	4	4	32
8	32	65	128
16	64	95	190

The results are also plotted in Fig. 4-18(a) through Fig. 4-18(c). The results show that there is significant improvements in system performance in terms of capacity due to increase in G_p and diversity.



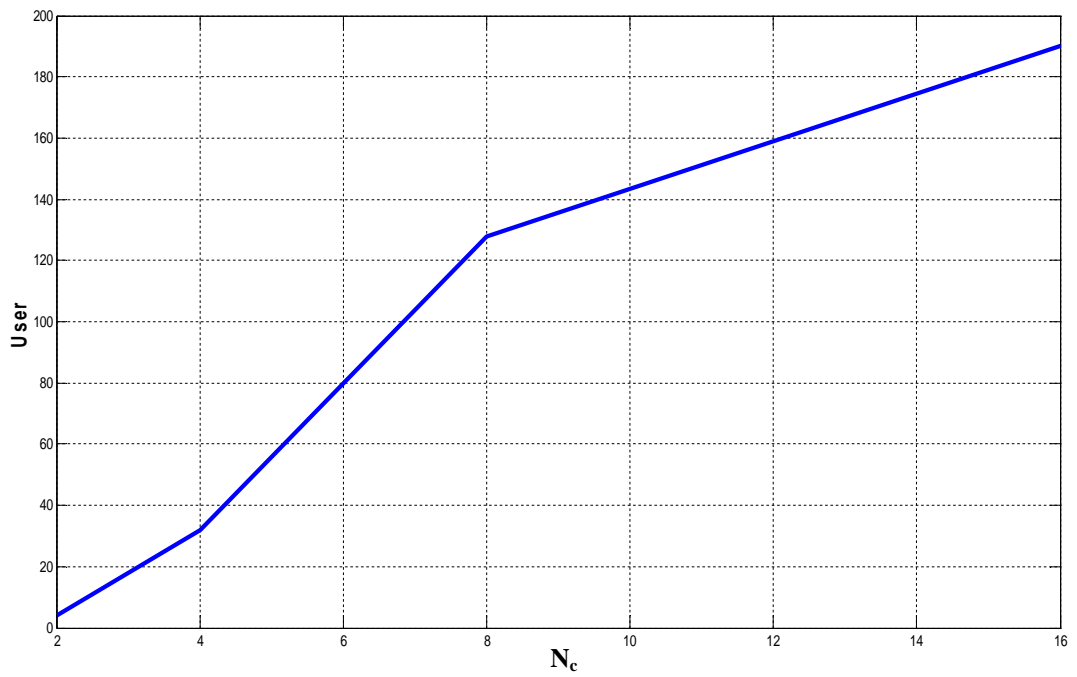
(a)

N_c Vs User at SNR=15 dB($G_p=256$), $N_r=3$



(b)

N_c Vs User at SNR=15 dB($G_p=256$), $N_r=4$



(c)

Fig. 4-18 Subcarrier (N_c) Vs User for a certain SNR (15dB) at $G_p=256$

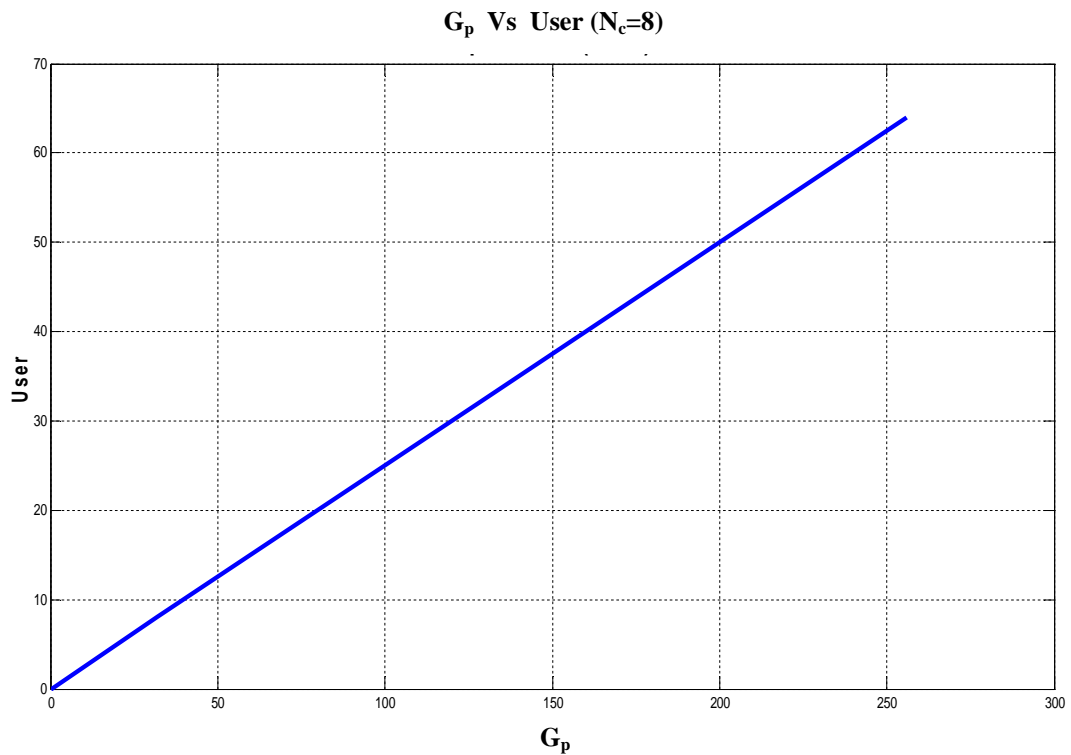
4.5.7 Processing Gain (G_p) Vs User for a Fixed Number of Subcarriers ($N_c=8$)

The receiver sensitivity for different processing gains for different users at a fixed number of subcarriers are depicted in Table 4-6 for $N_c=8$ and G_p ranging from 8 to 256 without diversity and with diversity employing rake receiver with number of rake fingers, $N_r=3,4$.

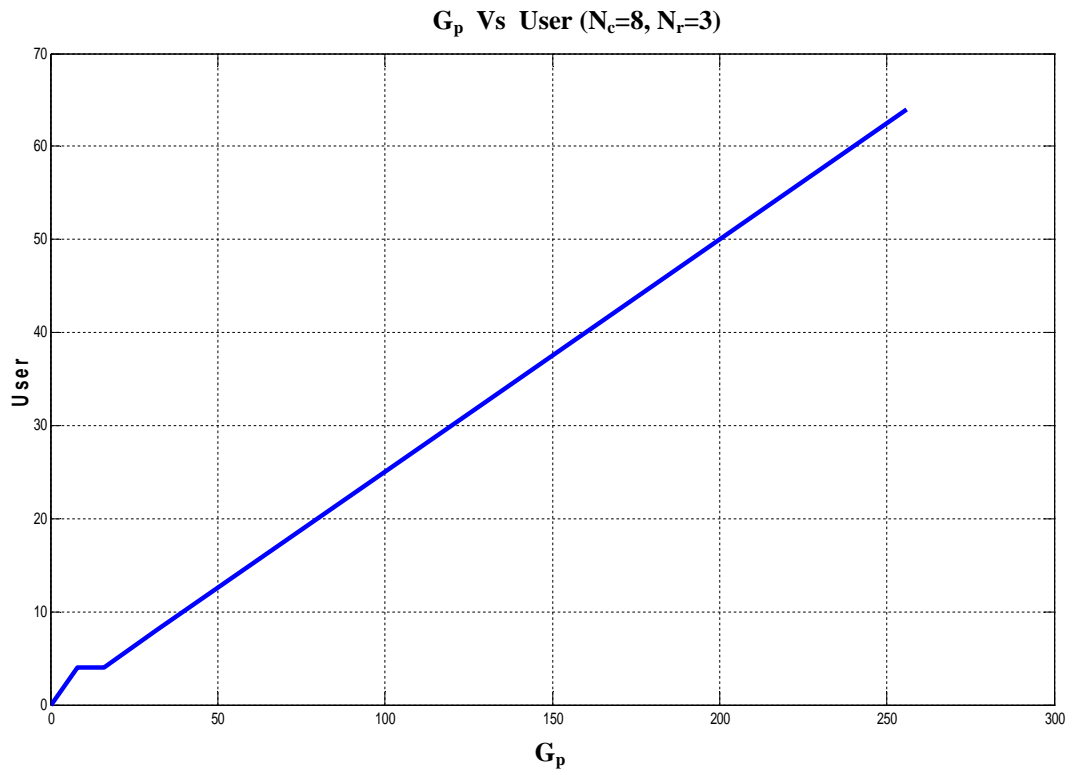
Table 4-6: Values of SNR(dB) for different processing gains for different users at a fixed number of subcarriers ($N_c=8$)

$N_c=8$																		
User ↓	Without Diversity						With Diversity											
	$G_p \rightarrow$						G_p with $N_r=3 \rightarrow$						G_p with $N_r=4 \rightarrow$					
	8	16	32	64	128	256	8	16	32	64	128	256	8	16	32	64	128	256
2	15	12.4	12	11.2	11.8	11	12	11.5	10.5	10	10	9.8	8.2	8	7.2	7	7	6.8
4		17.5	14.4	12.3	12.2	11.5	25	13.5	11.8	10.5	10.4	10	12	9.2	8.2	7.5	7.2	7
8			21.8	14.4	13	12			14	11.8	11	10.2		13.8	9.8	8.2	8	7.2
16				24.8	14.9	13			14	12	11				14.4	10	8.8	8
32					28.4	15					14.6	12				14.6	10	8.5
64						30.2						14.8					15	10
128																		15

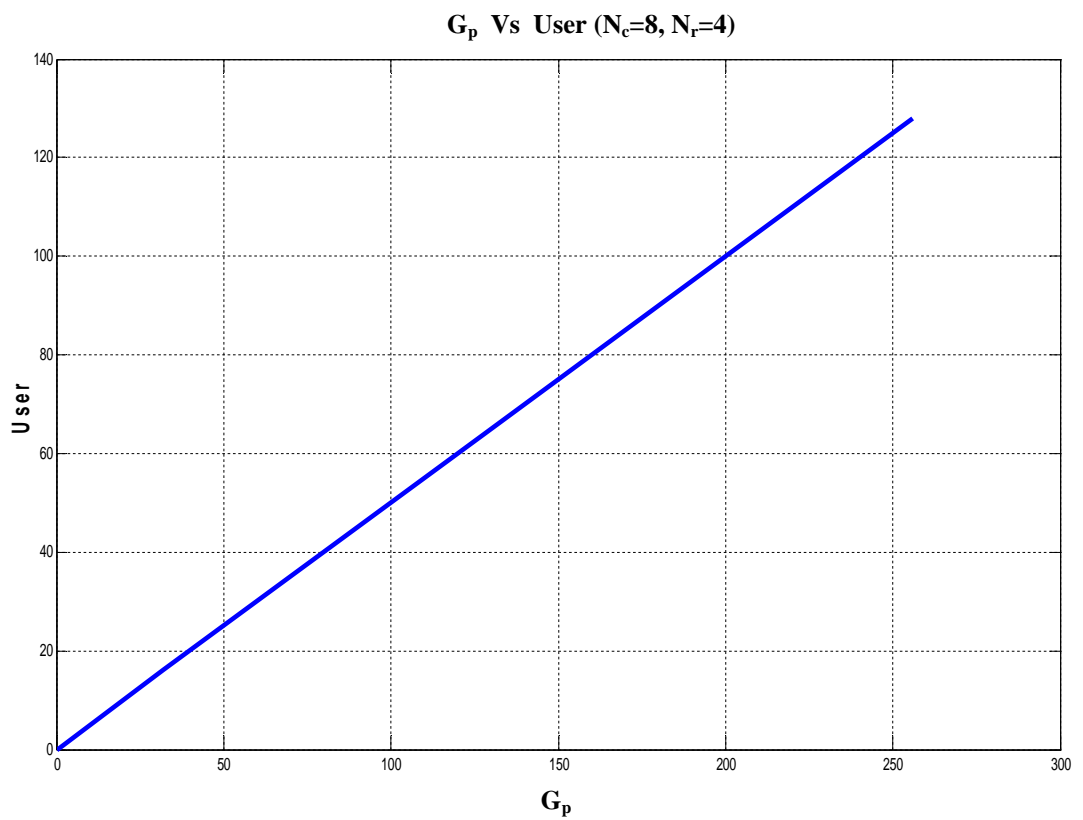
The results are also plotted in Fig. 4-19(a) through Fig. 4-19(c). Results show that system capacity in terms of user increases with the increase of G_p and it further improves for incorporating diversity.



(a)



(b)



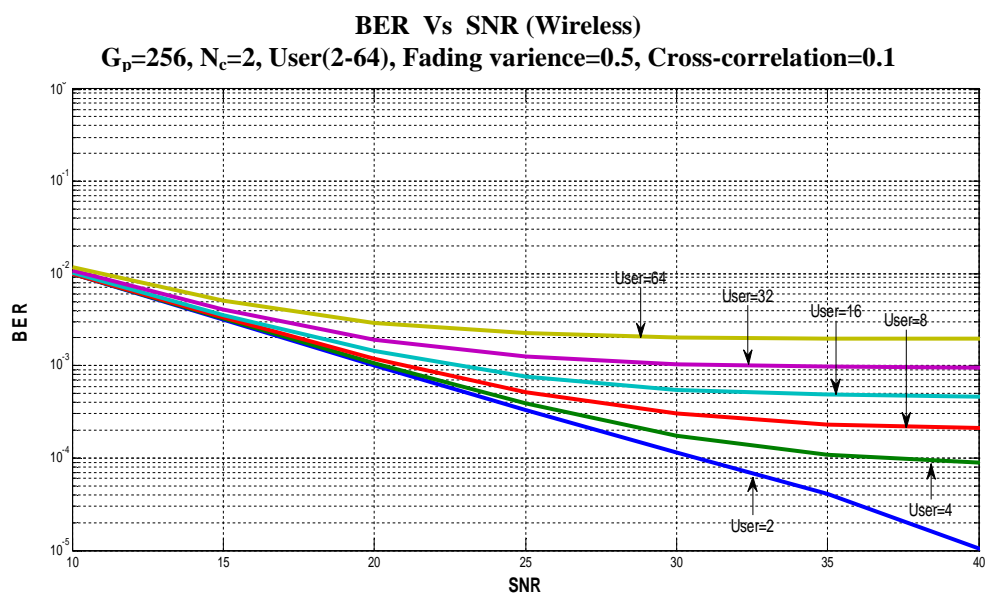
(c)

Fig. 4-19 Processing gain (G_p) Vs User for fixed number of subcarriers ($N_c=8$)

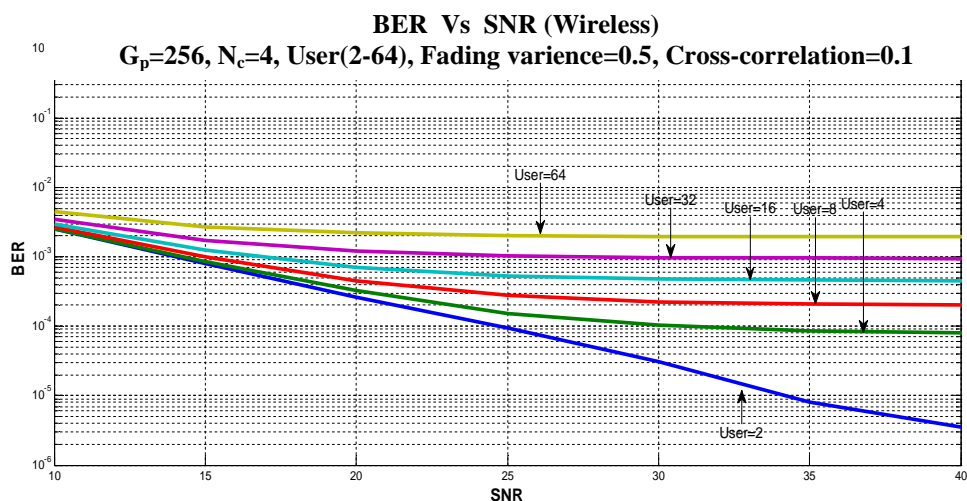
4.6 Performance Comparison of PLC with Wireless Communication

Fig. 4-20 and Fig. 4-21 show the BER versus SNR curves and User versus SNR curves for wireless communication for a given system parameters. It is noticed that, compared to Fig. 4-5 and Fig. 4-17(a) corresponding to PLC, for the same system parameters, the performance of PLC is better than wireless communication in terms of capacity. Table 4-7 shows the comparison of capacity between PLC and wireless communication at particular SNR(dB). It is noticed that, at BER level 10^{-3} and SNR=15dB, the number of user in case of wireless communication for subcarriers ranging from 2 to 16 is 1 to 42 whereas for PLC, number of user ranges from 2 to 64.

4.6.1 BER Vs SNR for Different Number of Subcarriers at Fixed Processing Gain ($G_p=256$) for Wireless Communication



(a)



(b)

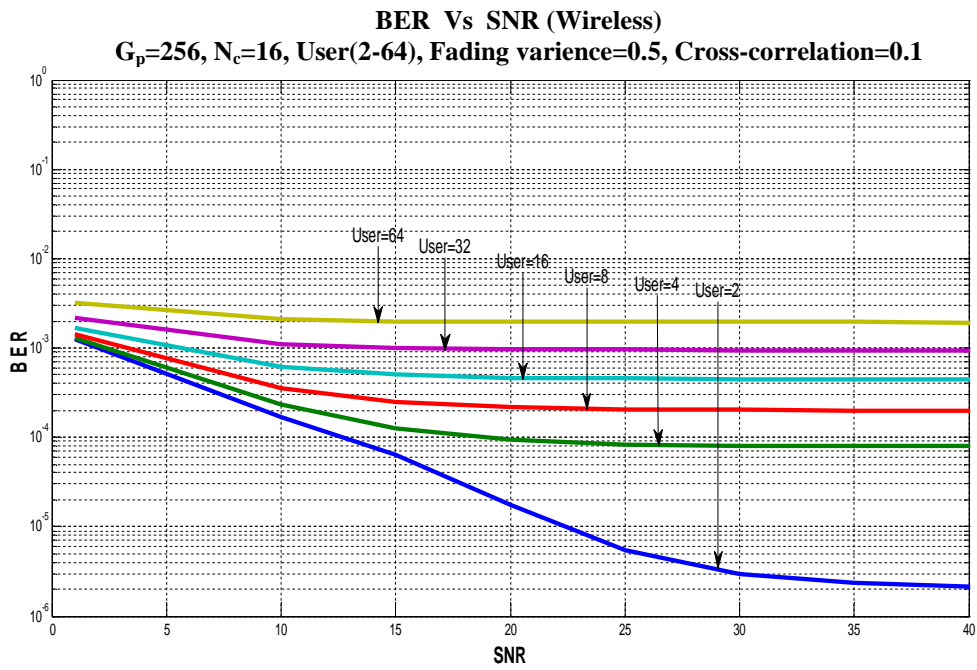
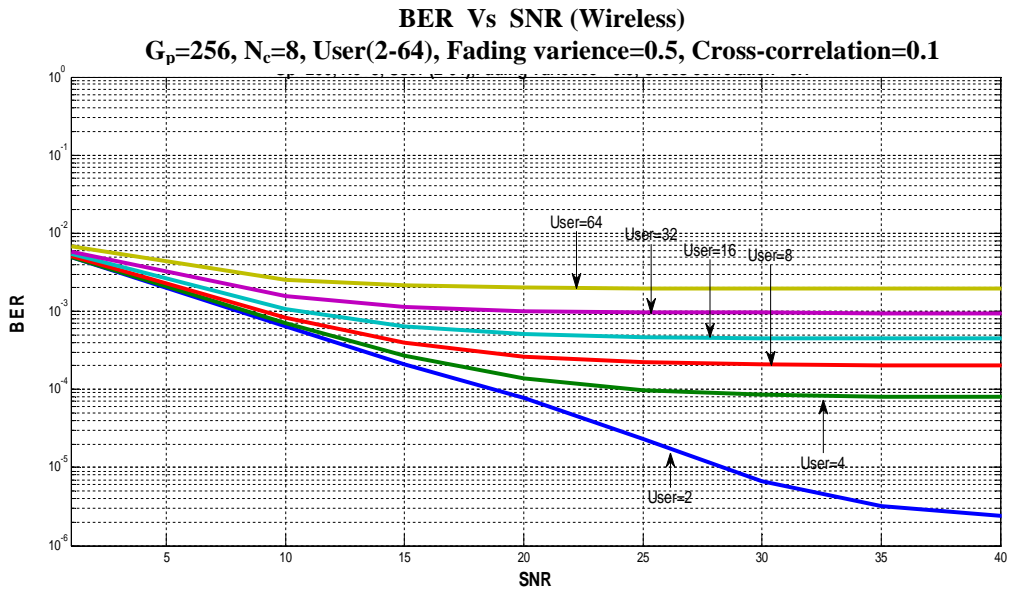


Fig. 4-20 Plots of BER Vs SNR for different number of subcarriers at fixed processing gain ($G_p=256$) for wireless communication

4.6.2 User Vs SNR for Different Number of Subcarriers (N_c) at $G_p=256$ for Wireless Communication

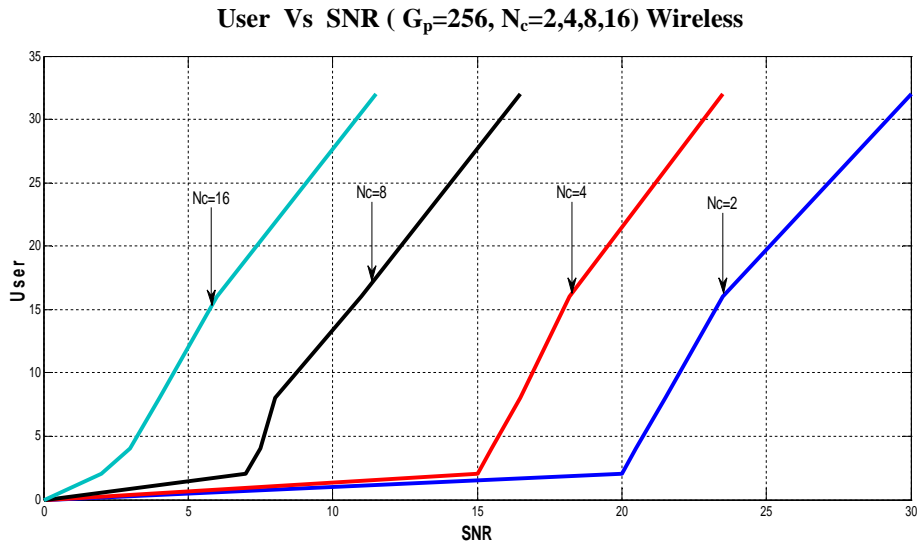


Fig. 4-21 User Vs SNR for different number of subcarriers (N_c) at $G_p=256$ for wireless communication

Table 4-7 : Comparison of capacity between PLC and wireless communication at particular SNR =15 dB, $G_p=256$

N_c ↓	At BER= 10^{-3}	
	Number of User	
	Wireless Communication	PLC
2	1	2
4	3	4
8	27	32
16	42	64

CONCLUSIONS AND FUTURE WORKS

5.1 Conclusions

An analytical model is developed and a theoretical analysis is carried out to evaluate the performance of a power line communication system with multicarrier DS-CDMA under the influence of channel effects. The analysis results in the development of an analytical expression for the SINR and BER at the output of an MC DS-CDMA receiver without and with diversity. The results are evaluated in terms of BER performance considering various system parameters and channel parameters to optimize the system parameters for a given BER.

The computed results show that there is deterioration in BER performance due to channel parameters. BER performance deteriorates with the increase of line impedances, number of branches, and branch lengths. The results show that performance can be improved by increasing the number of subcarriers. For a particular SNR, it is observed that, number of users can be significantly increased with the increase of subcarriers for a given BER. For a particular number of user, it is observed that, with the increase of subcarriers, there is improvement in receiver sensitivity. For example, the required SNR to achieve $BER \leq 10^{-3}$ is found to be 27 dB, 21 dB, 14.5 dB and 8 dB for number of subcarrier=2,4,8 and 16 respectively. For a given BER, number of users increase with increase of processing gain. For example, for $BER = 10^{-3}$, at $G_p=8$, the number of user is 2 whereas at $G_p=256$, the number of user is 64. At a value of processing gain, required receiver sensitivity in SNR(dB) is higher at higher number of user. It is noticed that there is significant improvement in receiver sensitivity at a given BER compared to $G_p=64, 128$ with 256.

It is noticed from the computed results that the performance of power line communication system with MC DS-CDMA can be improved by incorporating diversity technique. The results with path diversity using a rake receiver indicate that there is significant improvement in BER performance with increase number of rake fingers. Increasing the number of rake fingers allows more number of users at a given level of BER for a given number of subcarriers. For example, without diversity, the number of user that can be supported is about 4 for $N_c=10$ and is 16 for $N_c=15$. With diversity for $N_r=3$, the number of user is around 32 and for $N_r=4$, it is around 64. For a particular SNR, it is observed that, number of users significantly increases with the increase of subcarriers. For example, at $G_p=128$, without diversity, for number of subcarriers 2 to 16, user increased from 1 to 22. With diversity, for $N_r=3$, it is 2 to 57 and for $N_r=4$, it is 2 to 100 respectively. For a given BER, number of users increase with increase of processing gain. Achievable number of simultaneous user is found to be around 128 for $N_r=3$ and $G_p=256$ and 256 corresponding to $N_r=4$ and $G_p=256$ respectively. The optimum values of system parameters are also evaluated for a given BER.

It is noticed from performance comparison that PLC is better than wireless communication in terms of capacity. At BER level 10^{-3} and SNR=15dB, the number of user in case of wireless communication for subcarriers ranging from 2 to 16 is 1 to 42 whereas for PLC, number of user ranges from 2 to 64.

5.2 Scope for Future Works

Further investigations on MC DS-CDMA power line communication system can be initiated considering different types of user codes like PN- sequence, m-sequence, gold sequence etc. to find their efficiency in a PL communication environment.

Research can be done on PLC system with multiple input (transmitter) and multiple output (receiver) (MIMO) channel with relevant channel coefficients and their correlations to find the BER performance with multicarrier OFDM.

Further works can be carried out on a PLC system to find the effect of channel crosstalk due to coupling among the multiple conductors (phase, neutral, earth, protection) without and with diversity.

Further research works can be done on MIMO PLC system with MC DS-CDMA and MC FH-CDMA.

REFERENCES

- [1] Ma. Y. H., P. L. So and Gunawan. E., "Comparison of CDMA and OFDM Systems for Broadband Power Line Communication," IEEE Trans.on Power Del. vol 23 No. 4 October 2008.
- [2] Anatory J., Nelson T., Rajeev T., "Effects of Multipath on OFDM System for Indoor Broadband Power-Line Communication Networks," IEEE Trans. On Power Del. Vol. 24 No. 3 July 2009.
- [3] Marcel Nassar, Jing Lin, Yousof Mortazavi, Anand Dabak, Il Han Kim and Brian L. Evans, "Local Utility Powerline Communications in the 3-500 KHz Band: Channel Impairments, Noise, and Standards", IEEE Signal Processing Magazine, Volume 29, Number 1, January 2012.
- [4] Kamil H Zigangirov, "Theory of Code Division Multiple Access Communication", John Wiley and Sons Inc, IEEE Press, NJ, 2004.
- [5] Kiseon Kim and Insoo koo, "CDMA System Capacity Engineering", Artech House Mobile Communication series, Norwood, MA 02062, 2005.
- [6] R Prasad and T Ojanpera, "An overview of CDMA Evolution Towards Wideband CDMA", IEEE Communication Surveys, Fourth Quarter, Vol. 1 No. 1 of 1998.
- [7] Albenah Mihovska and R Prasad, "New Horizons in Mobile and Wireless Communication", Vol-1, Radio Interfaces, Artech House, Norwood, MA, 2009.
- [8] J. A. C. Bingham, "Multicarrier modulation for data transmission: An idea whose time has come", IEEE Communication Mag., vol. 28, no. 5 May 1990.
- [9] Ma. Y. H., P. L. So and Gunawan. E., "Performance Analysis of OFDM Systems for Broadband Power Line Communications under Impulsive Noise and Multipath Effects," IEEE

Trans. Power Del Vol 20 No 2 April 2005.

[10] Webpage www.hindaw.com/journals/wcn/2008/541410.html#B15

[11] Middleton D., "Statistical-physical model of electromagnetic interference," IEEE Trans. Electromagn. Compat, vol. EMC-19, no. 3. Aug 1977.

[12] Di Bert L., Caldera P., David S., and Tonello A. M , "On Noise Modeling for Power Line Communications," 2011 IEEE International Symposium on Power Line Communications and Applications (ISPLC). April 03-06, 2011.

[13] Bhatti S. A., Shan Q., Glover Ian A, Atkinson R., Illiana E O., Philip J M. and Richard R., "Impulsive Noise Modelling and Prediction of its impact on the performance of WLAN Receiver," 17th European Signal Processing Conference, Glasgow, Scotland, August 24-28, 2009.

[14] Khalifa S. A. M., Fawaz S. A.Q and Zahir M. H., "Adaptive Power Loading for OFDM-Based Power Line Communications Impaired by Impulsive Noise," 2010 IEEE International Symposium on Power Line Communications and Applications (ISPLC). March 28-31, 2010.

[15] Anatory J., Kissaka M M., and Mvungi N H., "Channel Model for Broadband Power-line Communications," IEEE Trans. Power Del. Vol. 22, no. 1, January 2007.

[16] Anatory J., Nelson T., Rajeev T., Kissaka M M., and Mvungi N H., "The Effects of Load Impedance, Line Length, and Branches in the BPLC-Transmission-. Line analysis for Indoor Voltage Channel," IEEE Trans. Power Del.vol.22 No. 4 October 2007.

[17] Ojanpera T., Ramjee P., Book on "Wideband CDMA for third generation mobile communications," Universal personal communications, Artech House, Inc Norwood MA, USA, 1998.

[18] John W Mark and Weihua Zhuang, " Wireless Communication and Networking", Prentice-Hall Inc, New Delhi, 2005.

- [19] Mosa Ali Abu-Rgheff, "Introduction to CDMA Wireless Communications", Academic press- An imprint of Elsevie.
- [20] Saimoon Ara Amin, Mahbulul Alam Rafel and S.P Majumder, "Performance Analysis of Multicarrier DS-CDMA wireless Communication System", Third UK European Symposium on Computer Modeling and Simulation, 2009.
- [21] S. Mallick and S. P. Majumder, " Performance analysis of an OFDM system in the presence of carrier frequency offset, phase noise and timing jitter over Rayleigh fading channels," ICECE 2008. Dec. 2008.
- [22] Phil Sutterlin and Walter Downey, "A Power Line Communication Tutorial Challenges and Technologies", Echelon Corporation, 4015 Miranda Ave. Palo Alto, CA, USA.
- [23] Masaaki KATAYAMA, "Introduction to Robust, Reliable, and High-Speed Power-Line Communication Systems", Center for Information Media Studies, Nagoya University, Nagoya-shi, Japan.
- [24] S. D. Paul, S. Asif and S. P. Majumder, "Performance Analysis of a MC-DS-CDMA Wireless Communication System with RAKE Receiver over a Rayleigh Fading Channel with Receiver Diversity", 7th International Conference on Electrical and Computer Engineering, 20-22 December, 2012, Dhaka, Bangladesh.
- [25] S.M. Navidpour, P Amirshahi and M. Kavehrad, "Performance Analysis of Coded MC-CDMA in Powerline Communication Channel with Impulsive Noise", Electromagnetic Compatibility, IEEE Transactions on Communication. Volume: EMC-19 Issue:3, 2006.
- [26] Kazi Abu Taher, Md Ruhul Minhaz and S. P. Majumder, "Performance Analysis of Multi-Carrier Direct Sequence (MC DS) CDMA with Fading", ICACT2013, January 27-30,2013.
- [27] Yong-tao Ma, Kai-hua Liu, Zhi-jun Zhang, Jie-xiao Yu, Xiao-lin Gong, "Modeling the Colored Background Noise of Power Line Communication Channel Based on Artificial Neural Netwrk", 978-4244-7596-4/10/2010 IEEE 2010.